NASA CR 112125
EDD W-3895

DEVELOPMENT OF AN ENGINEERING MODEL TRAVELING-WAVE TUBE AMPLIFIER FOR SPACE COMMUNICATION SYSTEMS

by

C. M. Eallonardo, J. Songli, A. Basiulis

HUGHES AIRCRAFT COMPANY
ELECTRON DYNAMICS DIVISION

prepared for

NATIONAL AERONAUTICS AND SPACE ADMINISTRATION

NASA Langley Research Center

Contract NAS 1-10417

Bruce M. Kendall, Technical Representative

NASA CR-112125
EDD W-3895

FINAL REPORT

DEVELOPMENT OF AN ENGINEERING MODEL TRAVELING-WAVE TUBE AMPLIFIER FOR SPACE COMMUNICATION SYSTEMS

by

C. M. Eallonardo, J. Songli, and A. Basiulis

HUGHES AIRCRAFT COMPANY
ELECTRON DYNAMICS DIVISION
3100 WEST LOMITA BOULEVARD
TORRANCE, CALIFORNIA 90509

prepared for

NATIONAL AERONAUTICS AND SPACE ADMINISTRATION

November 1972

CONTRACT NAS I-10417

NASA Langley Research Center
Hampton, Virginia

B. M. Kendall, Technical Representative

FOREWORD

The work reported herein was conducted at the Hughes Aircraft Company, Electron Dynamics Division, Torrance, California, under NASA Contract NAS 1-10417. The study was performed by Mr. C. M. Eallonardo of the Helix Tube Department, Mr. J. Songli of the Microwave Amplifier and Instrumentation Department, and by Mr. A. Basiulis and Mr. G. Cernik of the Mechanical Engineering Department. Mr. Bruce M. Kendall of the Flight Instrumentation Division, Microwave Techniques section, NASA Langley Research Center was Technical Representative for the program.

TABLE OF CONTENTS

TABLE OF CONTENTS (Continued)

LIST OF ILLUSTRATIONS

LIST OF ILLUSTRATIONS (Continued)

LIST OF ILLUSTRATIONS (Continued)

LIST OF ILLUSTRATIONS (Continued)

LIST OF TABLES

ABSTRACT

A design has been made of a 100 watt traveling-wave tube amplifier, including associated power supply, for use in space communication applications. The features of very high overall efficiency and heat rejection of waste heat at low thermal densities were predominant in the design concept. This high power unit can therefore be useful even in typical space craft applications with primary power and heat rejection capability being limited.

The design concept was proven by building a series of tubes, operating at efficiencies up to 50%. These tubes utilized heat pipe cooling and heat distribution such that 150 watts of waste heat was rejected at a density of less than 1.5 watts per square inch. A power supply to convert a 28 volt primary line of the needs of the TWT was built and operated at 85% efficiency. A combination of one tube and one power supply packaged as an integral amplifier was delivered at the end of the program in accordance with requirements.

I. SUMMARY

The work undertaken in this program falls into 3 major categories, traveling-wave tube development, power supply development, and heat pipe development with associated mechanical engineering.

A traveling-wave tube was designed utilizing the concept of a velocity tapered helix circuit to develop the RF power at high basic efficiency. To enhance this effect full advantage was taken of the increased interaction impedance resulting from the use of Anisotropic Boron Nitride for helix support material. A low perveance design was used to reduce the problem of beam control since intercept current reduces the effectiveness of a depressed collector. To raise the 35% anticipated basic efficiency to over 50% a two stage collector was used. Tubes were built which generate up to 100 watts of output power and operated at up to 50% efficiency, and which utilized heat pipe techniques to transfer waste heat into an integral baseplate. Heat was rejected from this baseplate at a density of 0.8 watts per square inch average.

The heat pipe development included a radial heat pipe which transfers heat from the collector while maintaining the required high voltage stand off for depressed collector operation. The low density of waste heat rejection is then accomplished by installing in the integral baseplate heat pipes which operate transverse to the tube axis. These heat pipes pull waste heat into the relatively thin baseplate and disperse it over 190 square inches of surface area.

A power supply was designed to provide the required tube voltages and power requirements within the expected range of line voltage (24 to 32 volts) and under the conditions of load variations and temperature extremes. Because of the high basic efficiency and the two stage collector employed, a large redistribution of current with drive level was expected. Helix current changes from 2.5% to 25% of total current, and Collector No. 3 current changes from 98% to 32% of total current, must be tolerated by the power supply. One breadboard and one packaged power supply were built.

The program concluded with assembly of one TWTA assembly, a tube, power supply, a heat sink baseplate, and associated hardware. After evaluation this unit was delivered to NASA.

II. INTRODUCTION

Traveling-wave tube amplifiers (TWTAs) have been used for some years now in communication satellites and as power amplifiers for deep space missions where data transmissions were required. In all cases to date the size of the spacecraft has dictated the power level of the TWTA (because of prime power limitations). This limit in turn is traded against ground receiving antenna size and noise figure and also data transmission rate.

New programs dictate the need for higher power output from on-board amplifiers and more prime power will be made available. As power goes up, however, two factors remain important in the TWTA design. First the efficiency must be maximized since prime power will always be limited, and secondly the rejection of waste heat, in large quantities, must be managed such that spacecraft thermal capabilities are not over-loaded. Of course, the basic highly reliable long life characteristics of the presently available low power units must be retained.

In consideration of these requirements a design for a 100 watt C-Band TWTA was undertaken. Primarily it serves as a model of the required amplifier for the Space Shuttle Vehicle. The intent of the program is to demonstrate that, in combination, the requirements of high power, high efficiency, high reliability, long life, and good communication characteristics can be obtained.

Since Hughes Electron Dynamics Division has constructed and evaluated many of the power amplifiers which have been successfully used in spacecraft, the requirements for high reliability and long life were well known. The high power requirement does not necessarily compromise life or reliability. Cathode loading and cathode temperature can be maintained by sizing the cathode properly for the load, and the use of high voltages does not degrade power supply operation if proper derating techniques are employed.

The most important question was whether high efficiency design would degrade communication characteristics, namely phase shift effects such as AM/PM conversion, and also the level of intermodulation noise products.

Our approach was to use a circuit which was to be operated at synchronism both in the driver section and in the output section by appropriate use of circuit tapering.

This report, including a collection of data taken on tubes and TWTA's, points out that this approach does indeed provide operation as predicted. The efficiency has been attained and AM/PM conversion and 3rd IM product levels are similar to those measured on space tube operating at much lower power and efficiency. Life and reliability have not yet formally been assessed by test but power supply derating factors, and the level of tube circuit operating temperature are well in line with stresses allowable for highly reliable units. The cathode loading and operating temperature, 750°C, are conservative for the required design life.

III. THE 279H TRAVELING-WAVE TUBE

SUMMARY OF THE TUBE PROGRAM

The major elements of the development program undertaken are illustrated in Figure 1. The program included the development of the required traveling-wave tube (TWT) and also the development of a heat pipe system. The heat pipe system is used for distributing waste heat along the tube axis and transversely into the expanse of a large base plate. In doing so the thermal load density due to rejected heat energy can be reduced, in this case, to 1.5 watts per square inch or less. This is a tolerable density for spacecraft cooling systems.

The initial tube design considered the efficiency requirement a prime consideration. By use of a large signal computer program a velocity tapered circuit was designed, giving rise in turn to choices for beam voltage and current. The remaining dependent designs for the gun, the collector, and the PPM array were then established. The mechanical design is very similar to other Hughes Electron Dynamics Division space tubes with the exception of the heat pipe cooling system.

The design phase, including cold testing of the circuit for phase velocity and impedance, and evaluation of the impedance watching system between helix and 50 ohm coaxial lines, took place in the first four program months.

As individual portions of the design were completed, materials and then parts were ordered. As subassembly levels were defined, assembly tools were designed and ordered. All parts of the basic tube were on order within 5 months and as sufficient parts were received tube assembly began.

As the tube design was being considered our Mechanical Engineering Department undertook the design of the heat pipe system. This involved first the choices as to operating temperatures of the copper collector core, of the relatively cool outer jacket, and of the axial heat pipes used to move waste energy along the tube body. Next choices of material (fluids, wicks, and containers) were made and sorted as to compatibility, power handling capability, and optimum operating temperature. Experimental heat pipes were built to check actual temperature rise as a function of power flow and heat pipe length for various material combinations. This work was conducted in the first three program months.

Mechanical design of the heat pipe system followed and culminated in a two part design. One, the collection heat pipe was made an integral part of the tube assembly. The heat pipe fluid was added only after the tube had been baked out and had been successfully pulse tested, indicating

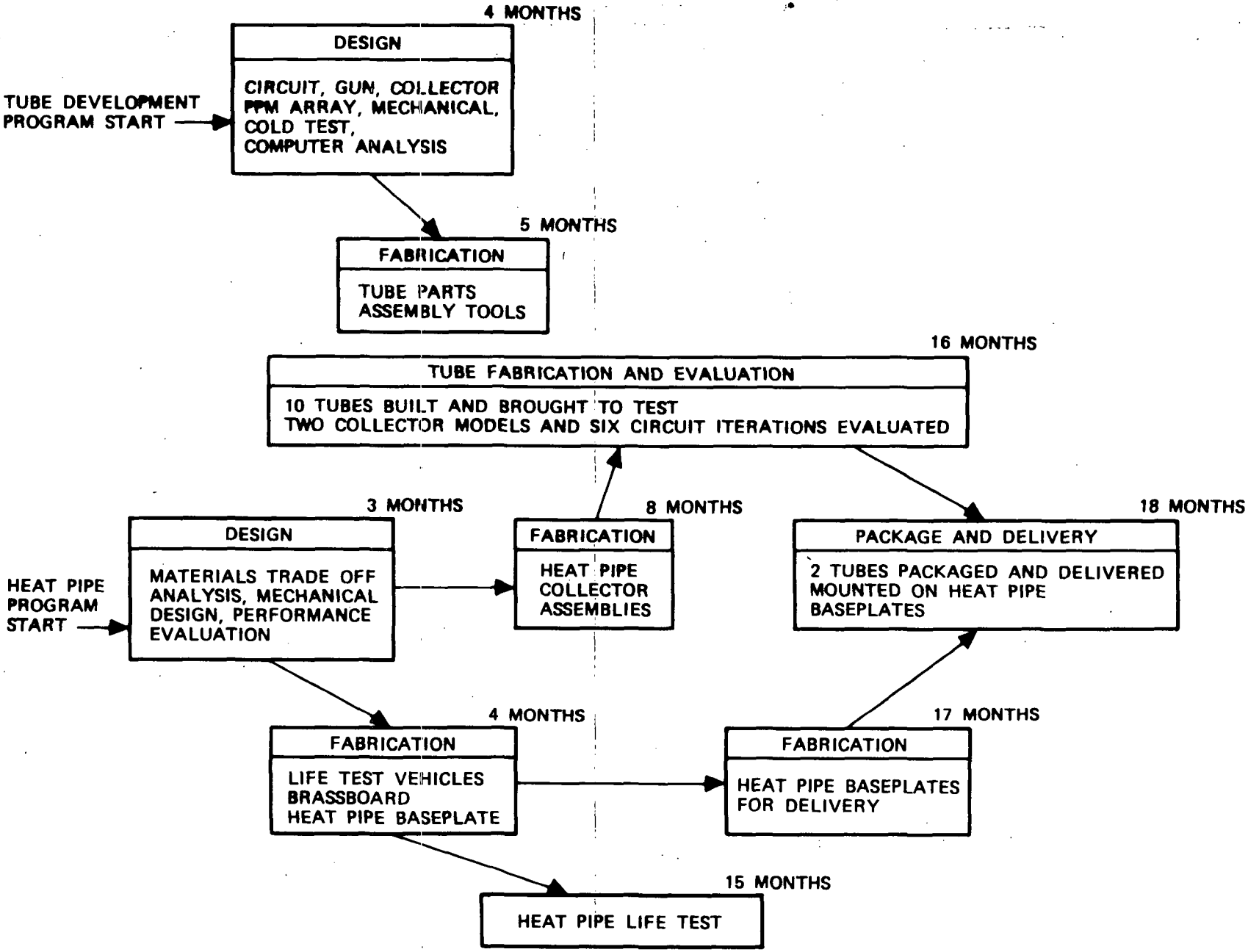

Figure 1 The 279H program summary.

that CW operational tests were desired. Fabrication of the first of these assemblies was completed in the eighth program month and was incorporated into the third tube assembly. Earlier tubes were built with interim oil cooled collectors. During the program 8 heat pipe collectors were used; 11 tubes were constructed.

The second part of the system, the axial pipes used to move heat energy from the collector and body of the tube out through a large base plate, was also designed and a brass-board version was built and tested. This base plate contained long heat pipes, transverse to the tube axis, soldered onto an aluminum frame. Heat pipes were spaced ~0.6 inches apart. Tests of this part of this system were successful and the design was tentatively selected to be used in final hardware.

Life test vehicles were constructed and placed on test. Axial heat pipes in a number of combinations of materials were started on life tests in the second month. Collector heat pipe tests were started in the eighth month. In this case three fluids were evaluated, all with the same radiator, condenser, and wick materials.

Tube fabrication started in the fourth program month. The first tube was brought to test in the sixth month. Approximately one tube per month was built and evaluated. Early tubes incorporated oil cooled collectors but the majority (eight) of the tubes were evaluated with heat pipe collectors. As tube evaluation proceeded a number of circuit design iterations were tried, six in all, following plans to improve basic efficiency. Only one electrostatic collector design was used and the possibility exists that improvements may be possible in this area. The gun design as originally selected was used on all tubes. Tube fabrication ended after completing the twelfth tube in the sixteenth program month.

The tenth and twelfth tubes built were packaged and mounted on heat pipe base plates. Tube No. 10 was delivered to NASA as an engineering model tube. Tube No. 12 was retained and integrated with a solid state supply, also built as part of this program, and the complete unit was then delivered to NASA in the eighteenth program month.

SPECIFICATION DESIGN GOALS

The object of the contract was to develop a traveling-wave tube amplifier package with a design capable of highly reliable operation in communication service. High efficiency was of prime consideration. The required characteristics of the package, translated into tube requirements, demanded that a high power, high efficiency tube be produced which would exhibit the communication characteristics of typical communication satellite output tubes.

The requirements are listed in Tables I and II. Inferred requirements are those which are determined by the overall requirement plus a consideration of the contribution of the power supply to overall performance.

In the electrical design the major consideration was efficiency. Our confidence in meeting this requirement lay in experience in similar power level tubes in which high basic efficiency was obtained by use of velocity tapers. Computer predictions lead to the belief that basic efficiencies could reach 35% with a proper circuit design in this application. The total of 50% efficiency would then be achieved through use of a two-stage collector. Here also the benefits of a computer analysis of collector electrode shapes were available to optimize the performance of the collector.

Also of major importance was the required output power level (100 watts). All space tubes to date had been required to deliver much lower power, in the 3 to 20-watt level, and subsequently much less waste power was handled. In this new application 100 watts of power had to be dissipated into the TWTA package in such a manner that the density of heat flux could be lowered to 1.5 watts per square inch.

Life was a major consideration also. Certainly an oxide cathode of the space tube type would be used. Three factors were expected to affect the life of the tube.

1. The circuit design called for a relatively small circuit diameter and, therefore, a small beam size. In order to provide the required beam density without using a high density cathode loading it was necessary to use a highly convergent gun. By doing so the impact of cathode loading on life was avoided.

2. The beam energy removal associated with a high basic efficiency meant that a high percent of the beam would not reach the lowest voltage collector. Instead it was estimated that 20% of the beam would strike either the helix or the body of the tube. Outgassing of these elements could give rise to contamination of the cathode and subsequent degradation of life. The key here was to heat sink the helix and body such that absolute temperatures are held to safe maximums. In addition, choice of materials to be used had to be limited to those which could be properly outgassed before installation in the tube.

3. The third consideration was the impact of beam defocusing as the voltages were raised to final values at turn on. The effect of this defocusing is controlled in lower power tubes by requiring a very short rise time for the helix potential. This, however, leads to the problem that the power drain from the source increases

TABLE I ELECTRICAL PERFORMANCE DESIGN REQUIREMENTS

Parameter	Value	Notes
Input Power	230 watts, max.	Inferred, assumes power supply efficiency of 85%
Saturated Output Power	100 $\pm$ 10 watts	
Frequency Range	5.925 - 6.425 GHz	
Efficiency	49.5% min.	Inferred, assumes power supply efficiency of 85%
Gain	33 dB min.	Saturation
Gain Variation	0.1 dB/MHz max. 2.0 dB over freq. range	Saturation or Small signal
Input VSWR	2:1 max, 40 MHz 3:1 max. over req. range	Operating
Load VSWR	1.3:1 max.	Meet all specs except gain variation
Load Mismatch	3:1 max.	No damage
Harmonic Output	-15 dB max.	
Spurious Output	-70 dB	Saturation
Noise Power Density	-70 dBw/MHz	
Phase Linearity	$\pm 8^{\circ}$/40 MHz	
Phase Sensitivity	0.8°/volt approx. 6°/volt approx.	Helix voltage Heater voltage
Amplitude Sensitivity	0.03 dB/volt max. 0.2 dB/volt max.	Helix voltage Heater voltage
AM/PM Conversion	15°/dB	8°/dB objective
Intermodulation	-10 dB	Saturation

TABLE II FORM FACTOR AND ENVIRONMENTAL DESIGN REQUIREMENTS

Cooling	Conduction	Tube package to provide for leveling heat flux along the tube axis.
Connectors	OSM Flying leads	RF High voltage
Size	3" x 4" x 18" max.	Inferred
Weight	5 lbs. max.	Inferred
Life	14,000 hrs. max.	
Stray Magnetic Fields	0.01 Gauss at 2 ft. from tube	
Temperature Range	$-55^{o}C$ to $+70^{o}C$	Operating
Vibration, Sine	6 g, 55-1500 Hz	Operating
Vibration, Random	$0.03\ g^2/Hz$, 20-2000 Hz	Operating
Shock	10 g, 11 msec.	Nonoperating
Acceleration	10 g	Nonoperating
EMI Control	per MIL STD 461	Design goal

momentarily as high voltage capacitance is charged. In this high power tube the effect would be even larger, yet if the turn on was slowed down there would be a danger of helix burnout during turn on.

The problem was resolved by specifying that the power supply would establish the helix and collector voltage slowly to avoid a power drain transient. However, beam power would be held off by using the anode as a control element. When tube operation was desired the anode would be raised to final operating potential by turning on a second power supply. With this type of turn on the defocusing is avoided as is the high transient power drain. The impact of increased complexity and lower efficiency in the power supply was accepted by the power supply designers as being within reasonable limits.

It appeared that the remainder of requirements would fall out of the design without special consideration. The significance of the circuit design and what effect it would have on AM/PM conversion was of considerable interest. The high efficiency (35%) of the circuit would yield an AM/PM of perhaps 15^{o}/dB if scaled from the lower power, lower efficiency space tubes. However, the design of the circuit was such that overvoltaging is not used to achieve high efficiency as is done in nontapered circuits. Since this is the case improvements in AM/PM conversion were expected and a design goal of 8^{o} dB was accepted.

THE FINAL ELECTRICAL DESIGN

The electrical design of the tube was pursued over a period of 16 months. This period included an initial design evaluation with the use of computer aided techniques. The electron gun, the RF circuit, and the two-stage collector were analyzed in this manner. A periodic permanent magnet focussing array was designed and the required transformers to match the helix to the 50 ohm coaxial lines were made.

Ten tubes were built and brought to test to evaluate the design. The ten tubes included a number of circuit modifications in attempts to produce the maximum possible efficiency. The final tubes produced came very close to meeting all requirements and two tubes were ultimately delivered to NASA.

A description of each portion of the design is included in this report. The variations undertaken are described, although it will be noted that the final tube differs very little from our initial proposal.

The Electron Gun

The electron gun is a standard Pierce type diode gun with an oxide emitter. The focus electrode and cathode are operated at the same

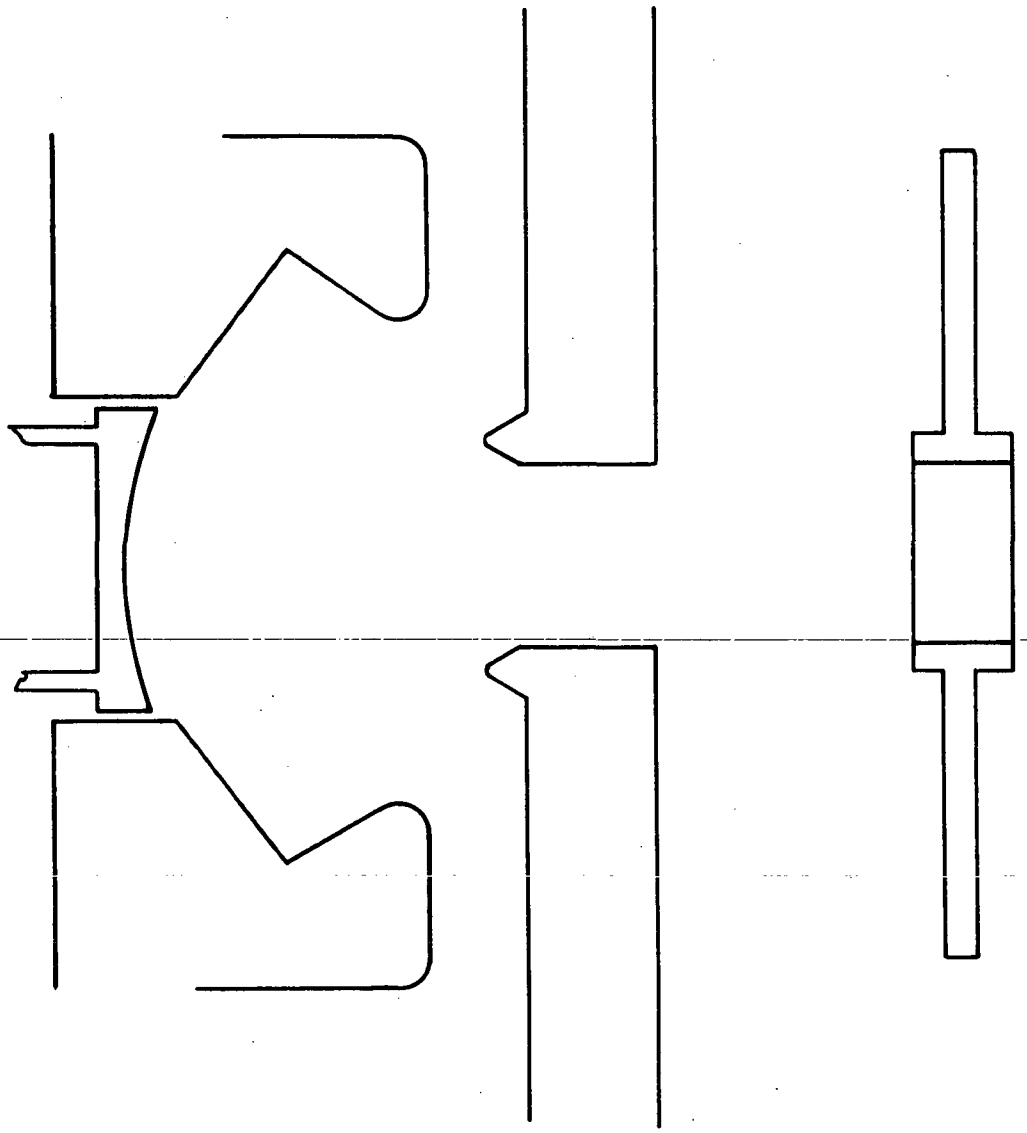

Figure 2 The 279H electron gun layout.

potential and the anode is isolated such that it can be operated at cathode potential (-3600 volts, beam off or at +200 volts, beam on). Figure 2 is a layout of the gun. The vacuum envelope components of the gun are brazed in three sections; the actual electrostatic elements of the gun are stacked into the vacuum envelope at final assembly after final cleaning and cathode coating. Perveance is set by the total of the precision length of a spacer ceramic and the focus electrode to cathode spacing which is also determined by a precision machining operation.

The electron gun parameters are listed in Table III.

TABLE III 279H ELECTRON GUN PARAMETERS

Anode voltage	3800	volts
Cathode current	85	mA
Cathode diameter	.196	inches
Cathode loading	435	mA/cm^2
Emitter type	Oxide, double carbonate base	
Operating temperature	750	^oC, brightness
Heater voltage	6.0	volts
Heater current	350	mA

The electron gun design was evaluated initially by a computer program and by testing an actual gun in a beam analyzer. No changes were made in the design after completion of evaluation, perveance requirements did not change, all guns were therefore identical.

No problems were encountered with perveance or emission level other than in Tube No. 3 which had a leak following bakeout. The high resultant on internal pressure caused degradation of that cathode. All other tubes were operated at the design heater power after an initial 24 hours age.

The RF Circuit

The requirement for extremely high basic (undepressed) efficiency led to the use of a velocity tapered circuit. This circuit was designed using a Hughes Electron Dynamics Division large signal computer program.

Basically the reason for the use of a velocity tapered circuit is to retain synchronism between the helix and the beam as energy is removed from the beam. Since essentially all of the energy is removed near the output end of the helix, only that end is affected by the design. A properly designed circuit for this application is one for which a single operating helix voltage will produce both maximum small signal gain and maximum efficiency at saturation. Figure 3 is a description of the helix circuit design. This circuit operates within the conditions mentioned in both small signal and saturation modes. The voltage is 3650 volts. This voltage with beam current of 85 mA is sufficient to produce the required output power.

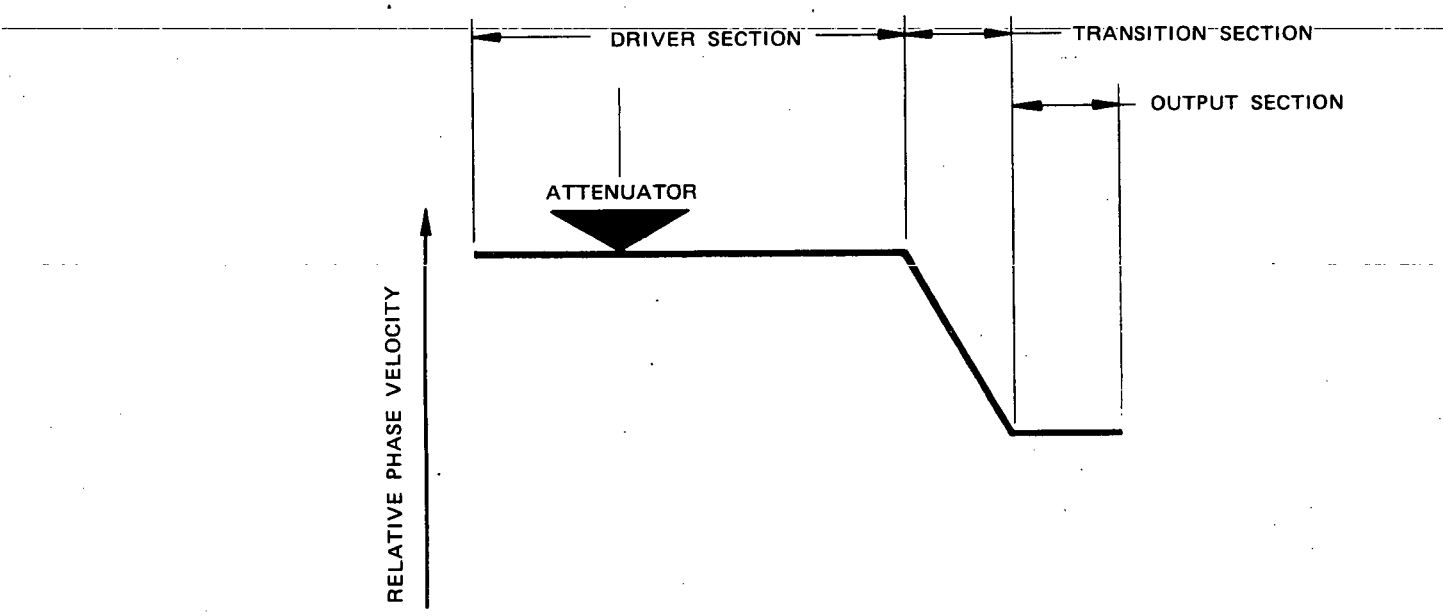

Figure 3 The velocity tapered helix.

A major factor in the generation of power at high efficiencies is the interaction impedance of the circuit. The shape factor of the helix material, the helix loss, the shell loading, and the dialectic loading of the helix supports all contribute in effecting impedance and each was considered in the design. Table IV is a list of the significant parameters.

TABLE IV 279H CIRCUIT PARAMETERS

Helix mean diameter	.059 inches
Support material	Boralloy (Anisotropic Pyrolytic Boron Nitride)
Number of supports	4
Shell diameter	.123 inch
Reduced impedance (midband)	105 ohms
DLF (midband)	.81
Loss (midband)	1.0 dB/inch

Computer runs estimating the gain and efficiency of the circuit as a function of axial position along the tube are shown in Figure 4 for the two band edge frequencies. The projected efficiencies of 40% and 36% for low and high band edges respectively were not attained in actual tubes. The best figures achieved were 33% and 30% (in Tube No. 10). Approximately 2 percentage points are associated with RF heating of the circuit and subsequent power fade. This should be reduced in future tubes. The remainder is an offset which has been noted in other designs, that is, the computer prediction is optimistic with respect to practice. The original proposal, however, took this into account and an efficiency of 35% at the low band edge was predicted. Our performance, therefore, closely approaches the expected results.

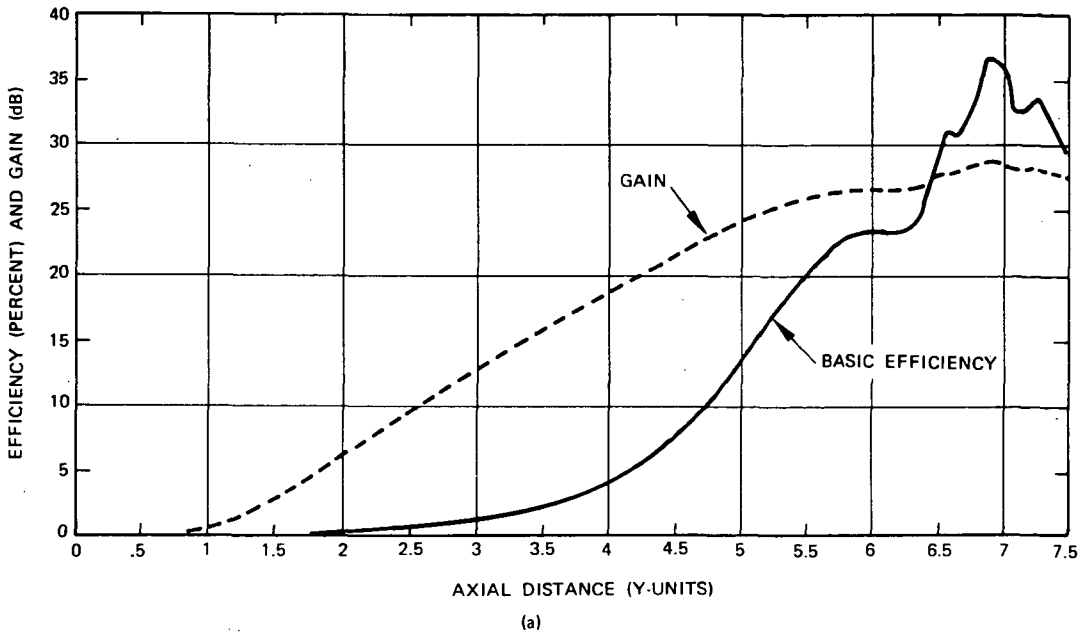

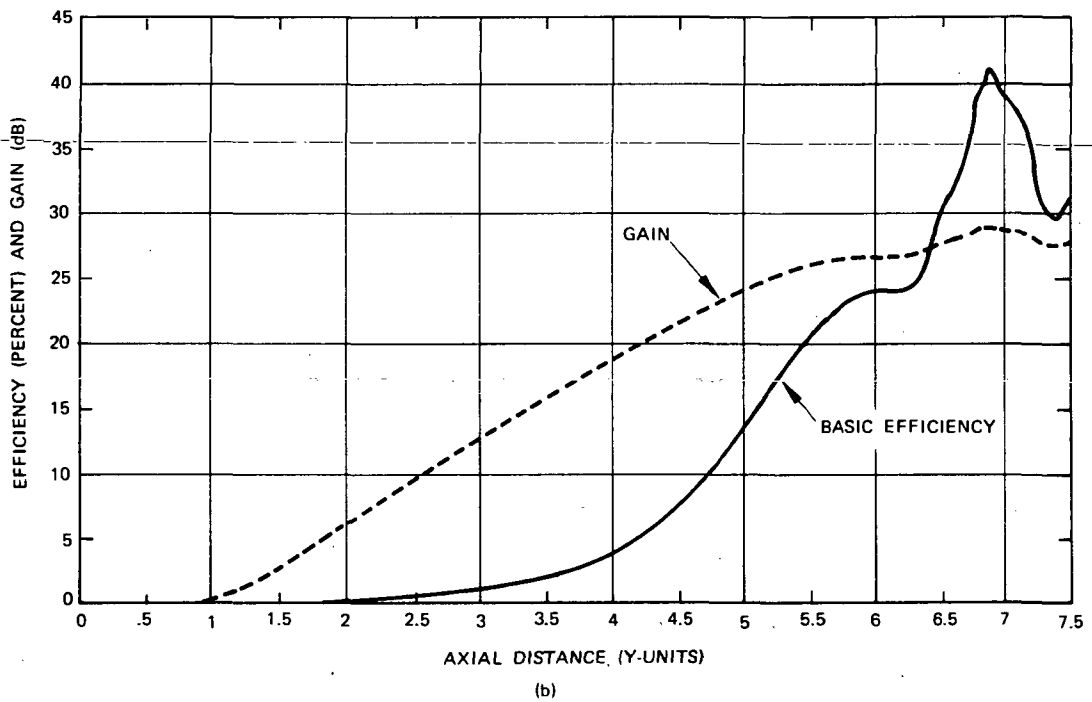

Figure 4 Calculated basic efficiency without depression and gain at (a) 6.4 GHz and at (b) 5.9 GHz.

The Collector Design

Because of the large amount of energy removed from the beam through generation of RF power, collector depression becomes very critical. Required electrode shapes within the collector become dependent on the energy distribution in the beam. This energy distribution in the spent beam was approximated by groups of electrons at five different energy levels for computer analysis in the case of the 279H development. The collection of the beam for different electrode shapes was then evaluated. A typical computer run is shown in Figure 5. Note that there is one undepressed stage, equivalent to helix potential. The other two electrode potentials can be varied in order to maximize collector efficiency for the given choice of five energy levels. If necessary the electrode shapes can be changed and again the collector efficiency can be evaluated for all combinations of electrode voltages. Since we have predicted basic efficiency of 35%, the collector efficiency must be at least 46% in order that our goal of over 50% efficiency be reached. A number of electrode shapes were considered and a design which performed at greater than 46% efficiency was determined. This was translated into the collector design shown in Figure 6.

The collector design work pointed up the fact that the undepressed collector face and the first depressed stage receive the greatest portion of the spent beam (both in electron numbers and watts) when the beam is operating at saturation. This can be seen in Figure 5 by the number of trajectories striking those two surfaces. It was, therefore, necessary to make those two members good conductors of heat and have them present as large a surface as possible to the cooling medium.

The undepressed stage is attached directly to the tube base and cooling is accomplished by conduction radially to the edge of the collector stage and then directly to the tube base. The first and second depressed stages have no such conduction path. They are cooled instead by heat pipe action; this is described in another section of this report. It is important to note, however, that heat flow by conduction radially from the center of the collector to the periphery is still required to keep the metal collector members from overheating. A thick copper member was adapted for this purpose. Table V illustrates how the beam power is distributed in the actual tube for one particular frequency and beam current condition. The tube is No. 10. This tube operated best at 3200 to 3300 volts, helix potential. Basic efficiency was 31.2%; overall efficiency was 50.1%; collector efficiency was, therefore, 54.5%.

The predicted basic efficiency of 35% was not achieved. Better collector performance compensated and the goal of 50% overall efficiency was achieved. Exactly how efficient the collector would be at a basic efficiency of 35% cannot be estimated. It is, to be sure, a function of beam energy distribution which is in turn dependent on basic efficiency. If a basic efficiency of 31.2% were accepted as standard, a program to optimize the collector for that particular beam condition should be undertaken.

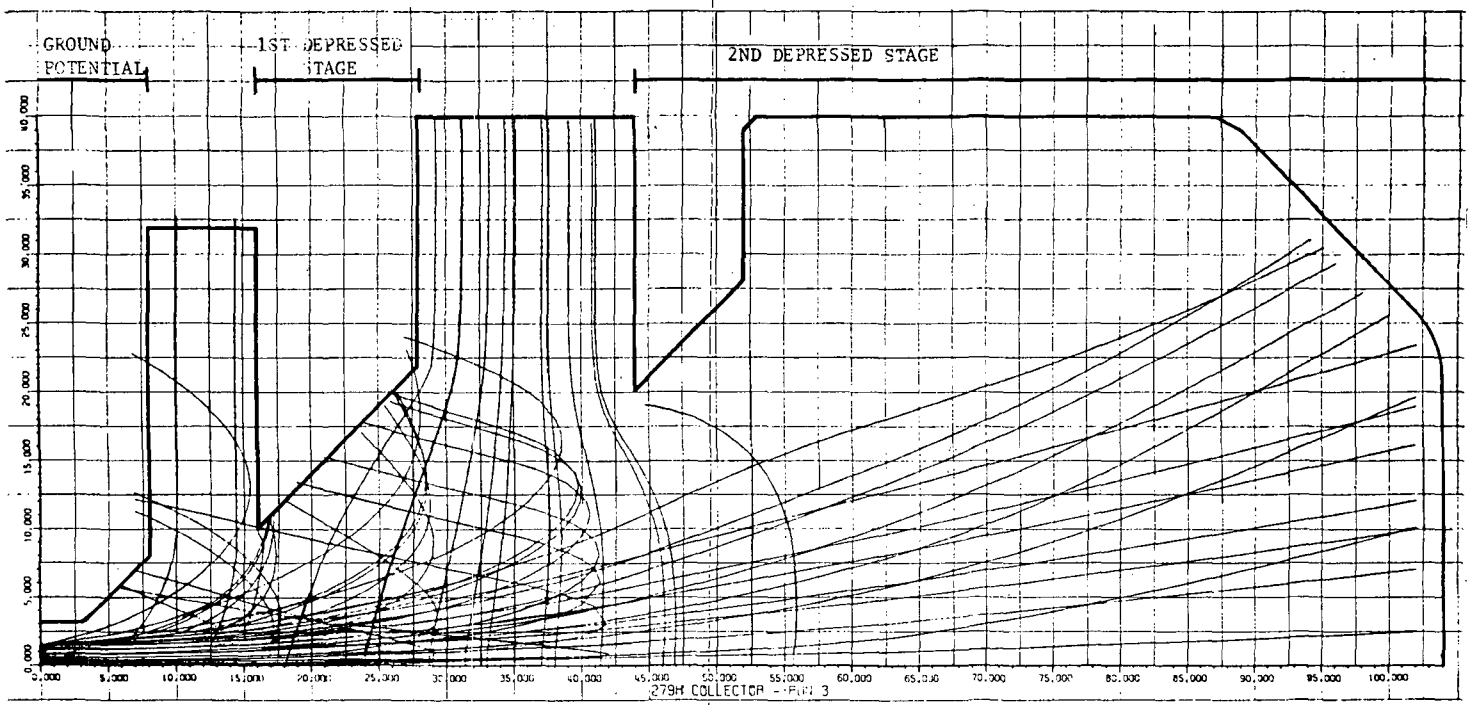

Figure 5 Calculated trajectories and equipotentials in an improved collector design. The spent beam is represented by five energy groups.

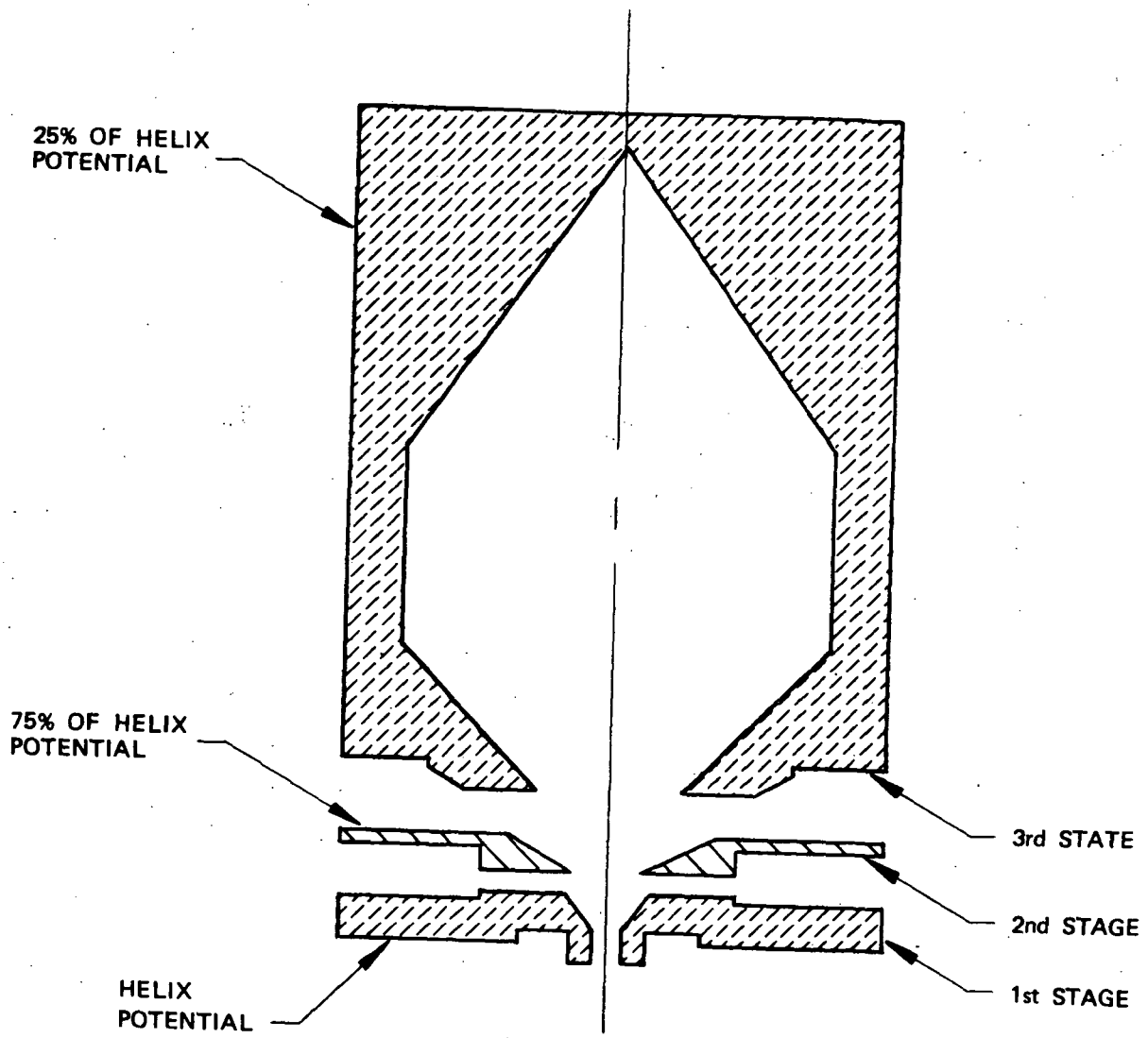

Figure 6 The 279H collector layout.

TABLE V DISTRIBUTION OF BEAM POWER

Collector No. 1 (and helix) potential	3200 volts		
$Ic_1 + Iw$	21.5 mA		
$Ew \times (Ic_1 + Iw)$ (metered helix + collector no. 1 current)		71.0 watts	
(Actual thermal helix + collector no. 1 power)			30 watts
Collector No. 2 potential	2350 volts		
Ic_2	33.7 mA		
$Ec_2 \times Ic_2$ (metered collector no. 2 power)		79.2 watts	
(Actual thermal collector no. 2 power)			34.7 watts
Collector No. 3 potential	820 volts		
Ic_3	28.8 mA		
$Ec_3 \times Ic_3$ (metered collector no. 3 power)		23.6 watts	
(Actual thermal collector no. 3 power)			22 watts
RF output power			87.1 watts
Total Power		173.8 watts	173.8 watts

The PPM Focussing Array

The focussing requirements for this tube were quite standard. One important feature of the tube operation, however, became a very constraining influence on focussing array design. As energy was removed from the beam the magnetic field required to maintain the beam at the required diameter and the plasma wavelength of the beam changed drastically. The focus array could have been designed for worse case conditions or could have been tapered along the axis to match changing beam requirements. The taper may include both reversal period length and field strength alternations. The ultimate choice was to maintain the period for worse case conditions and to vary field strength along the axis as required. Table VI illustrates the effect of energy level in the beam.

TABLE VI FOCUS ARRAY DESIGN CONSIDERATIONS

	Full Energy (DC Beam)	34% Energy Removal (RF Saturation)
Average accelerating voltage	3600 v	2340 v
Lowest accelerating voltage		~1000 v
Beam current	85 mA	85 mA
Beam current density	14.5 amp/cm^2	>14.5 amp/cm^2 (due to beam modulation)
Peak required field	1400 gauss	2000 gauss
Plasma wavelength	.98 inch	.376 inch
Maximum reversal period for stable operation ($\lambda p/L = 2.0$)	.49 inch	.188 inch

Table VI indicates that 1000 volts of energy is a level below which we have estimated an insignificant level of electrons will be found in the spent beam. There is actually no discrete energy distribution cutoff. However, if the interception on the helix at saturation is a small percent of the total beam, then the assumption is adequate. Initial computer analysis indicated that the beam electron energies were largely above 1000 volts. Table VII describes the parameters of the focus array actually used on the operational tubes. Under saturation conditions the interception was 5 to 7 mA. This is without use of the depressed collector and verifies the choice of design parameters since the intercept current is less than 10% of the total beam.

TABLE VII FOCUS ARRAY DESIGN PARAMETERS

Reversal period	.228 inch
Magnet length	.090 inch
Magnet OD	.500 inch
Gap length	.064 inch
Peak field at input	1500 gauss
Peak field at output	2800 gauss
Magnetic material	Samarium Cobalt

It is also interesting to note that depressing the first collector stage to -800 volts causes a modest increase in helix or body current. At -1100 volts the helix current begins to increase sharply, an indication that a large portion of the beam indeed is at an energy equivalent to approximately 1000 volts of acceleration. These data are given in Table VIII.

TABLE VIII BEAM CONTROL CHARACTERISTICS

Total beam	85.0 mA
Body interception (no RF)	1.0 mA
Body interception (full RF, 32% basic efficiency)	7.3 mA
Body interception (full RF, collector no. 3 depressed to -2300 v)	8.0 mA
Body interception (full RF, collector no. 3 depressed, collector no. 2 depressed to -1000 volts)	23.0 mA

The RF Lines, Input and Output

The RF lines are coaxial, both input and output, and are terminated in type TNC connectors. This represents a change from the desired SMA size, a change made in consideration of both power level and electric field strengths involved at the 100 watt level. Because of the application (orbiting vehicle) the ambient pressure will approach a hard vacuum. In this case multipactor can be a serious problem in the small RF lines. TNC connectors offer the advantage of a solid teflon dielectric medium with the mating line between connectors being a stepped surface, thereby lengthening the path length. In addition, the larger size lowers the electric field gradient between center and outer conductor.

The RF line is designed in three parts. The connector is a 50 ohm mechanical transition from a standard TNC jack to the coaxial line which is part of the tube. The vacuum seal window section is an alumina disk, electrically short, and compensated for step discontinuities. The third section is a transformer section used to match the helix to the 50 ohm line. Since the pitch of the helix (and therefore the transmission line impedance of the helix) is different on the two ends, the transformers

are adjusted for the two cases. The adjustment is made by using a smaller center conductor in the output RF line transformer section. A primary transformation is also made on each end of the helix by tapering the pitch of the last three helix turns.

THE MECHANICAL DESIGN FEATURES

The 279H mechanical design was centered on the requirement of generation of power at high basic efficiency, and efficient rejection of waste heat because of the large amount of waste heat in a 100-watt level tube.

The RF Circuit Thermal and Electrical Considerations

The RF circuit is a tungsten tape, supported by anisotropic pyrolytic boron nitride (APBN). The circuit is held together by radial compression forces. The loading is accomplished by inserting the circuit into a body which has temporarily been expanded by increasing its temperature. After the body is cooled the reduced diameter loads the circuit properly. The temporary expansion used in this design is .001 inch, accomplished by heating the body to approximately 700°C. The .001-inch expansion suggests the precision with which the circuit must be assembled. Its diameter must be correct to a tolerance of approximately $\pm$.0002 inch. To attain this precision the tungsten tape is OD ground after winding and the APBN rods are trimmed as required for each individual helix used. Figure 7 shows a cross section of the circuit and points out areas of concern in manufacture.

The use of APBN rods contributes to both electrical and thermal performance. Its relatively low dialectic constant yields a high interaction impedance which in turn contributes to high basic efficiency. The good thermal properties permit the dissipation of power without significant rise of helix temperature. The cross section shown in Figure 7 yields a thermal impedance of 0.7°C/watt for the power generating section of the helix (the last half inch). The expected temperature rise in that section would then be 21°C based on the 30 watts of thermal loading at saturation indicated in Table V. This is, of course, only the rise in temperature from body to helix. Additional thermal impedances contribute to raise the helix to its actual operating temperature.

The 30 watts of power, having been transformed to the body, must be removed by conduction to the mounting base. This is accomplished by the use of copper thermal shunts installed between each pair of polepieces at the output end of the tube. Figure 8 illustrates their use. Since the shunt paths are radial the magnets have to be slotted to permit their passage. The removal of magnet material lowers the capability to produce peak field on the axis, but there is adequate margin in the design for this effect.

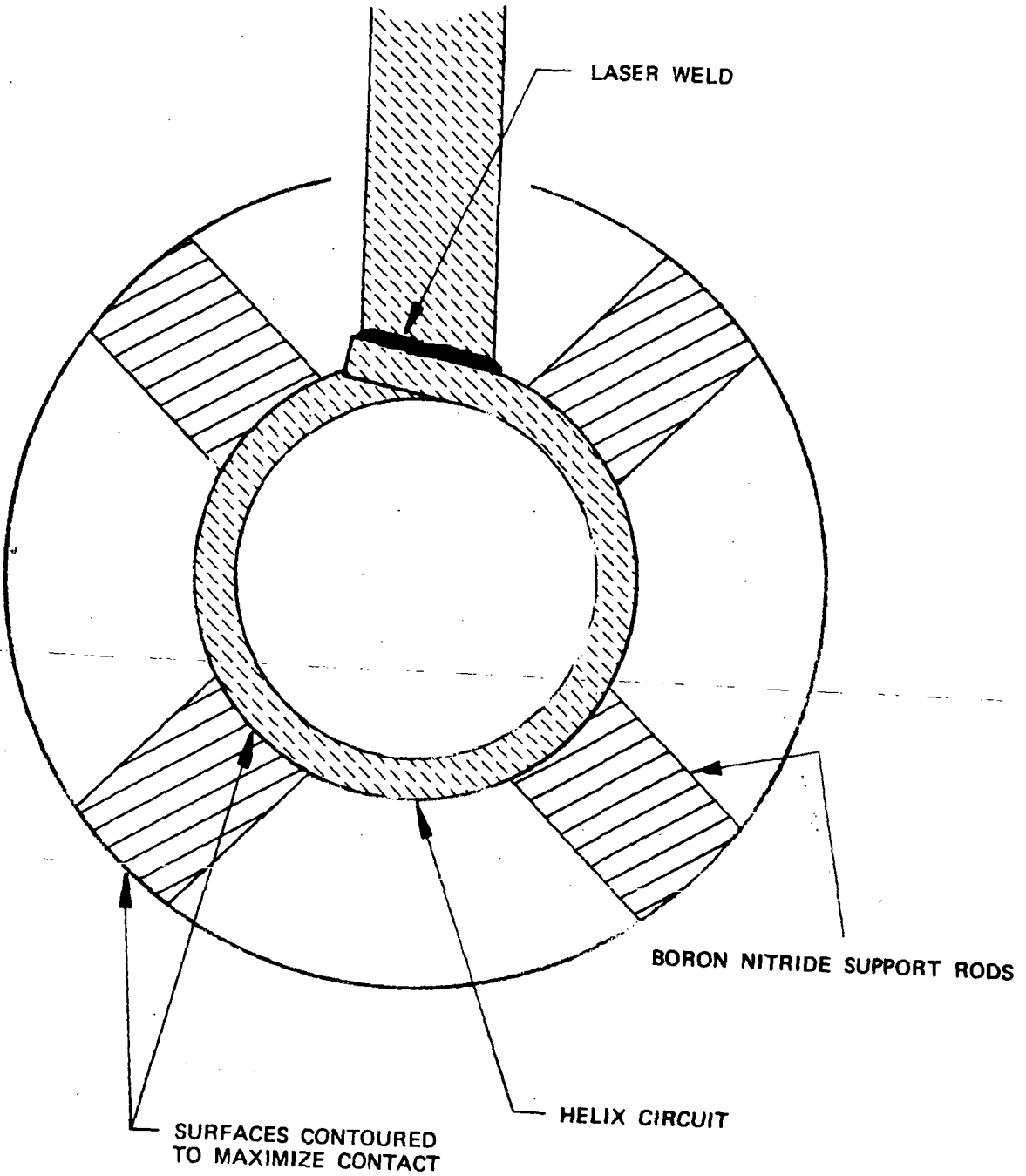

Figure 7 The 279H circuit assembly.

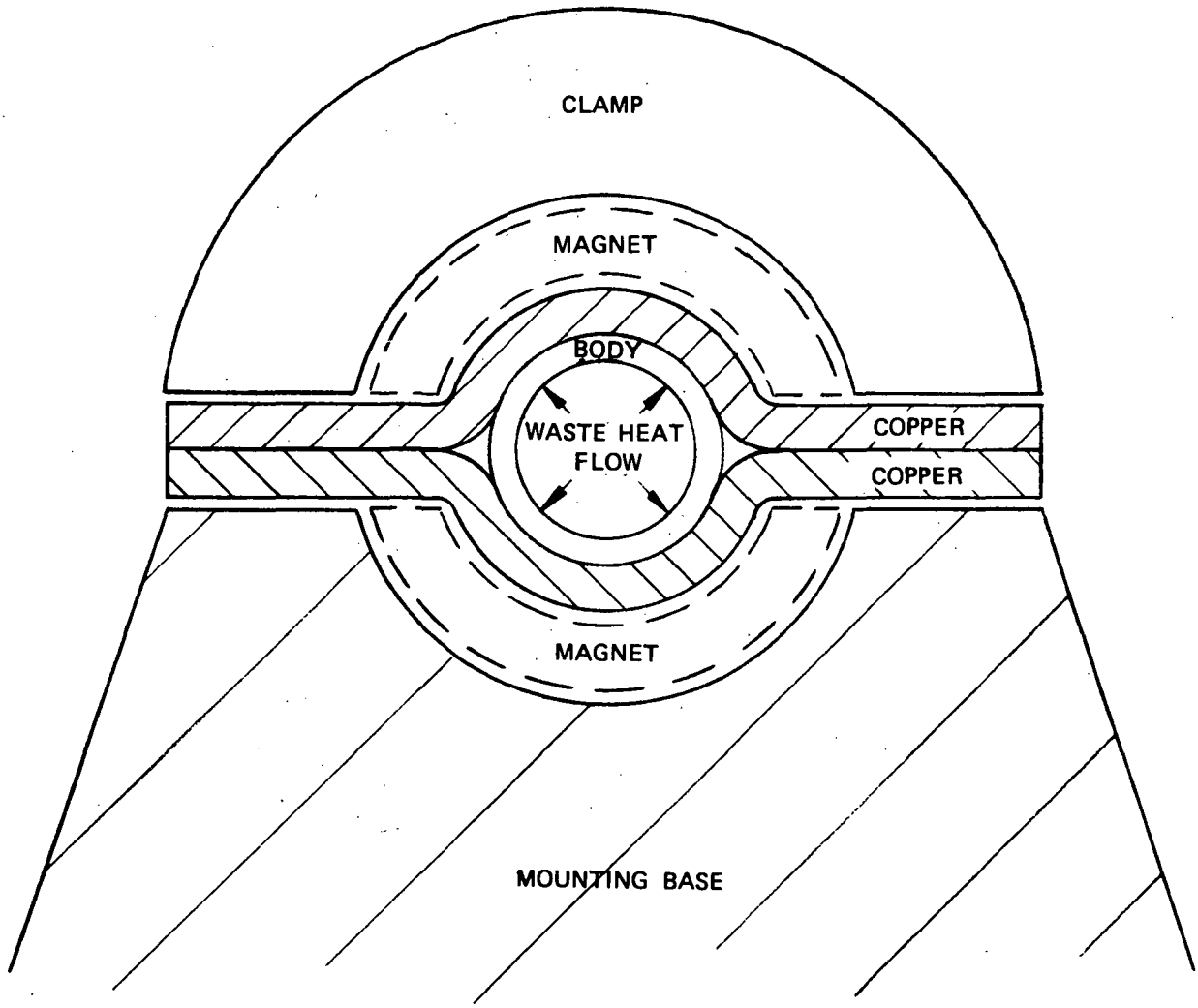

Figure 8 Removal of waste heat with thermal shunts.

Measurements indicate that a temperature rise from mounting base to the circuit body of 15°C exists when 30 watts of power is dissipated at the output end of the circuit. The helix temperature rise above the mounting base temperature is, therefore, 36°C. The mounting base temperature will be approximately 10°C above the external heat sink temperature, controlled by the use of the system. The heat sink temperature is allowed to reach 70°C under worst case conditions. The absolute helix temperature should, therefore, be 70°C plus the total rise of 46°C or 116°C maximum. This is a minimum number assuming perfect fits at all interfaces and the actual temperature is probably slightly higher. The fact, however, that power fade is less than 0.1 dB indicates that helix temperature is well controlled.

The Collector Design for Power Dissipation and Mechanical Integrity

The two isolated collector stages which must be provided are a conflict in design in two ways. First, the isolation reduces the ability to reject heat while being required to enhance efficiency. A second effect centers on the redistribution of interception current with changes in RF drive. The no drive condition causes almost 100% of the beam current to impact on Collector No. 3. The power dissipation is 100 watts in this case. The size of Collector No. 3 must, therefore, be selected in consideration of this amount of dissipation power. Since Collector No. 3 is furthest from the helix it is supported through two ceramic isolators. At full drive its thermal load drops to 22 watts and the massive collector is no longer required while loading on Collector No. 2 increases. The collector design requires that these varying conditions be met including heat rejection and mechanical integrity under shock, vibration, and acceleration.

The need for heat rejection by conduction through ceramic isolators is eliminated by the use of a radial heat pipe cooling apparatus. This device is described in detail in another section of this report.

The system for mechanical support is not complete. A tentative solution, used in engineering model units, consists of ceramic support rods supporting the collector by radial force much in the manner that the helix is supported. The rods in turn are held in place by the same cylinder which acts as the condenser surface for the radial heat pipe. Since the cylinder is fairly thin, inadequate force is applied to sufficiently restrain the collector in transverse vibration modes. Improvements in this mounting system are planned for future units.

The 279H Tube Package

A single mounting base is used to serve several purposes. First, the tube body is held in place and a sink for heat transferred through the copper heat shunts is provided at the output end of the circuit. Also, mounting surfaces are provided to tie down the RF connector

adaptors, so that external stresses on the TNC connectors are not transmitted to the tube itself. A support for the collector heat pipe is provided and this support also becomes a conduction path for heat rejected from the heat pipe condenser surface.

In order to insulate the electron gun, a potting mold is provided which is retained as an EMI shield after the gun is encapsulated.

Finally the mounting base also supports a set of six axial heat pipes which drain heat from the collector end of the tube and reject it along the tube body. This heat pipe system serves to lower the waste heat density at the interface between the tube and TWTA base plate.

A picture of the tube mounted on its base with axial heat pipes in place is shown in Figure 9. The final package with RF hardware in place and with gun shield installed is shown in Figure 10. In this picture the tube is mounted on its heat pipe base plate. The heat pipe channels can be seen along the edge of the base plate.

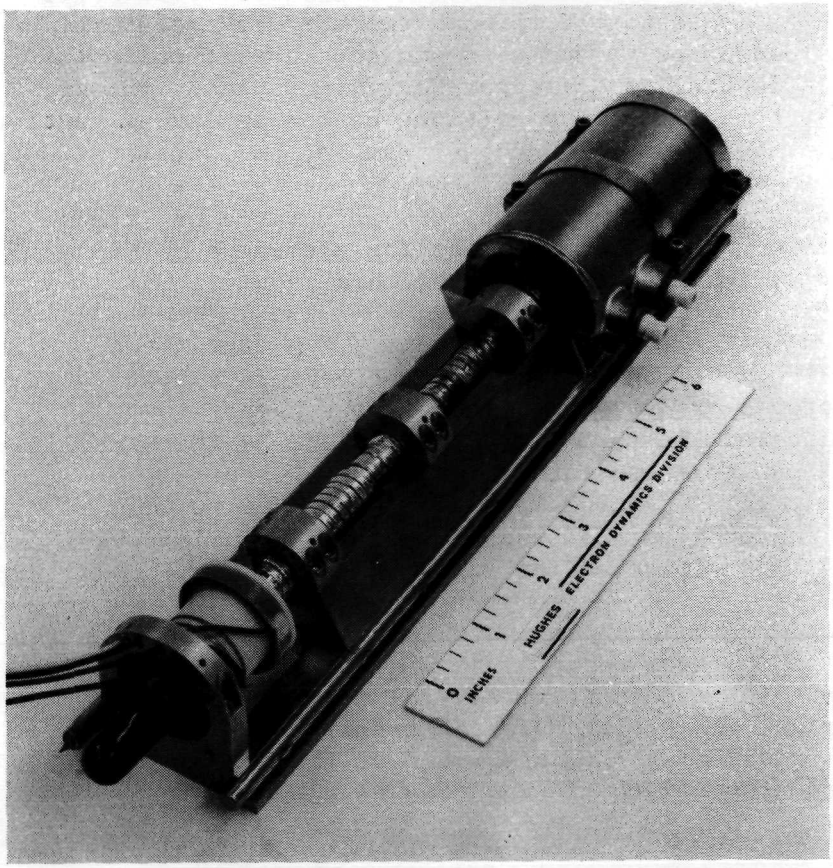

Figure 9

The 279H prepared for finishing operations.

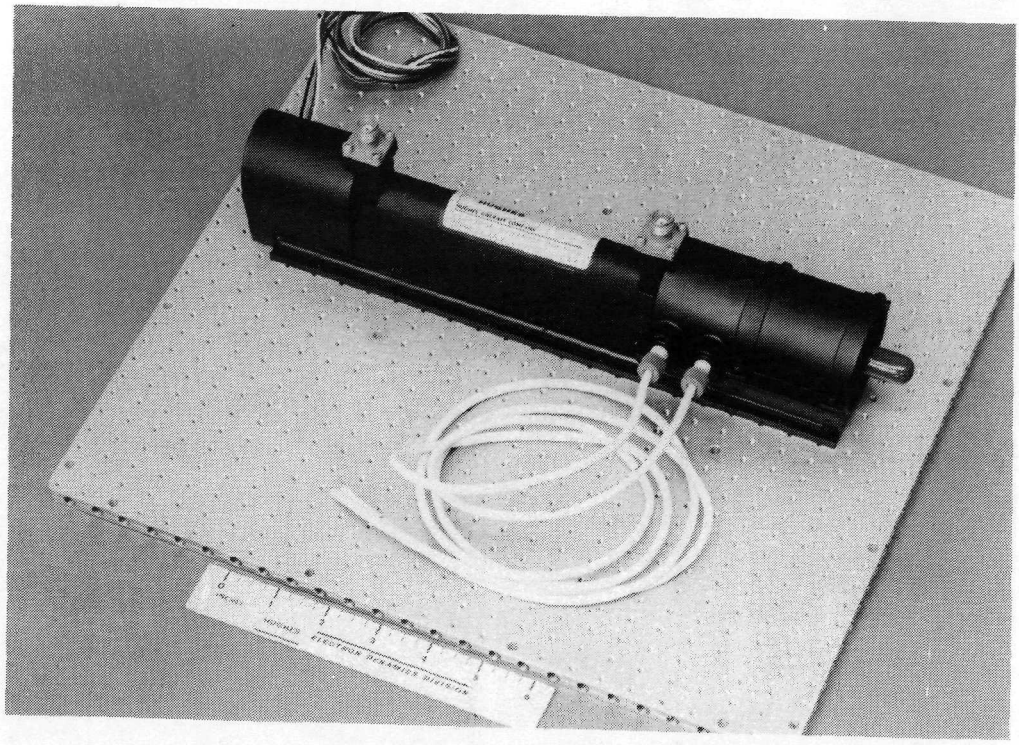

Figure 10 The 279H, packaged and mounted for power supply integration.

PERFORMANCE OF THE 279H TWT

The development program was terminated after evaluating ten tubes. Eight of these were synchronized at 3300 volts, two at 3650 volts. The higher voltage tube differed in performance mainly in that more power was consumed and more power was generated.

The data included in this section does not describe the best or worst performance. It is typical of the majority of tubes, and in addition two figures serve to illustrate the major difference between the 3300 volt and the 3650 volt designs. The importance of the data is that it illustrates the major sensitivities of the tube. Independent variables were considered to be power supply voltages, RF drive level and frequency. Dependent variables examined were output power, gain, efficiency, phase length, intermodulation, gain ripple, and phase ripple.

Figures 11 and 12 display power, gain and efficiency versus frequency for the two different voltage designs. The tube design is presently centered low. Over 500 MHz, the rated bandwidth, the efficiency is 43% minimum for either design. Individual tubes have exhibited 50% efficiency at single frequency points and power output above 100 watts. Further work could raise the efficiency 3 to 4 percentage points. This

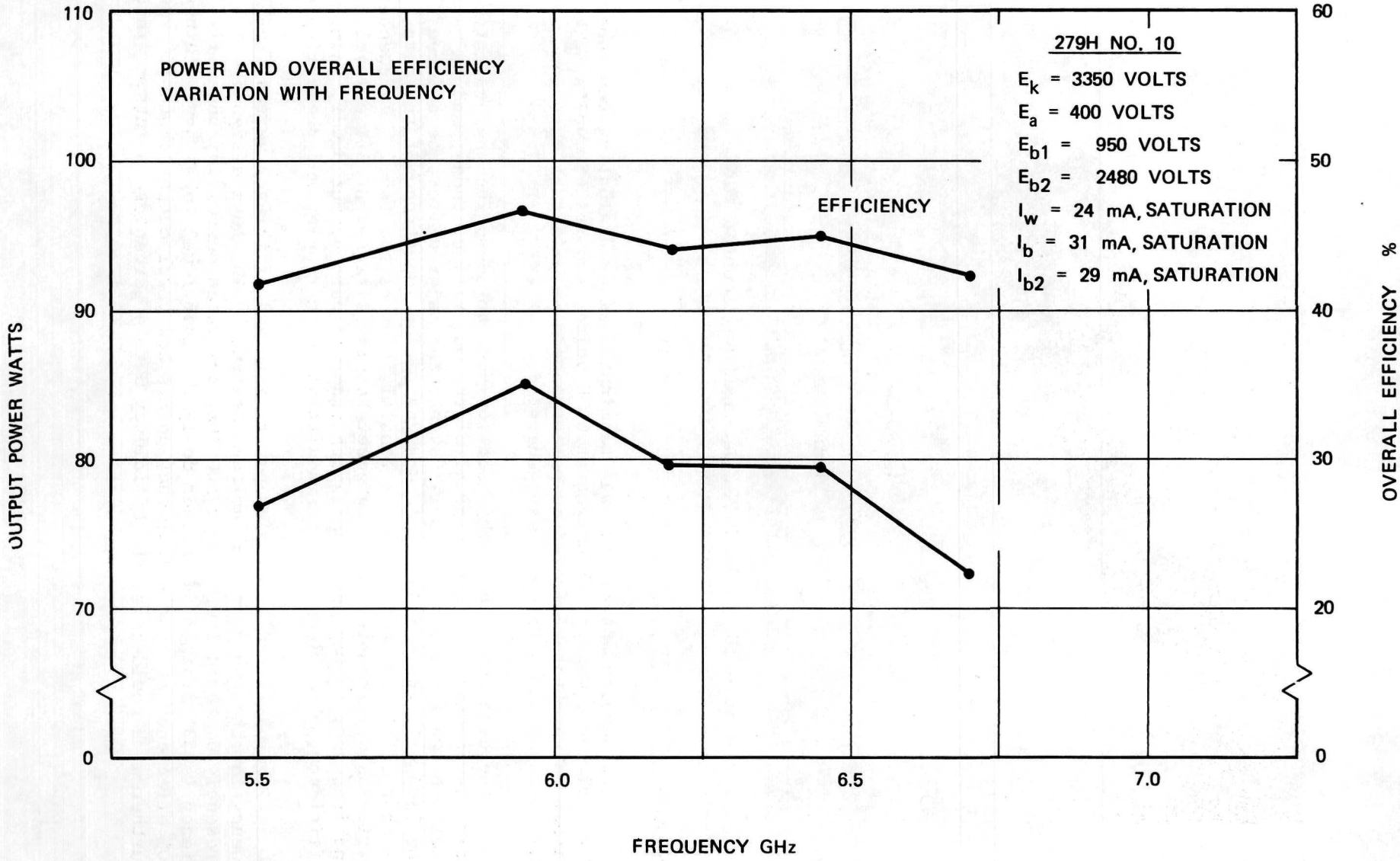

Figure 11 Power and efficiency versus frequency 279H No. 10.

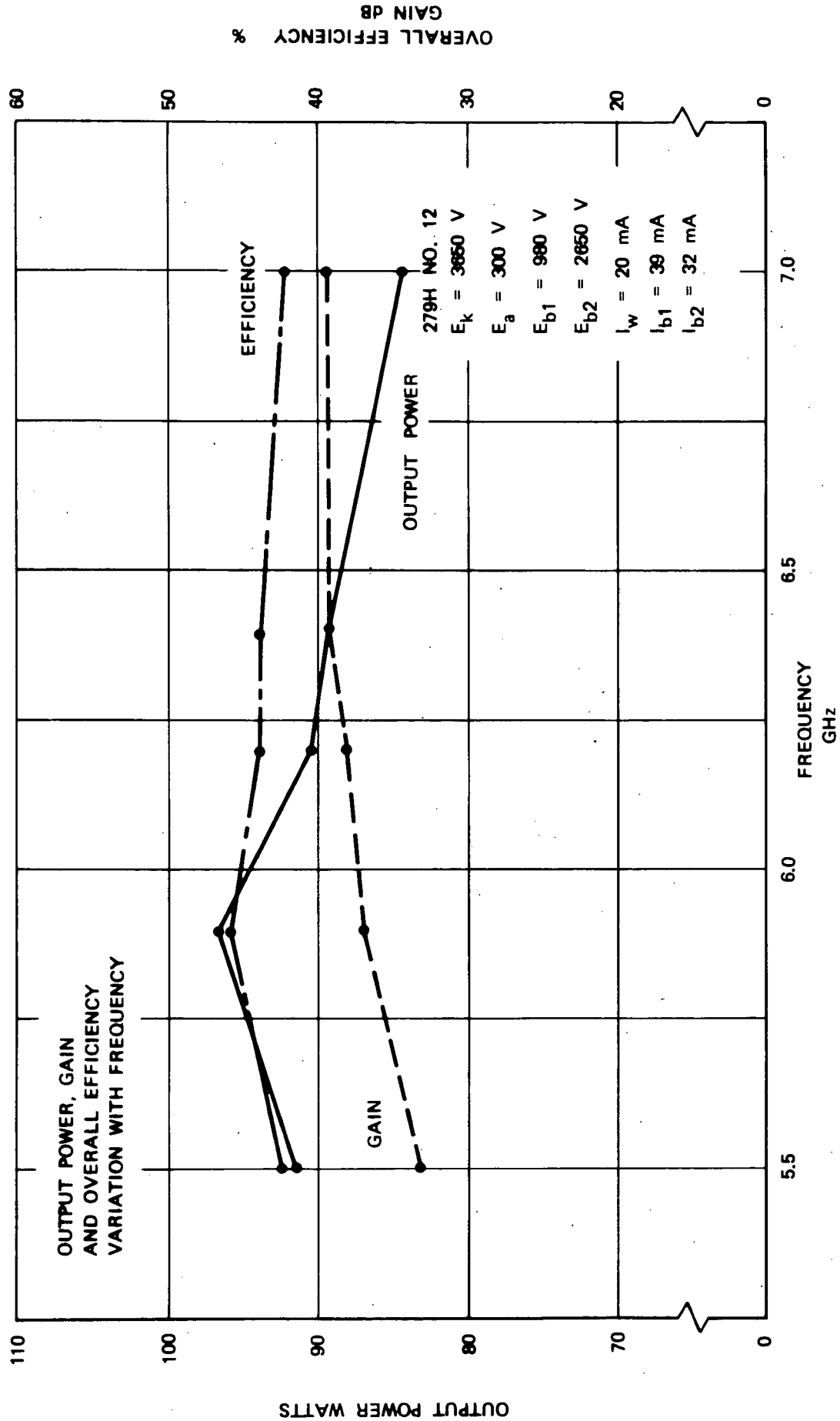

Figure 12 Power, efficiency, and gain versus frequency 279H No. 12.

statement is based on data which shows that the output section should be lengthened for better performance. The program minimum goals can, however, be met with the present performance. Gain variation across 50 MHz is approximately 2 dB. This is within requirements and is not expected to be improved because of the gain slope inherent in the lower γa design.

Figures 13 and 14 illustrate statements made earlier in a discussion of the design. The tube, No. 9, operates at best efficiency and at highest small signal gain at or near 3300 volts. The tube is, therefore, not overvoltaged in the input or driver section as is common to some high voltage designs. Note also in these figures that by being at the peak of the two curves a precise voltage for neither gain level nor efficiency is required.

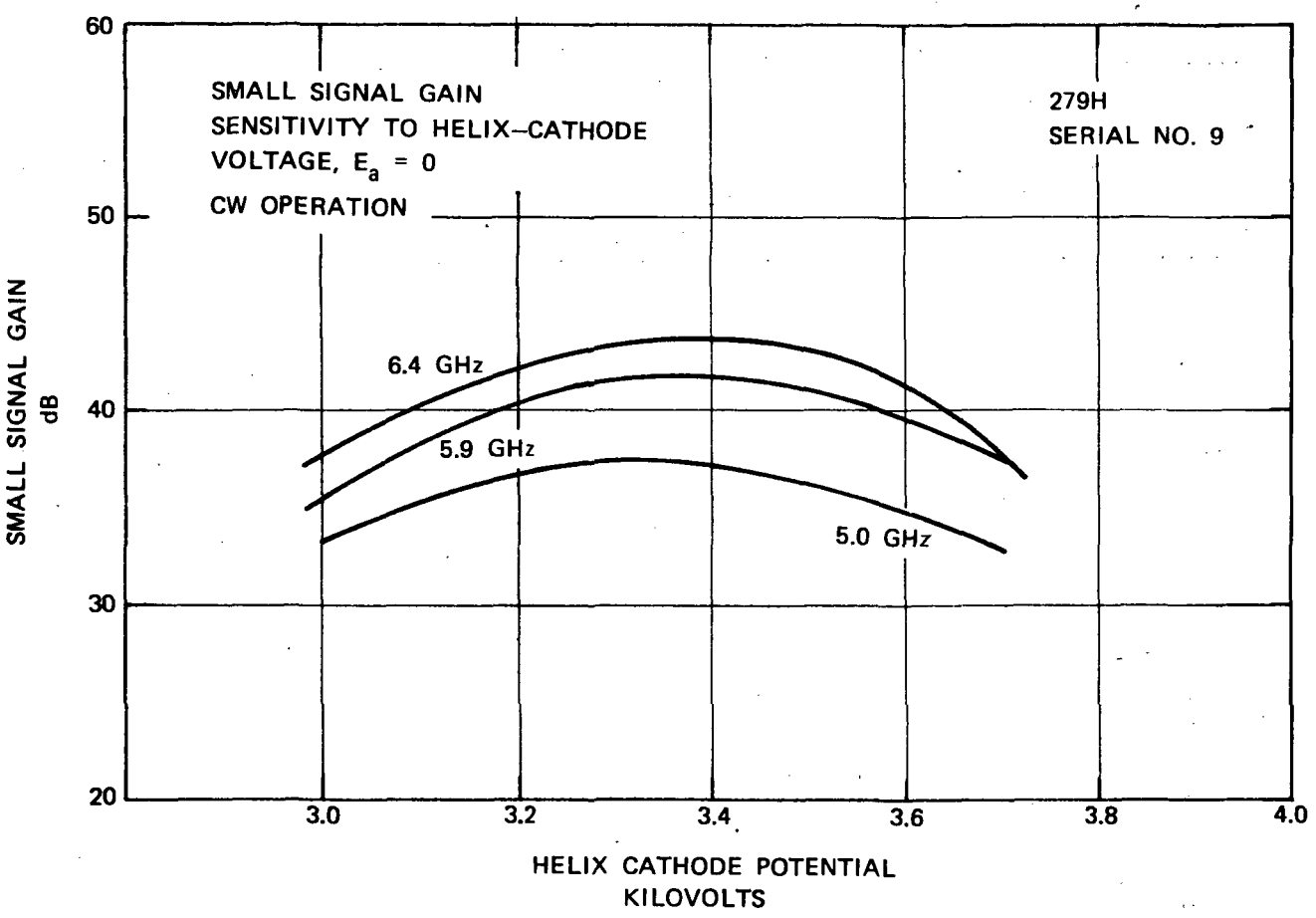

Figure 13 Small signal gain versus helix potential, 279H No. 9.

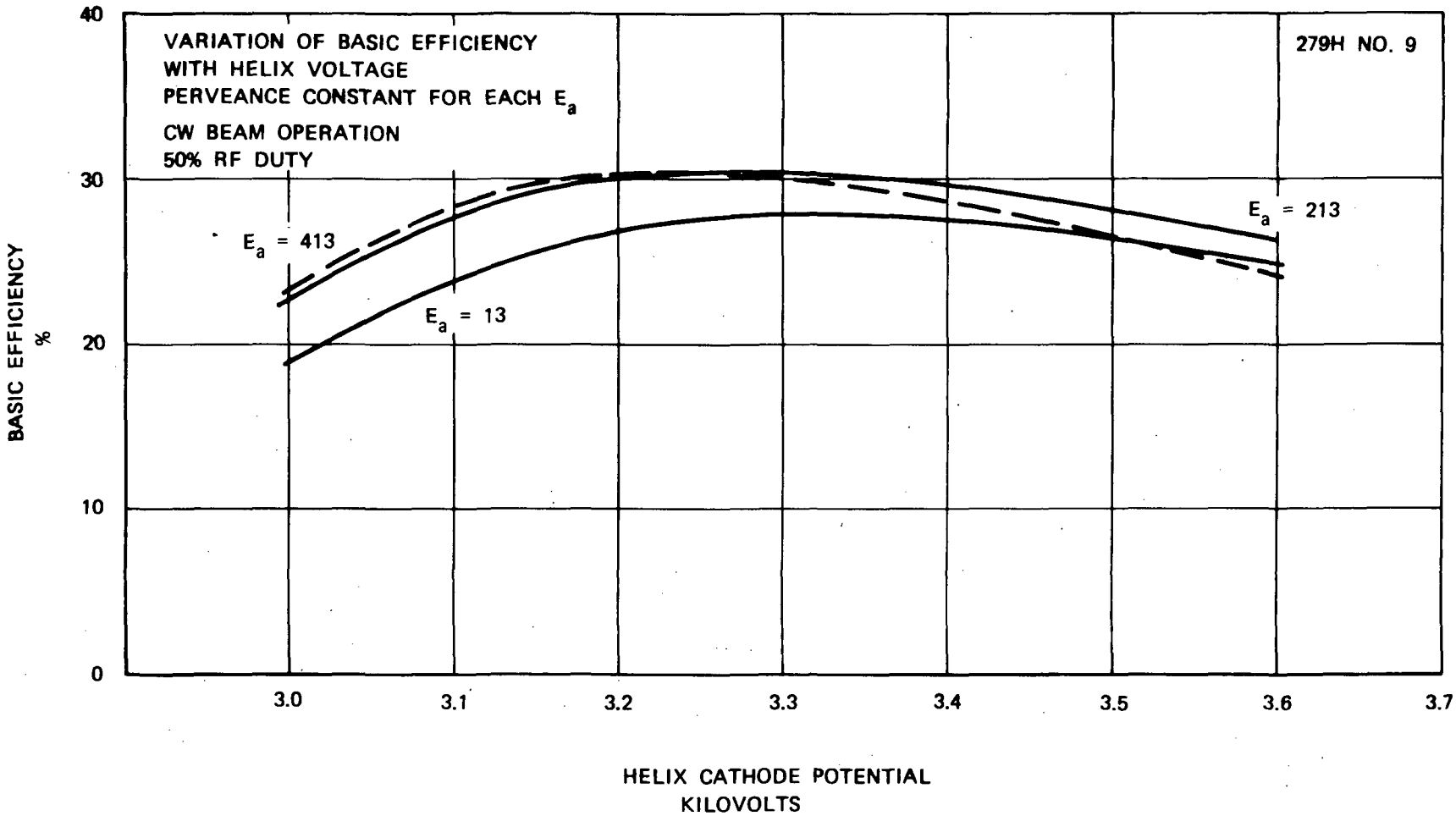

Figure 14 Basic efficiency versus helix potential, 279H No. 9.

Output power and phase length sensitivity is shown in Figures 15, 16, and 17. Anode voltage effect on output power is based on changes in beam power. Phase length effects are second order in that they are due to efficiency changes caused by changes in beam current. In a similar fashion the heater voltage effects the beam power, and, therefore, output power and phase length. This is shown in Figure 16. Phase length variation with helix potential is important in that it is usually the variable causing the most phase ripple in the TWTA. The data in Figure 17 indicates a slope of 0.8^{o}/volt. Output power, for fixed drive levels, has a slope of only 0.002 dB/volt indicating that the usual levels of helix voltage ripple would not cause significant AM modulation. This again is due to being able to operate at the gain/voltage peak. In this tube the PM noise specification, coupled with the given helix voltage phase sensitivity, dictates the allowable helix voltage ripple.

Intermodulation, as affected by drive level, for three different helix potentials is shown in Figures 18, 19, and 20. Note that although efficiency does not increase at higher helix potentials the typical degradation of intermodulation levels does occur. As the helix voltage is increased, a discontinuity appears at a drive level of -20 dB, relative to saturation drive. The discontinuity has the effect of reducing carrier to IM ratios with respect to the more linear curves illustrated in Figure 18 for the lower helix voltage.

The basic problem is seen in Figures 21, 22, and 23 which are transfer curves, output power as a function of driver power. At the lower helix voltage, Figure 21, the curve is quite normal. As the voltage is raised the curves take the characteristic overvoltage shape at -20 dB drive level. An inflection point occurs in the curve and the slope rises to a value greater than one.

Figures 24, 25, and 26 illustrate the phase length change with drive level. These curves again show odd effects below saturation. Again the highest voltage, Figure 26, shows the largest sensitivity to drive level. In this case the total phase length change with drive level is approximately 50^{o} (83.9 mA beam current). At the lower voltage, Figure 24, the total phase change is only 30^{o}. Consequently the AM/PM conversion (the slope of the phase length, drive level curve) is significantly higher at the higher voltage. The two figures are 3.0^{o}/dB and 1.5^{o}/dB for the highest and lowest voltage cases. Both figures are wll within acceptable limits for communication service, but considering that no improvement in efficiency is achieved by the use of the higher voltage the higher level of AM/PM conversion need not be tolerated.

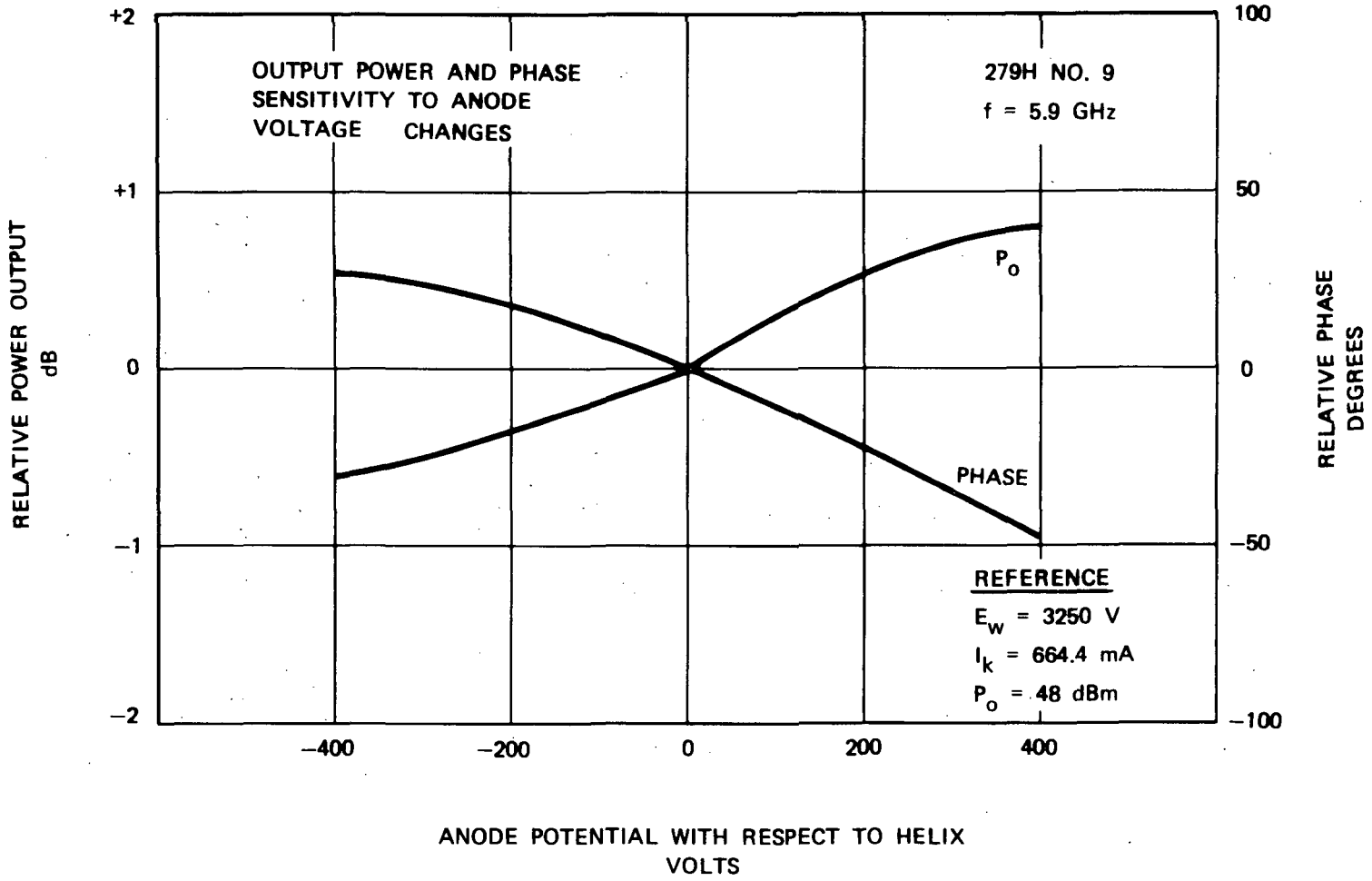

Figure 15 Phase length and output power, sensitivity to anode potential.

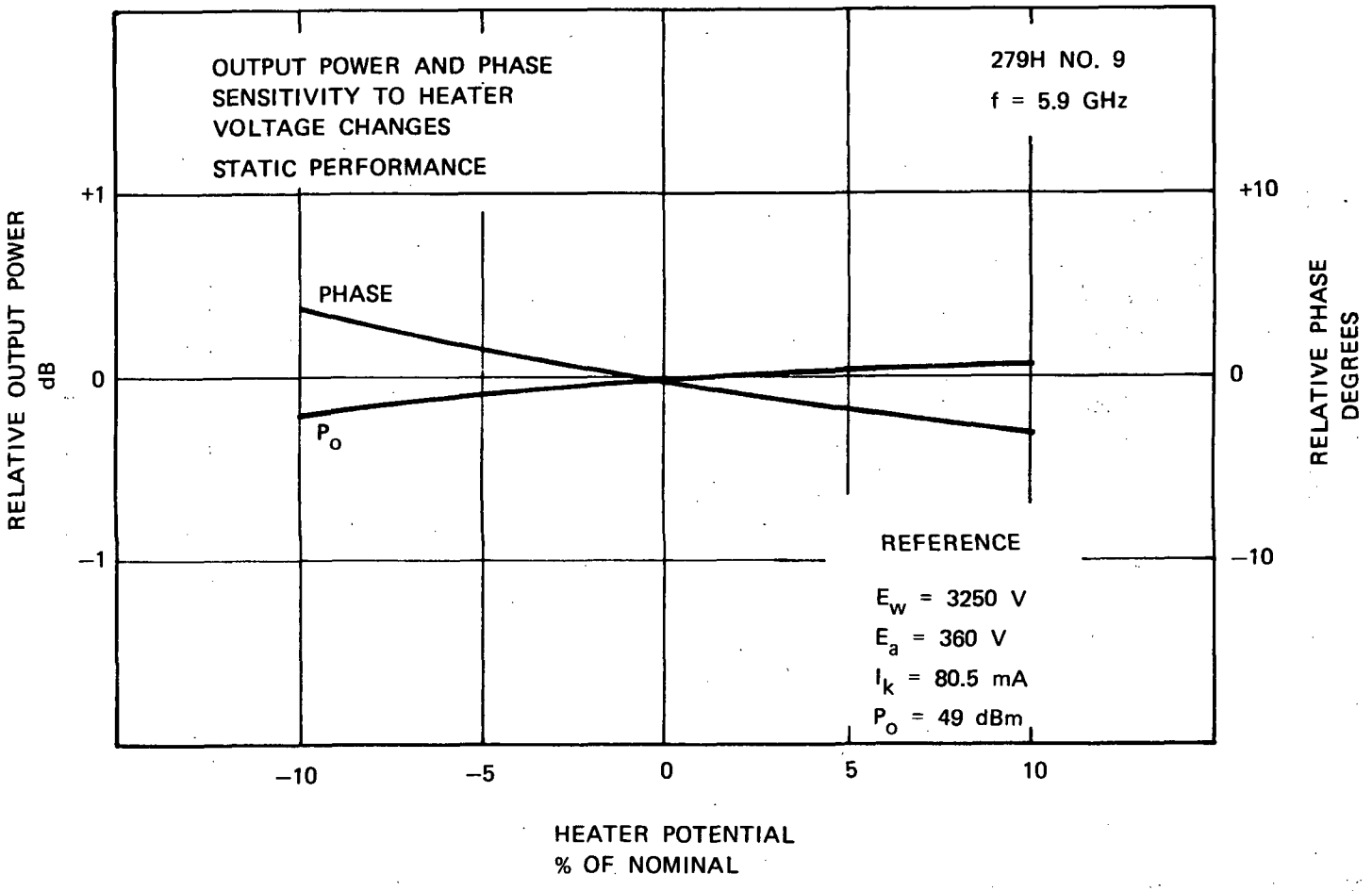

Figure 16 Phase length and output power, sensitivity to heater potential.

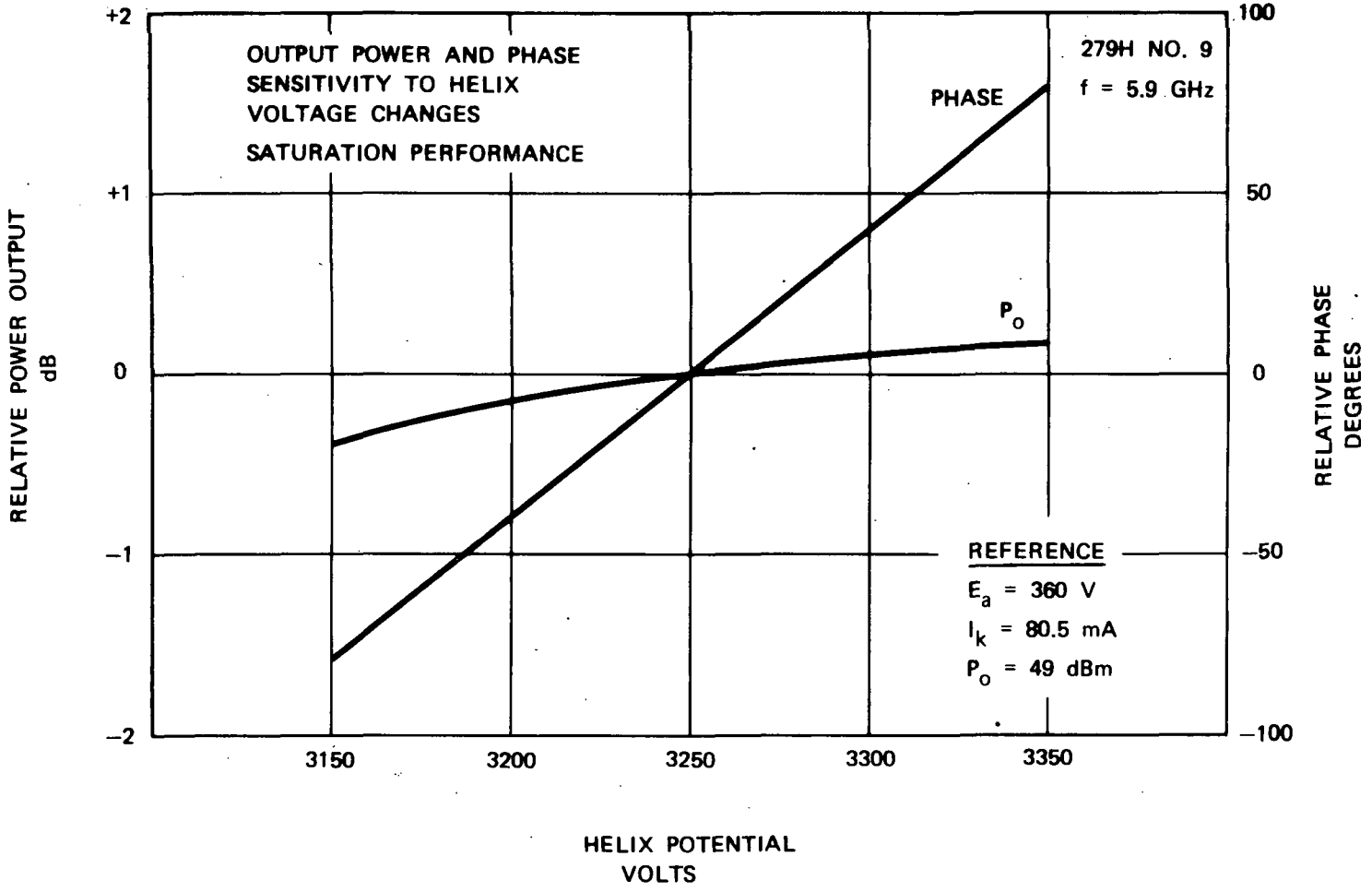

Figure 17 Phase length and output power, sensitivity to helix potential.

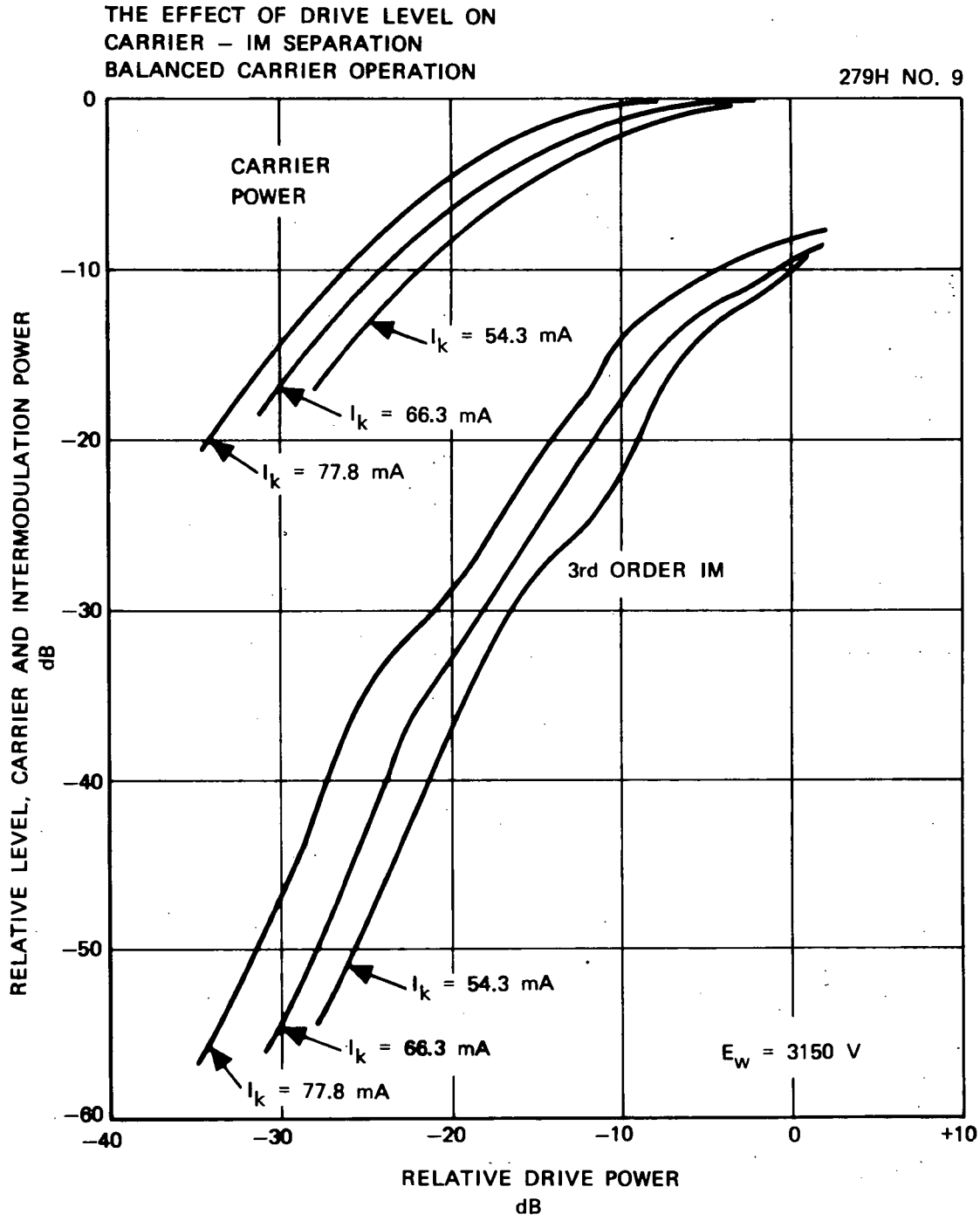

Figure 18 Intermodulation levels for balanced two carrier operation, E_w = 3150 V.

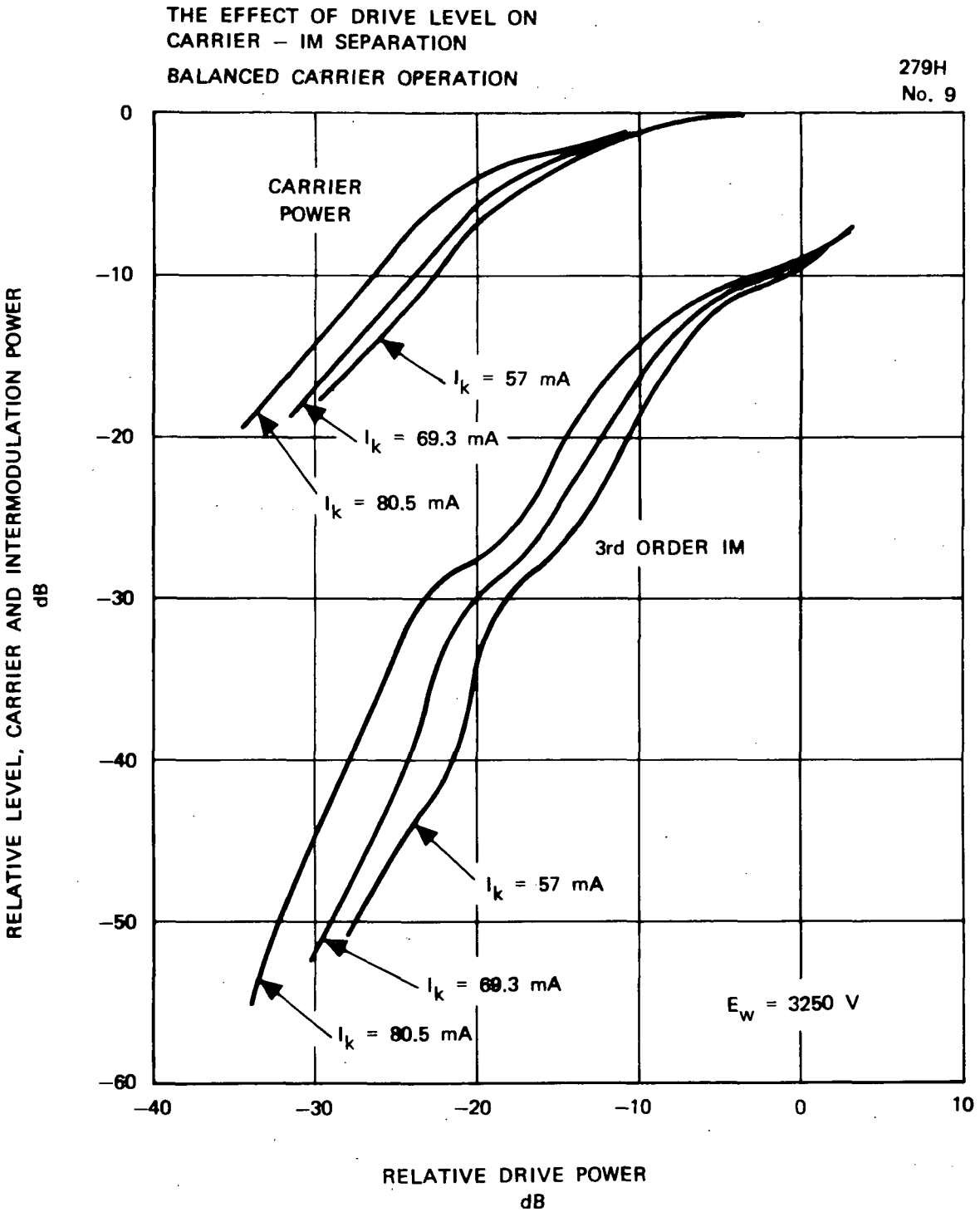

Figure 19 Intermodulation levels for balanced two carrier operation, E_w = 3250 V.

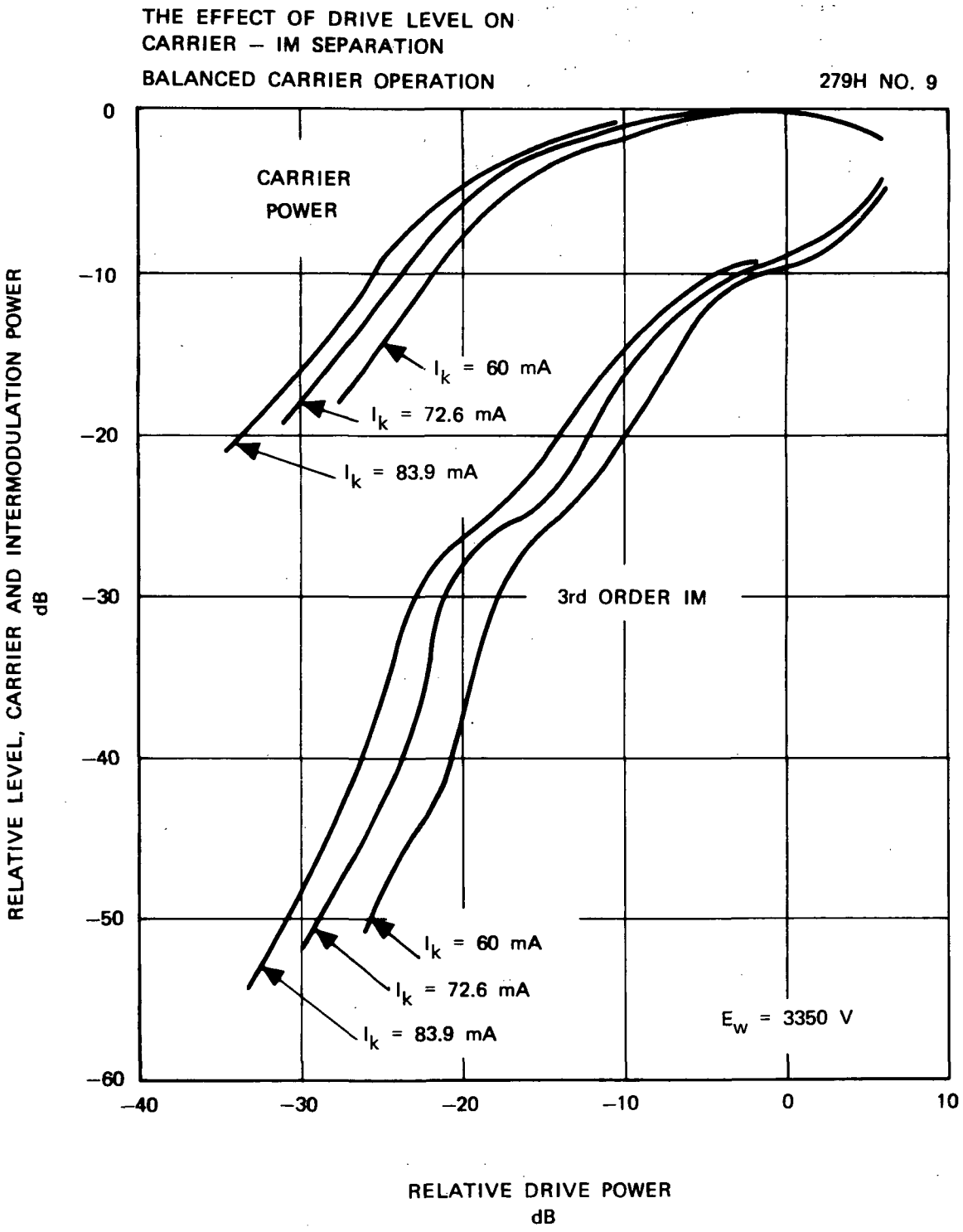

Figure 20 Intermodulation levels for balanced two carrier operation, E_w = 3350.V.

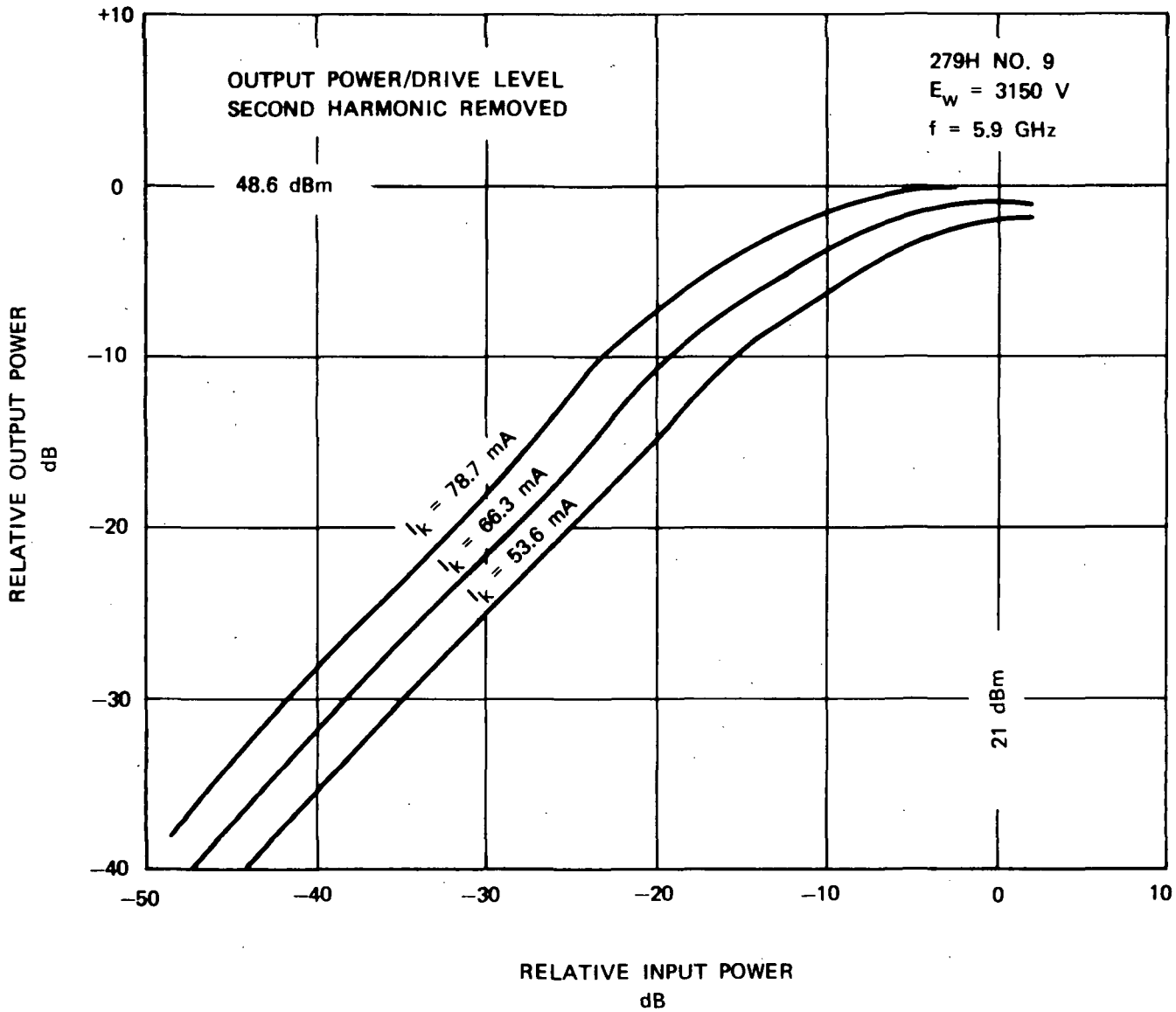

Figure 21 Output power variation with drive level, E_w = 3150 V.

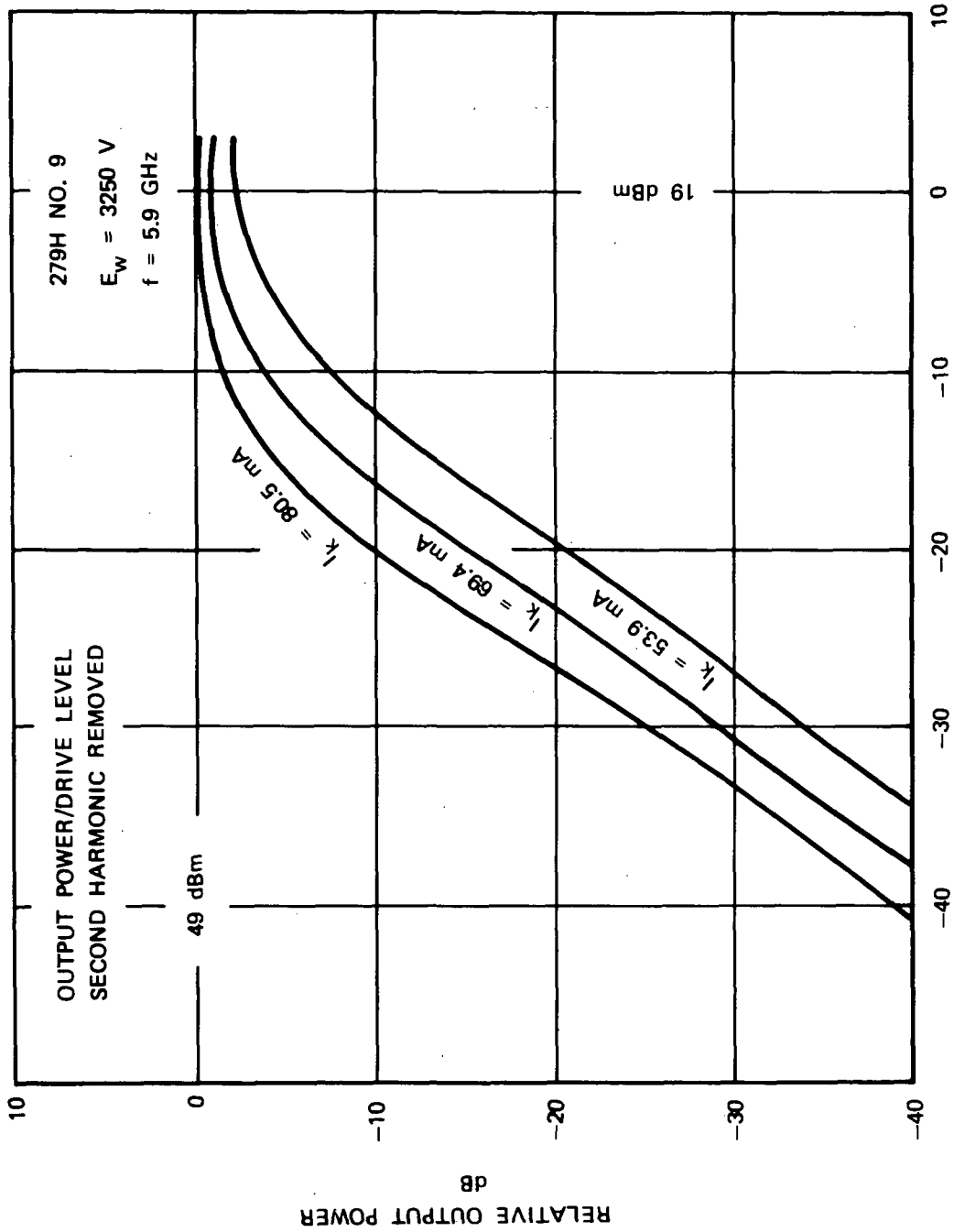

Figure 22 Output power variation with drive level, E_w = 3250 V.

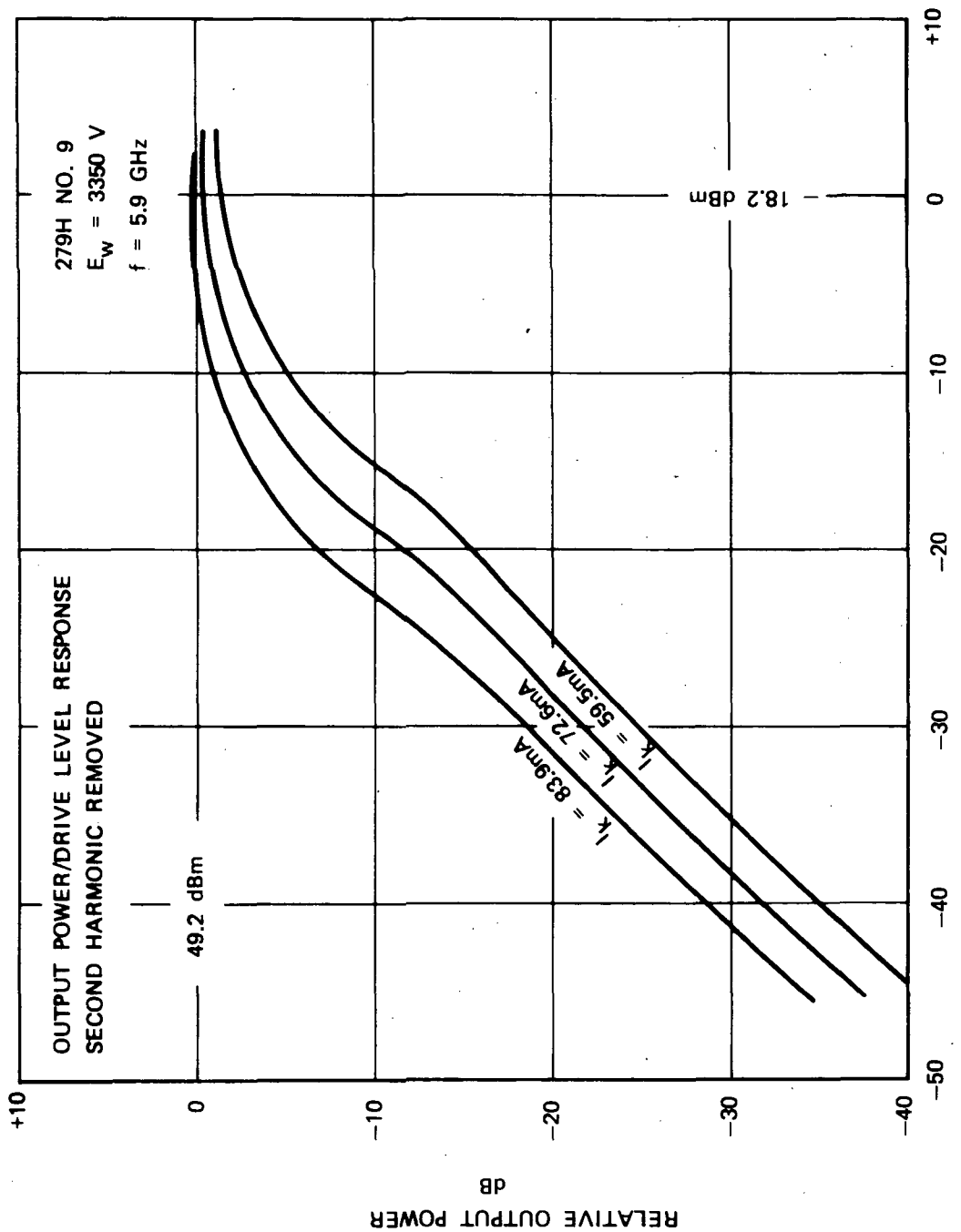

Figure 23 Output power variation with drive level, E_w = 3350 V.

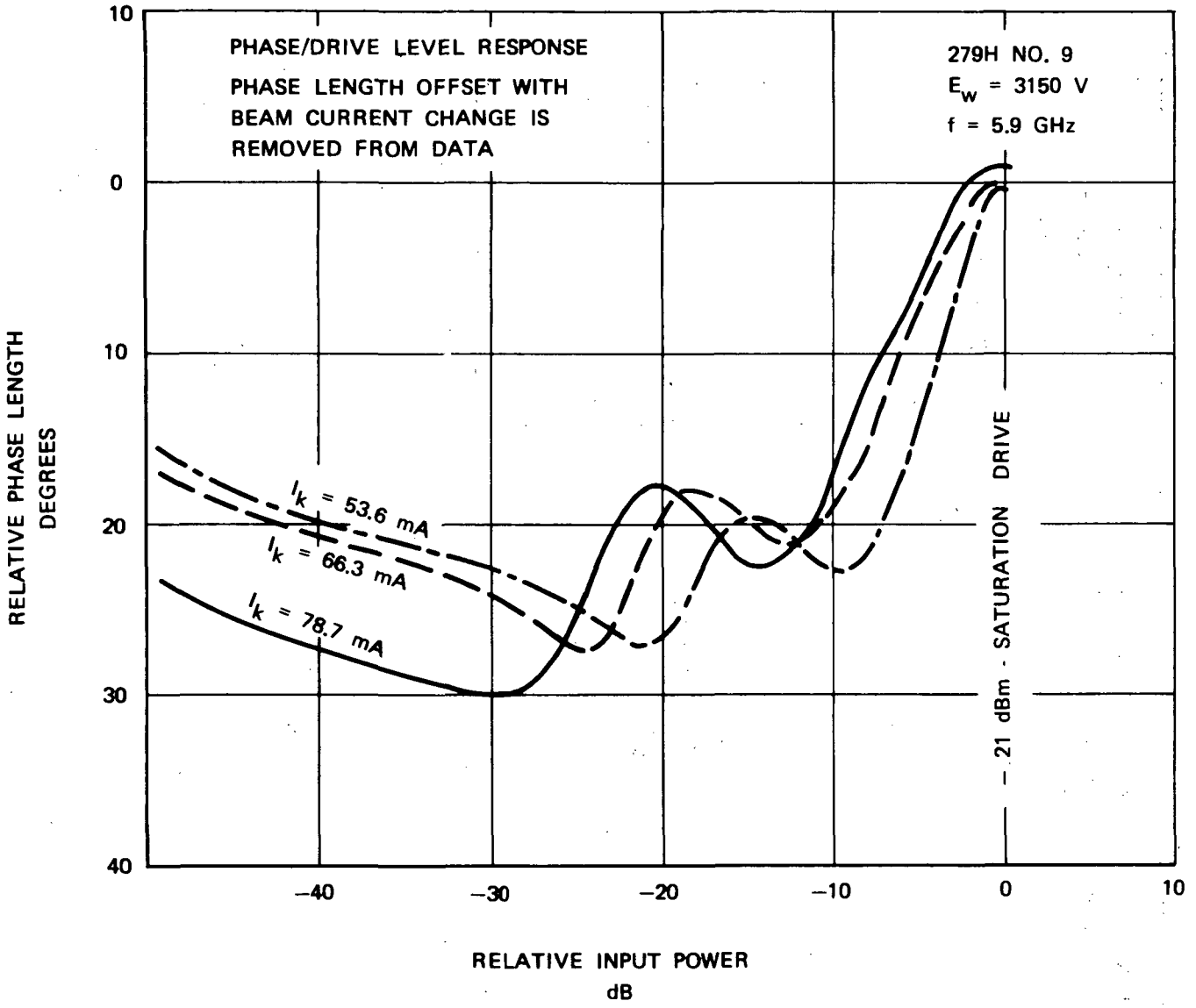

Figure 24 Phase length variation with drive level, E_w = 3150 V.

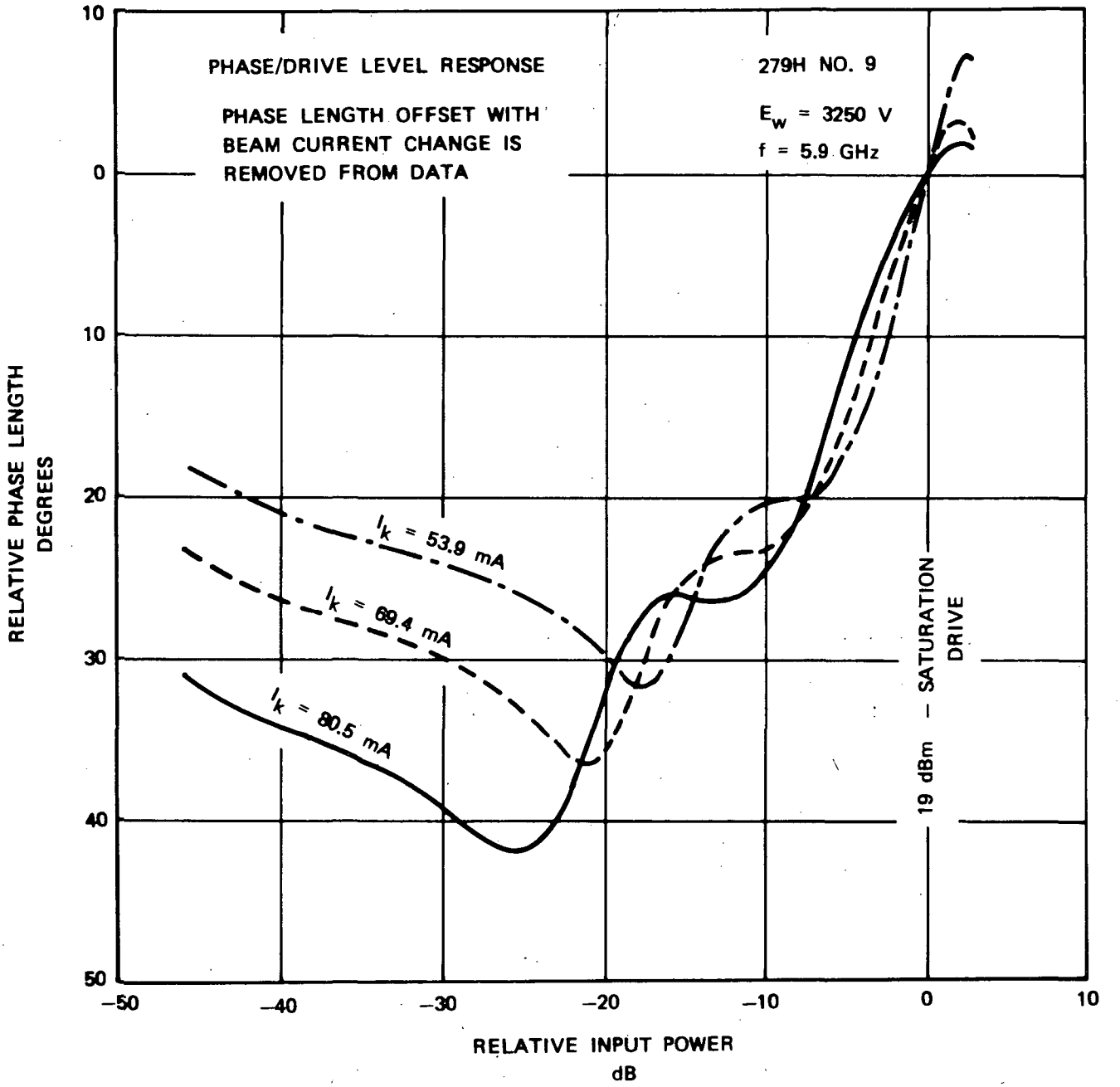

Figure 25 Phase length variationwwith drive level, E_w = 3250 V.

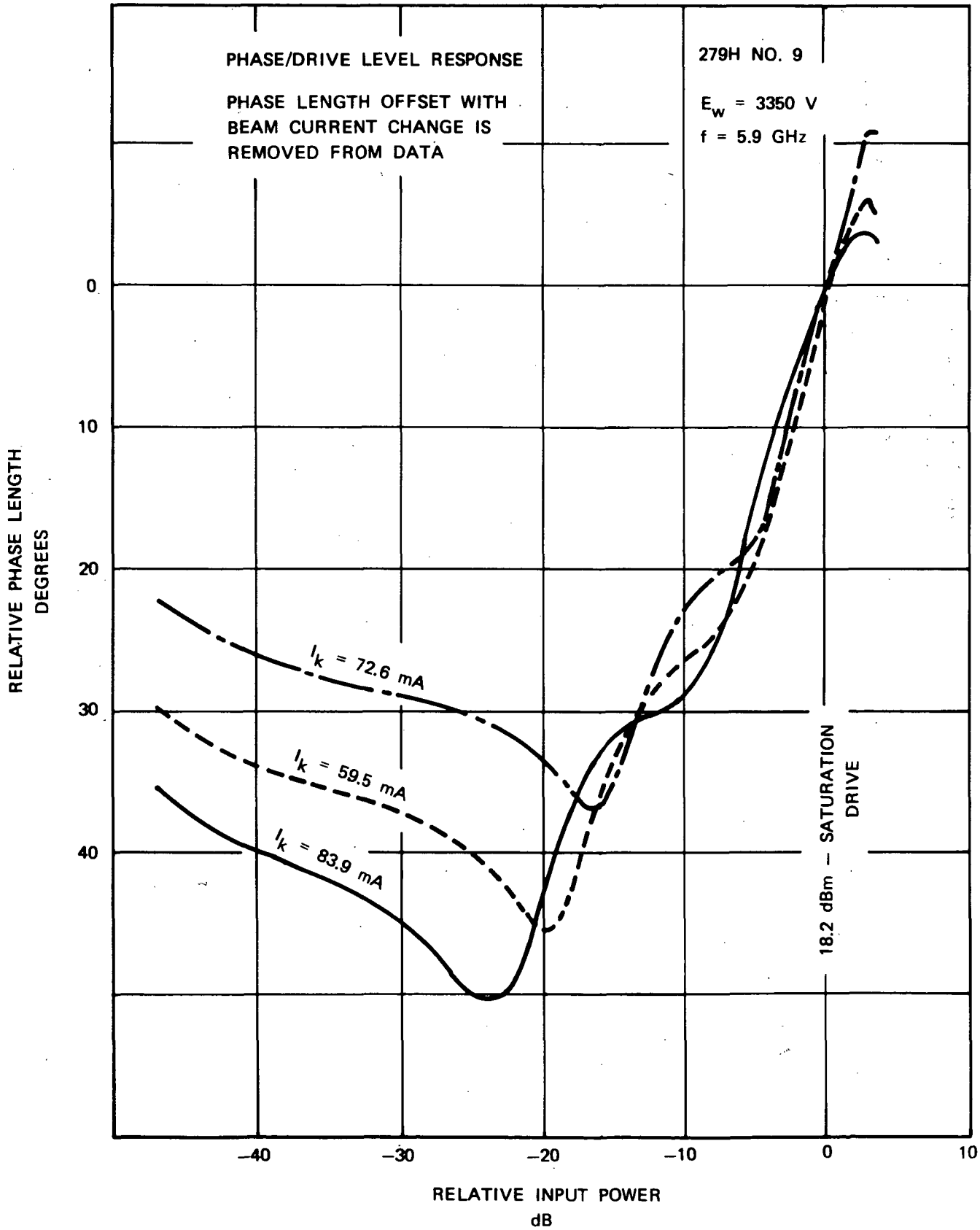

Figure 26 Phase length variation with drive level, E_w = 3350 V.

Gain and phase ripple are two additional factors which determine distortion levels. They are both related to reflections of signals within the tube, magnified by the gain of the tube, therefore are a measure of the construction of the tube as well as an indication of the usefulness of the tube in a particular communication system. Figure 27 is a plot, small signal, of the phase ripple with frequency. Note that the calibration lines are not constant with frequency. The phase ripple should be read, therefore, as a departure from the shape of the calibration curve. When this is down the true phase ripple is seen to be less than $\pm 20^{\circ}$ from an arbitrary straight line across the entire band. The maximum slope occurs near midband and is about $8^{\circ}/40$ MHz which corresponds to the specified limit.

Gain ripple is shown in Figure 28. The calibration lines are again not constant with frequency, but in this case apparently contain ripple due to reflection which was reduced in magnitude when the tube was introduced into the test circuit. The data trace itself contains very little ripple but shows a slope over 500 MHz of 2.5 dB. This is slightly over the goal of 2.0 dB.

In total the data presented point out that best performance, for both efficiency and communication type parameters, is attained when the tube is operated at synchronism in the driver section and at peak efficiency in the output section simultaneously. The ability to do this is a function of the RF circuit design, the demonstration of which has been a major part of this program. The overall efficiency at this operating point has been as high as 50% on individual tubes, at best frequency, and presently is over 43% over the entire 500 MHz band.

By operating at synchronism good communication type performance is obtained. In terms of comparison with other devices not making use of this type of circuit but operating at comparable power levels, superior characteristics have been obtained.

Further improvements in efficiency and corrections in frequency centering are foreseen as straightforward results of continued development and changes to accomplish these results will be implemented in following programs.

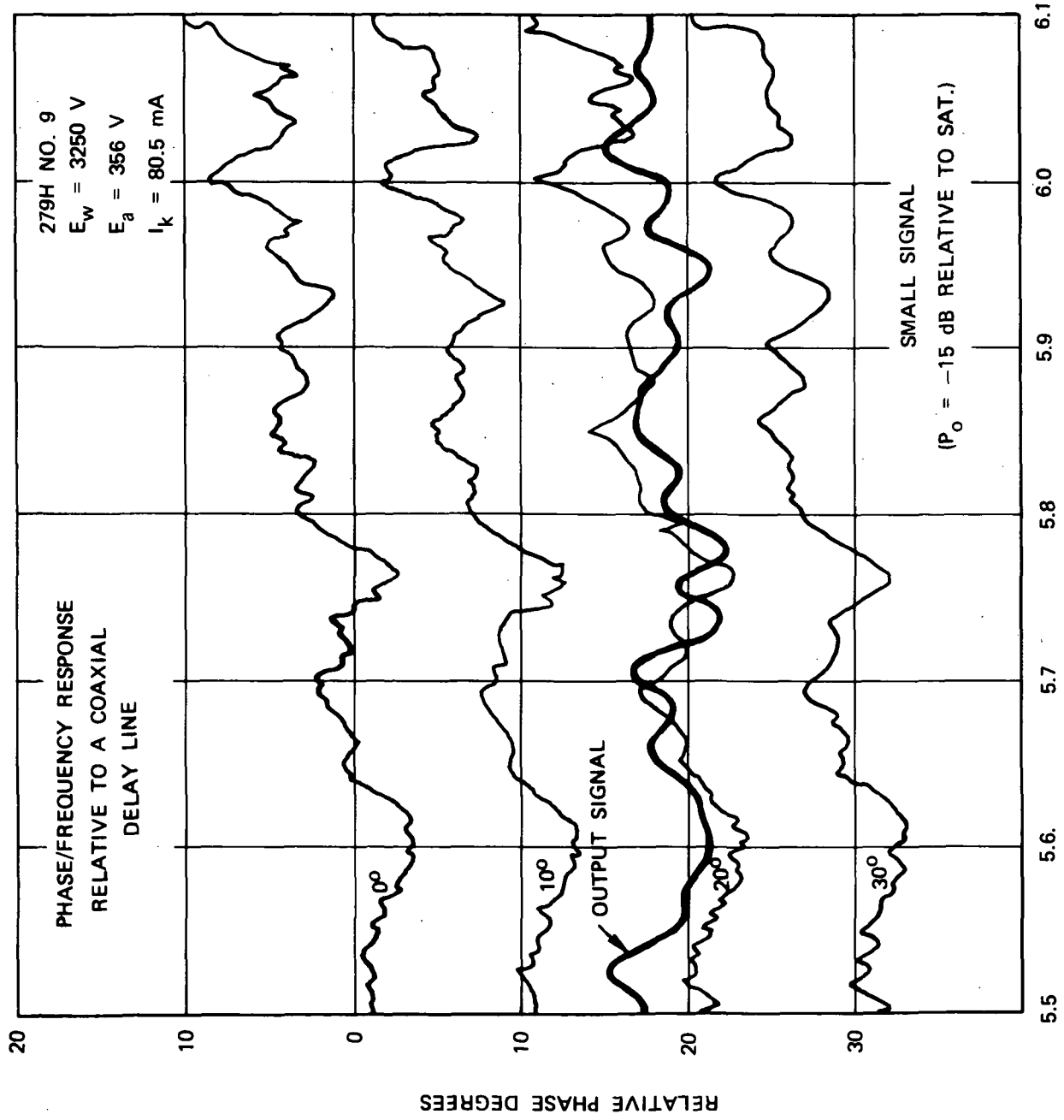

Figure 27 Phase ripple variation with frequency.

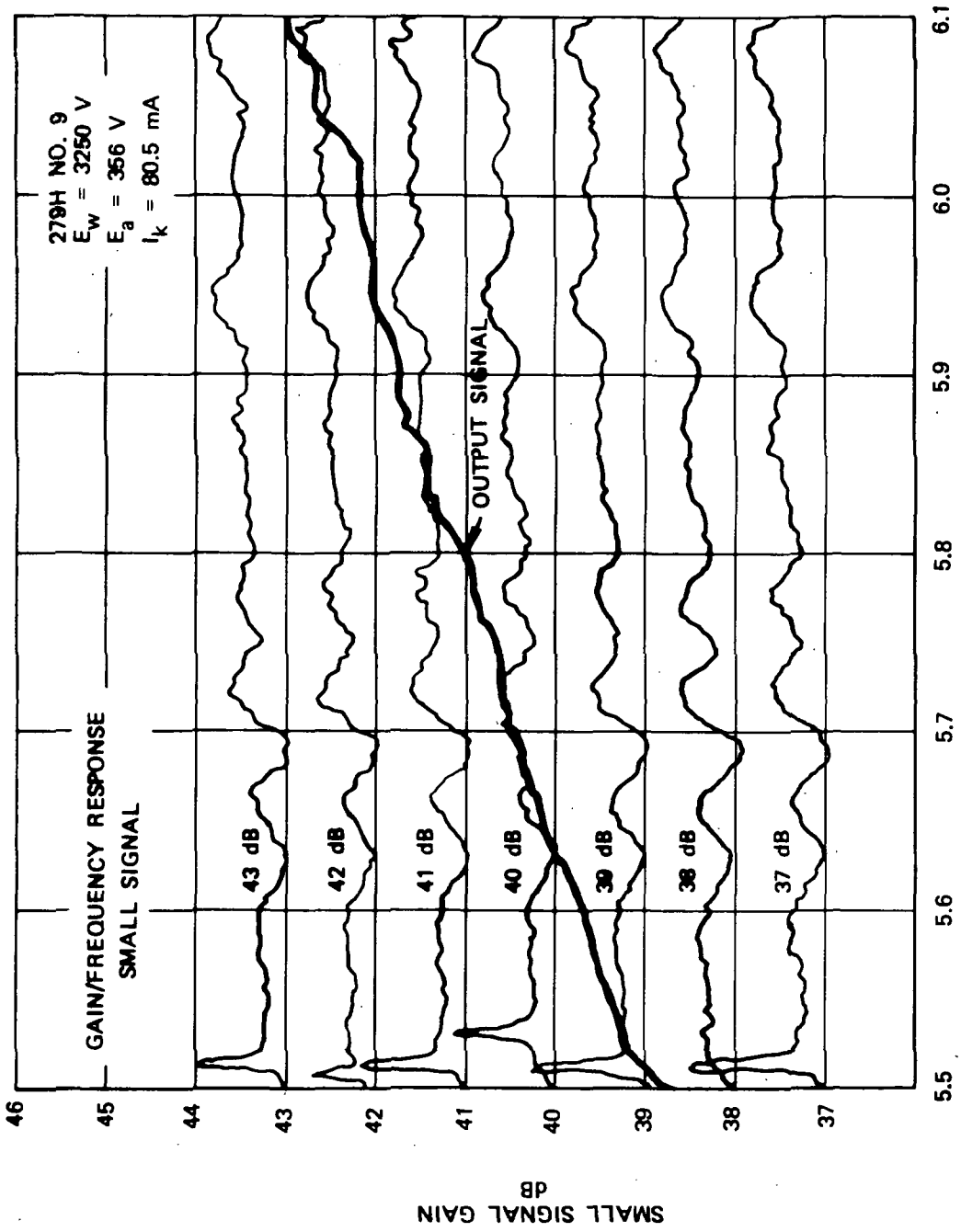

Figure 28 Gain ripple variation with frequency.

IV. THE 1221H POWER SUPPLY

SUMMARY OF THE POWER SUPPLY PROGRAM

The major phases of the development program are illustrated in Figure 29. The program consisted of developing five different stand-alone power supply modulates, and concluded with integrating said modules and the 279H TWT.

The program was initiated by devoting considerable effort to preliminary design and trade-off analysis. Attempts were also made to anticipate future requirements resulting from the TWT development program. Self imposed specifications were therefore added to existing requirements resulting in stringent performance requirements over wide operating conditions. Actual design was initiated after two months of preliminary work. Detailed paper design and lab experiments were conducted through the third month. At this stage electronic circuit design had advanced sufficiently to yield detail specification for the critical magnetic components. Efforts on all tasks were moving forward through the ninth month at which time the total power conditioner system was placed under test. By this time setbacks and redesign of magnetic components had occured. Overall achievements, however, had been quite satisfactory. A high voltage converter with a recorded efficiency of 97% had been designed and implemented into the cathode-helix supply. Acquiring this favorable experience it was decided to initiate a parallel effort of redesigning the transformer in the pulse width modulator. Integration of the power supply and a TWT to place during the eleventh and twelfth months. At this time final stabilization of all feedback loops was also completed, and preliminary product design was initiated.

During the thirteenth month of the program exclusive efforts were made to acquire the same excellent performance of the PWM as was obtained previously in the cathode-helix supply converter. However, schedule requirement precluded complete follow-through and productizing was started with an intermediate transformer design. Productizing and fabrication lasted through the sixteenth month, at which time all power supply modules had been potted and electrically tested from $-60^{o}C$ to $+70^{o}C$.

The final integration was completed during the seventeenth month. At this time, when the TWTA was in its final electrical testing phase, a corona type failure caused severe delay to the delivery schedule. The failure was simple, however, and caused no major damage. The module in concern was repotted and the TWTA was ready for shipment to NASA during the eighteenth month.

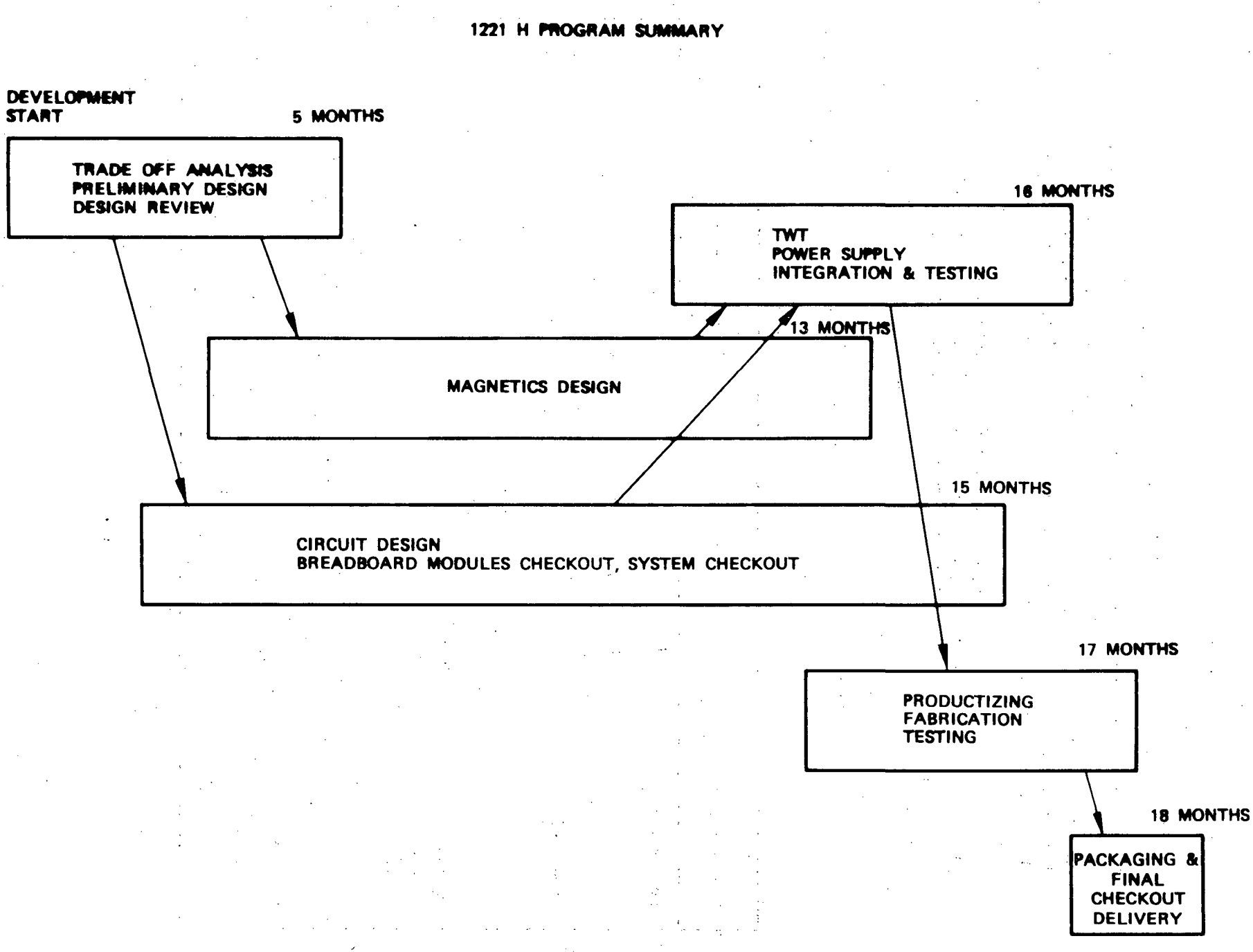

Figure 29 The 1221H program summary.

STATEMENT OF DESIGN GOALS

The design goals of the power conditioner are shown in Table IX. As apparent from the initial specifications, the supply had to furnish a wide range of output voltages and currents. The engineering model was designed to meet these requirements by utilizing tapped transformers and some overvoltaged outputs.

Table X shows the input and interface specifications. It should be noted that the power supply modules were designed for operation through critical pressure and to meet all mentioned electrical specifications from -55°C through +80°C.

TABLE IX POWER CONDITIONER OUTPUT TO TWT

Required Outputs	Parameters	Limits		
		Minimum	Typical	Maximum
Heater voltage	Current mA	400	500	600
	Regulation %			± 3
	Ripple, mA P/P			30
	Voltage ac	5.0	5.6	6.5
Anode voltage	Current mA		.05	.2
	Regulation %			3
	Ripple, V P/P			.5
	Voltage, dc with respect to helix	+50	+100	+350
Collectors with respect to cathode	Regulation %			± 3%
	Ripple %			± .5%
Collector II	Voltage volts dc	+2400	+2600	+2800
	Current mA	30	40	45
Collector III	Voltage volts dc	900	1100	1500
	Current mA	30	34	40
Cathode with respect to helix & Collector I	Regulation %			± .5%
	Ripple %			± .02%
	Voltage volts dc	3400	3600	4000
	Current, helix & Collector I mA	10	15	20

TABLE X POWER CONDITIONER SYSTEM INTERFACE

Inputs/Outputs	Parameters	Limits		
		Minimum	Typical	Maximum
Input dc	Voltage volts dc	24	28	32
Ripple	Volts P/P	TBS	TBS	TBS
Input current				
a. Warm up	Amps dc	.3	.4	.6
b. Operate steady state	Amps dc	7.5	8.5	10
Inrush current at application off:				
a. Warm up command	Peak current Amps			
	Rate of increase Amps/sec			
	Duration of current Pulse msec			TBS
b. High voltage on command	Peak current Amps			
	Rate of increase Amps/sec			
	Duration of current Pulse msec			

INTRODUCTION

The different modules comprising the power conditioner are functionally shown on Figure 30. The power buss is connected to the EMI filter which in turn connects to the Pulse Width Modulator. (The ON/OFF logic is considered a part of the PWM block). The PWM is shown to be feedback controlled, and the indicated "ramp" symbolizes controlled turn-on and low inrush current.

All other blocks are powered by the 100 volts buss. The Anode and Heater circuit and the Cathode Helix Supply are turned on with the PWM. The Modulation Anode circuit is turned on after a 2-1/2 minutes delay. This circuit feeds current into the clamp network to bring the anode of the TWT up to proper potential.

The detailed circuit and functional descriptions are described in the following sections.

SPACE SHUTTLE FUNCTIONAL BLOCK DIAGRAM

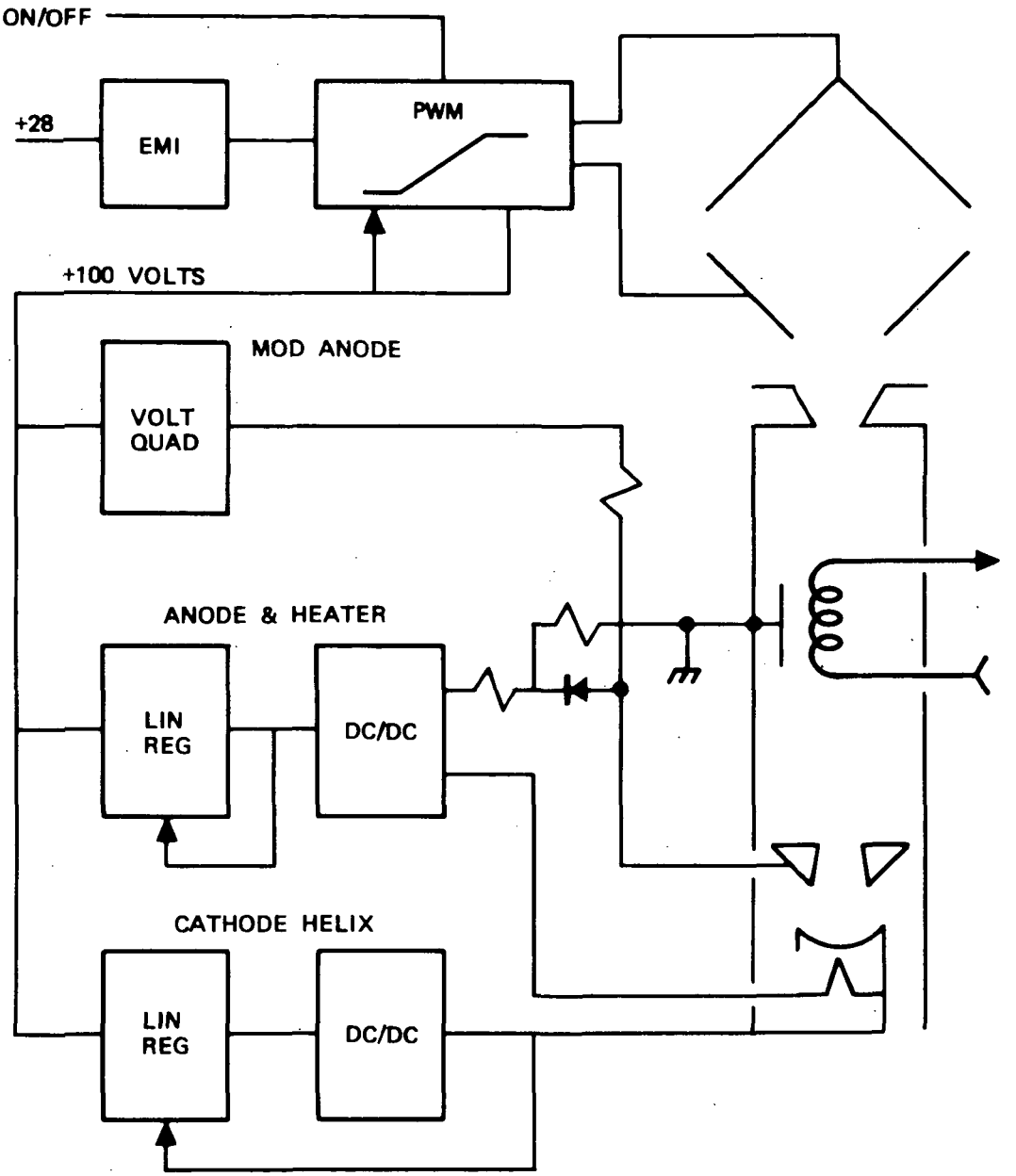

Figure 30 Functional block diagram.

ON/OFF LOGIC

The ON/OFF logic is shown in Figure 31. The ON/OFF circuit consists of an and-gate with an inhibitor circuit. When activated the output sinks current to ground to turn on the PNP transistor switch in the oscillator circuit (See Figure 32).

The ON/OFF input threshold level is approximately 7 volts. The input signal should be free from switch bounce noise, and to maintain good noise immunity its high level should be brought well above 7 volts, preferably equal to the buss voltage. The other and-gate input facilitates the under-voltage protection. If the power buss is not 22 volts or more the gate will be off and an ON-command will not be transmitted to the oscillator. The inhibitor gate will be activated if the power buss exceeds 35 volts. In such case an ON-command would likewise be inhibited.

As shown on this Figure a 2-1/2 minute delay circuit is also implemented. This circuit delays the turn-on of the modulation anode circuit (See Figure 33). The circuit is composed of a UJT timing circuit and a latch. The voltage is activated by the presence of the housekeeping supply voltage. After the specified delay, the unijunction transistor fiers and turns on the latch circuit. The latch in turn clamps the voltage across the timing capacitor to ground and prevents the timing cycle from restarting. As long as the housekeeping voltage is present the latch remains energized and the modulation anode circuit remains activated.

It should be noted that these circuits are intended for use with the engineering unit only. The final logic circuits will have more functions implemented and all circuits will feature defined hysteresis levels and better accuracies.

MODULATION ANODE SUPPLY

The modulation anode supply is shown in Figure 33. The function of this circuit is to furnish a 4000-volt capable current source which when referenced to the cathode and connected to the anode can be used to control the anode voltage and thereby the TWT beam current.

This supply is turned on by the time delay circuit shown in Figure 31. When this circuit times out all supply voltages are up to operating levels and the cathode is up to full emission. Base drive will then be furnished to the converter circuit and the anode voltage, which up until this time have been resistively held at cathode potential, will move up until it is clamped by the clamp diode in the anode supply. In this manner the TWT is brought from cutoff to full conduction.

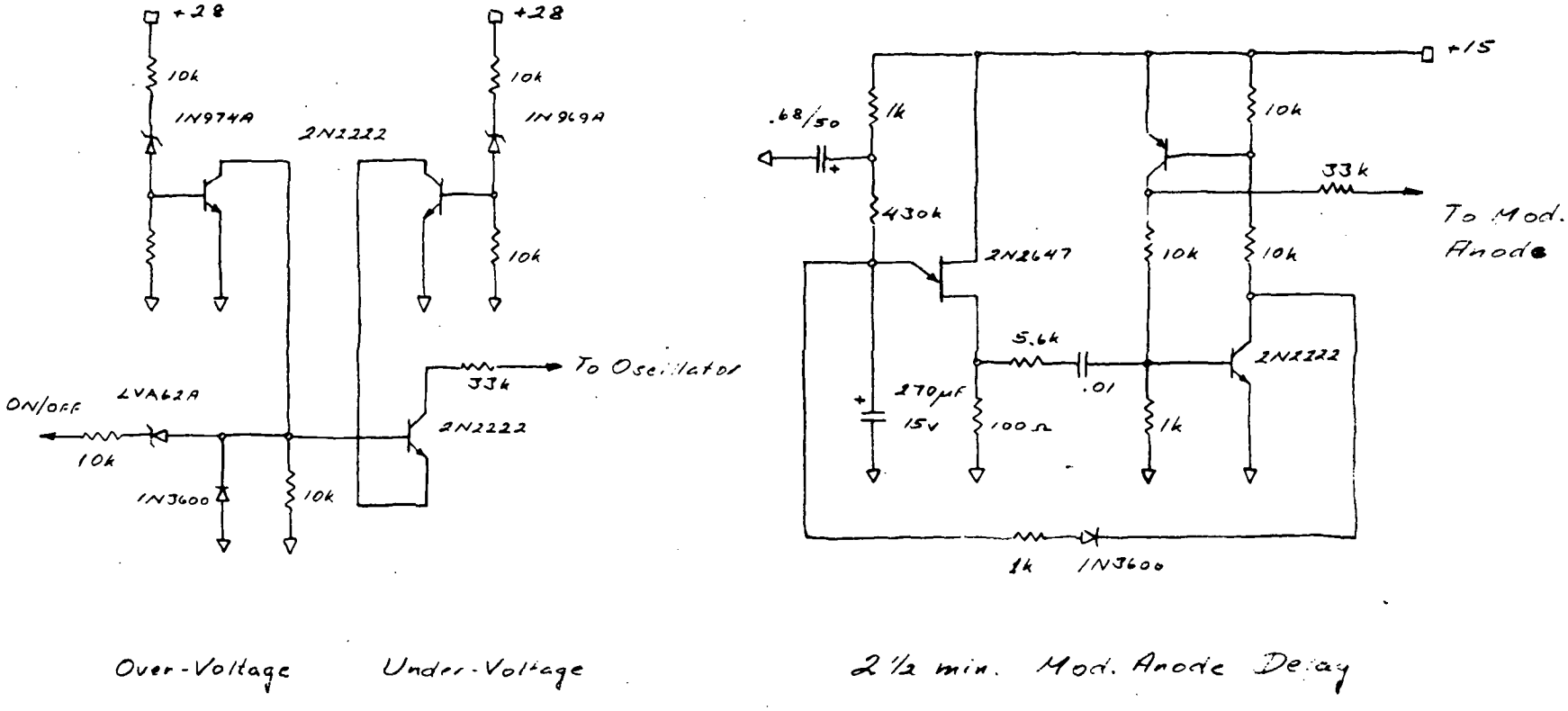

Figure 31 Power supply ON/OFF logic and time delay circuit.

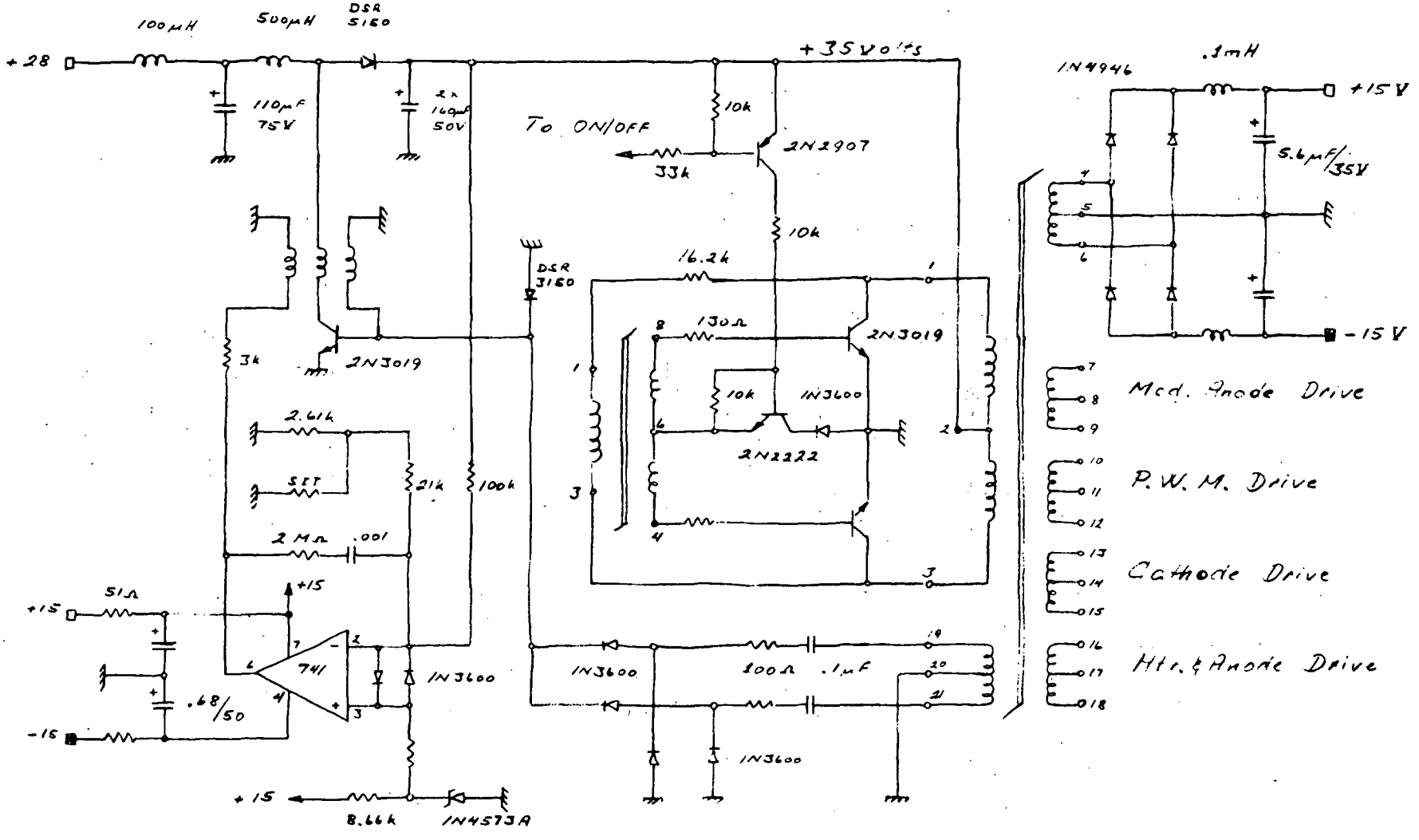

Figure 32 Oscillator and auxiliary power supply.

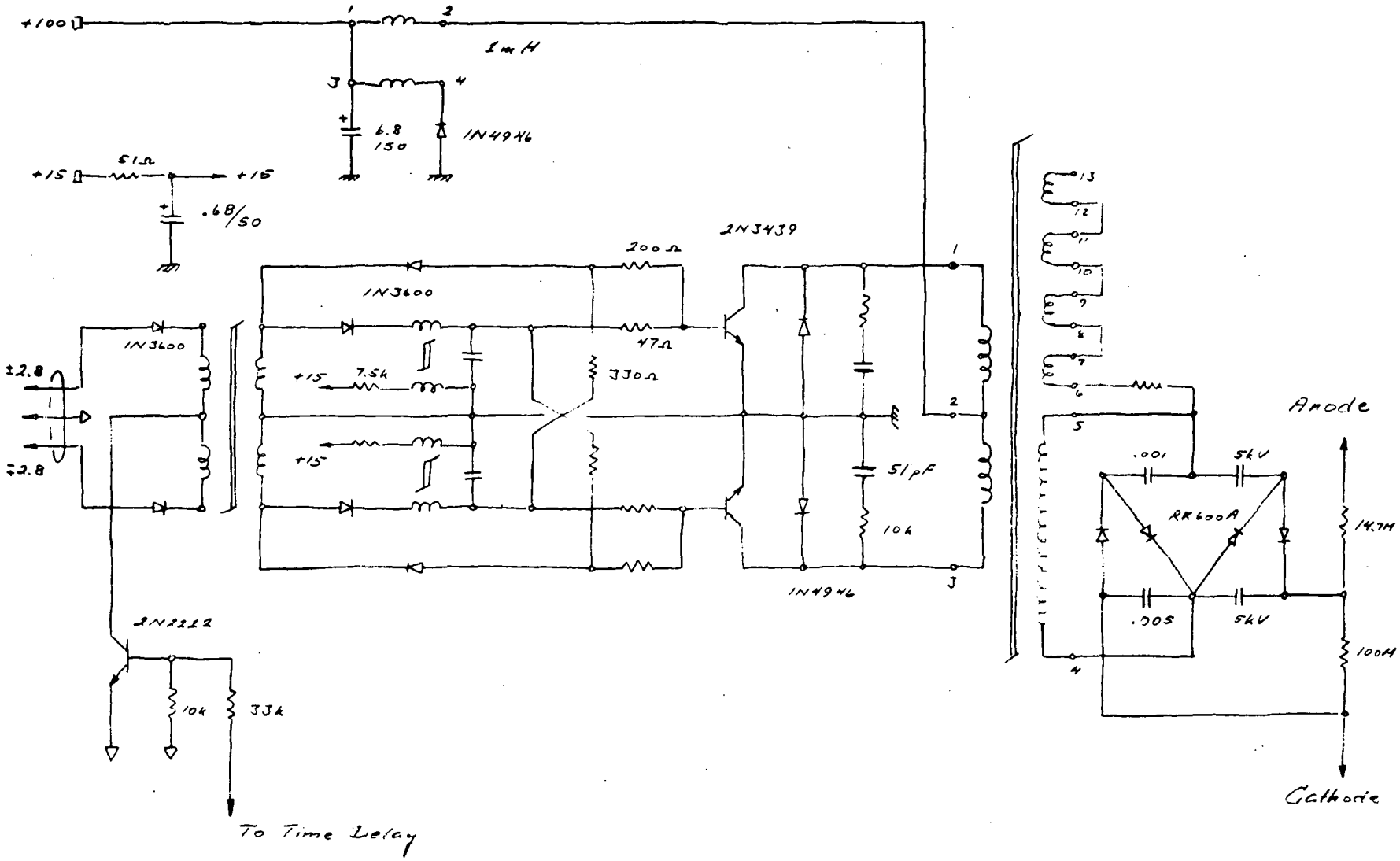

Figure 33 Modulation anode supply.

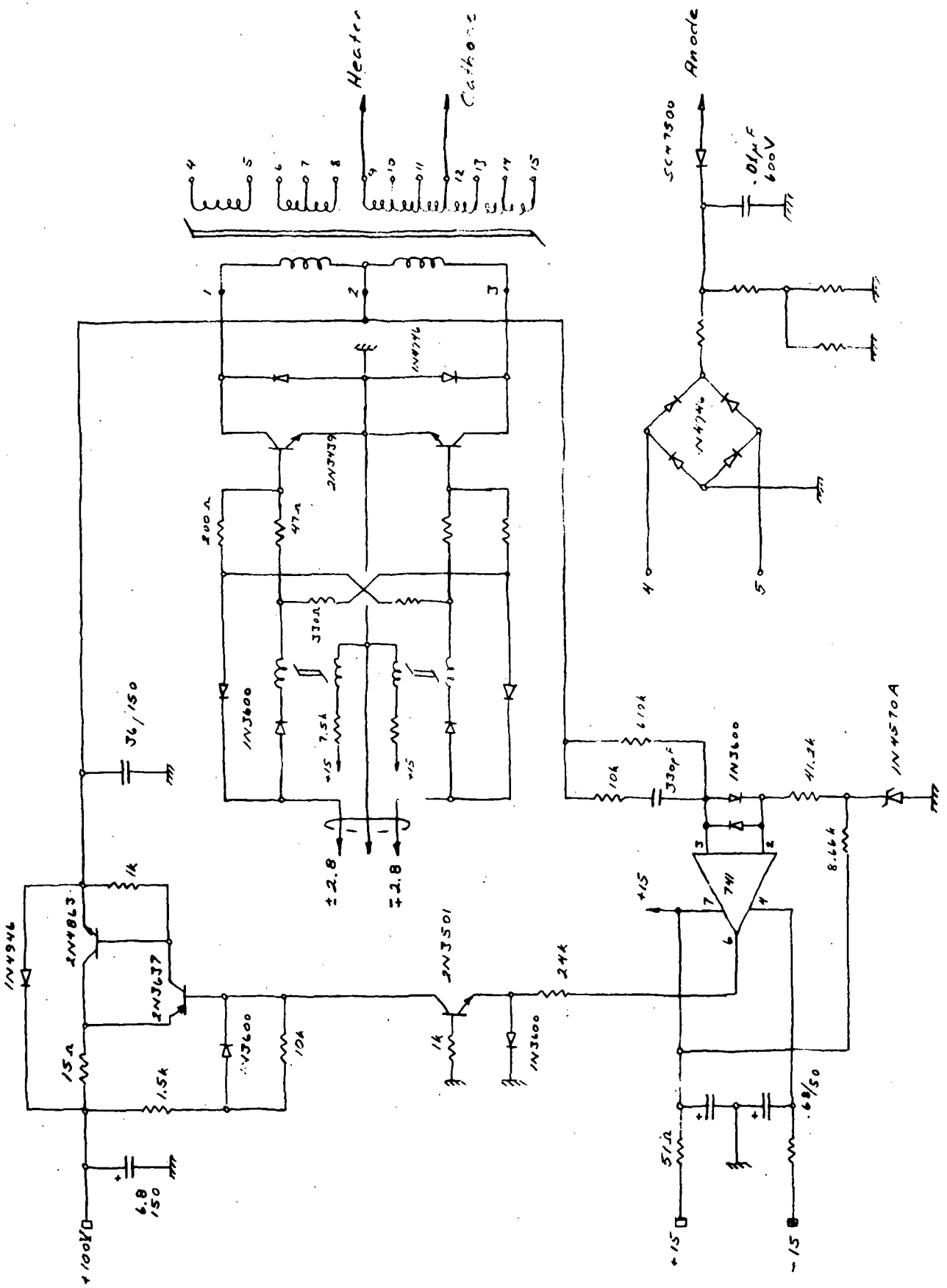

Figure 34 Heater and anode supply.

This converter circuit is driven with a gated base drive circuit identical to the circuit used in the cathode supply. Similarly, an inductance transformer is also connected to the center tap of the step-up transformer. Please refer to the mentioned supply description for detail explanation. Since the power demand from this circuit is less than 250 mW, the highest efficiency was obtained by going to a voltage quadrupler. This quadrupler is being charged during both half cycles and exhibits less ripple in the output. Since the transformer winding is connected as described, it will also float at only half the cathode potential and thus stress the winding insulation only half of an ordinary quadrupler winding. The circuit operates well from -55°C to +80°C.

HEATER AND ANODE SUPPLY

This supply is schematically shown on Figure 34. The primary function of this module is to furnish a current limited low voltage supply floating at cathode potential, and to furnish a ground referenced clamp voltage equal to the anode voltage. The supply must feature good regulation and low aduio susceptibility.

This supply is functionally identical to the cathode supply; please refer to said supply for detail description.

The heater voltage output winding is shown as a centertapped tapped winding. This was done to facilitate full wave rectified heater voltage if desired. The other three taps are for course selection of heater voltage. Finer resolution can be obtained adjusting the linear regulator. To protect the heater element in the TWT during the warm-up period the linear regulator will current limit at approximately 50% overload.

CATHODE SUPPLY

The cathode helix supply is shown in Figure 35. The function of this supply is to convert the preregulated +100 volts to a 1/2% regulated -3650 volts supply at highest possible efficiency. The supply must also feature low ripple and low audio susceptibility.

As shown in the schematic, the supply consists of a linear regulator and a dc/dc converter. The primary functions of the linear regulator are to minimize audio susceptibility and to provide proper regulation. The pass elements are designed to reject up to +1 volt of ripple; they drop the voltage by less than 4 volts to yield an efficiency of approximately 96%. The regulator current limits at 1.5 amperes.

The dc/dc converter transforms the regulated voltage to -3650 volts DC. A bridge rectifier is used for minimum component voltage stress, and the filter is of the choke input type.

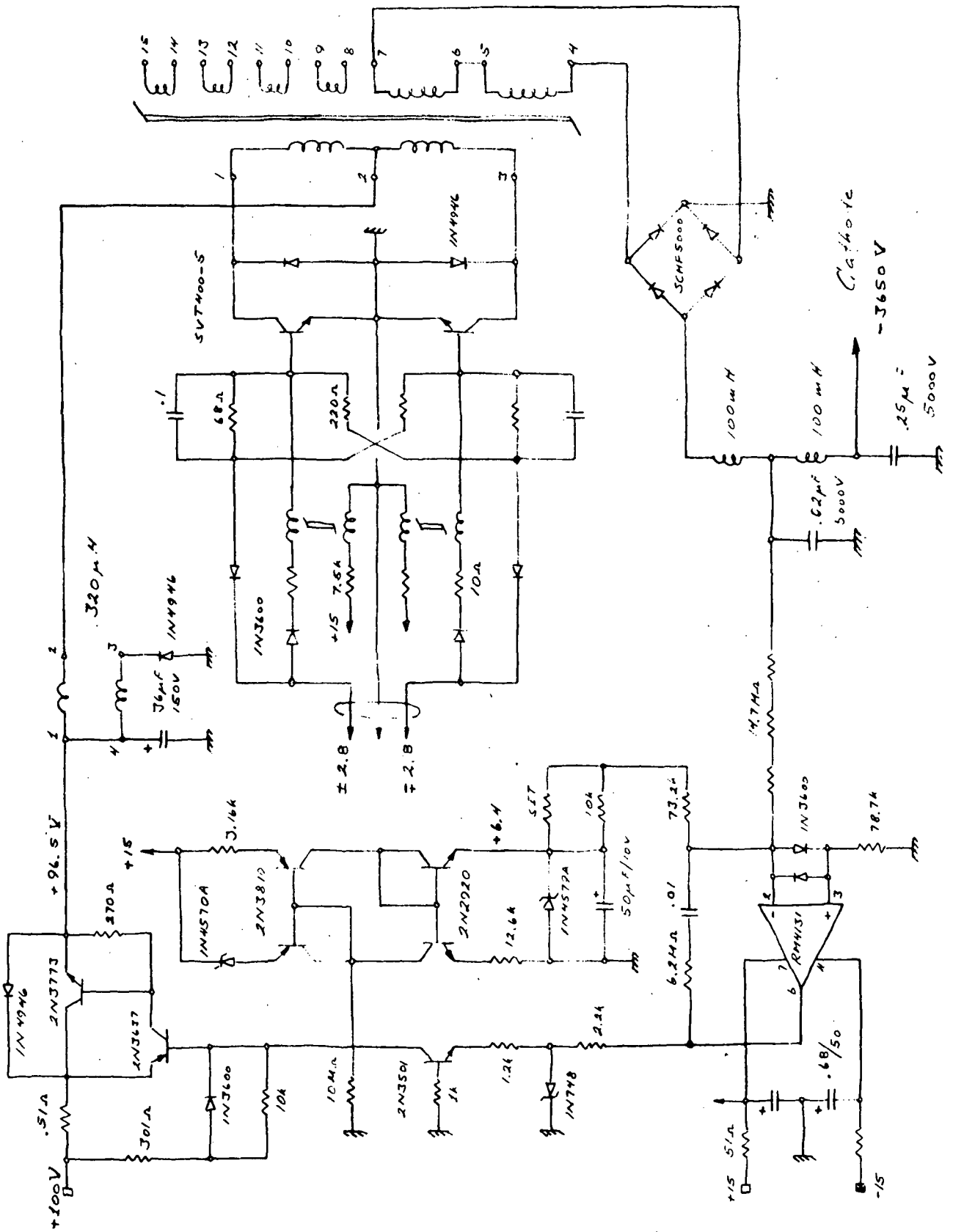

Figure 35 Cathode supply.

The converter circuit is specially designed for high efficiency. The base drive source is again a $\pm$ 2.8 volt, 5 KHz square wave. However, a set of adjustable saturable inductors are connected in series to facilitate a quasi square wave drive for the actual base current. Independent adjustments can thus be made such that collector current overlap during switching is prevented. Equally important, however, since the converter drives into a choke input filter, more advantages can be obtained by further increasing the "dead zone." There is a significant amount of power dissipated during the charging and discharging of the stray winding capacitance in the transformer high voltage secondary. This effect is reduced by increasing the "dead zone" to such an extent that the continuing current demand by the filter choke will completely eliminate this stored charge. The charge depleted is transferred as useful power at the same time as the actual voltage change across the capacitor is reduced by a factor of 2 and in turn reducing the power dissipation by a factor of 4.

Although reduction of the leading edge current spikes have been achieved, further reduction and improved efficiency was obtained by inserting an inductance transformer at the centertap of the converter transformer. This device eliminates the high capacitive currents to the converter transformer, The energy stored in the inductor primary during load current demand is coupled to the secondary when the demand seizes. Current will then flow from the secondary through the diode to the filter capacitor and thereby efficiently returning the stored energy to the power buss.

To maintain overall high efficiency, the high voltage transformer output is furnished with four binary stepped auxilliary windings. Connected in an aiding or bucking manner an output adjustment range of + 450 volts with a resolution of 30 volts (0.83%) is obtained. This enables the voltage drop across the linear regulator to remain within 0.83% of its optimum efficiency over the total specified voltage output range at infinite resolution. The efficiency of the converter is larger than 94%, and total supply efficiency is approximately 91% at 75 watts output.

The feedback factor as a function of frequency is shown on Figure 36. The midfrequency value of the factor is 11.7 at full load. At 40 Hz the filter capacitor of the linear regulator starts rolling off at 6 dB/octave. This slope is kept up to 1 KHz, 2-1/2 octave above unity cross-over. At this frequency the first double pole of the filter occurs and roll-off approaches 18 dB/octave. The second filter double pole occurs at approximately 3.8 KHz. To avoid subharmonic oscillations cross-over occurs at 450 Hz, a decade below the chopping frequency.

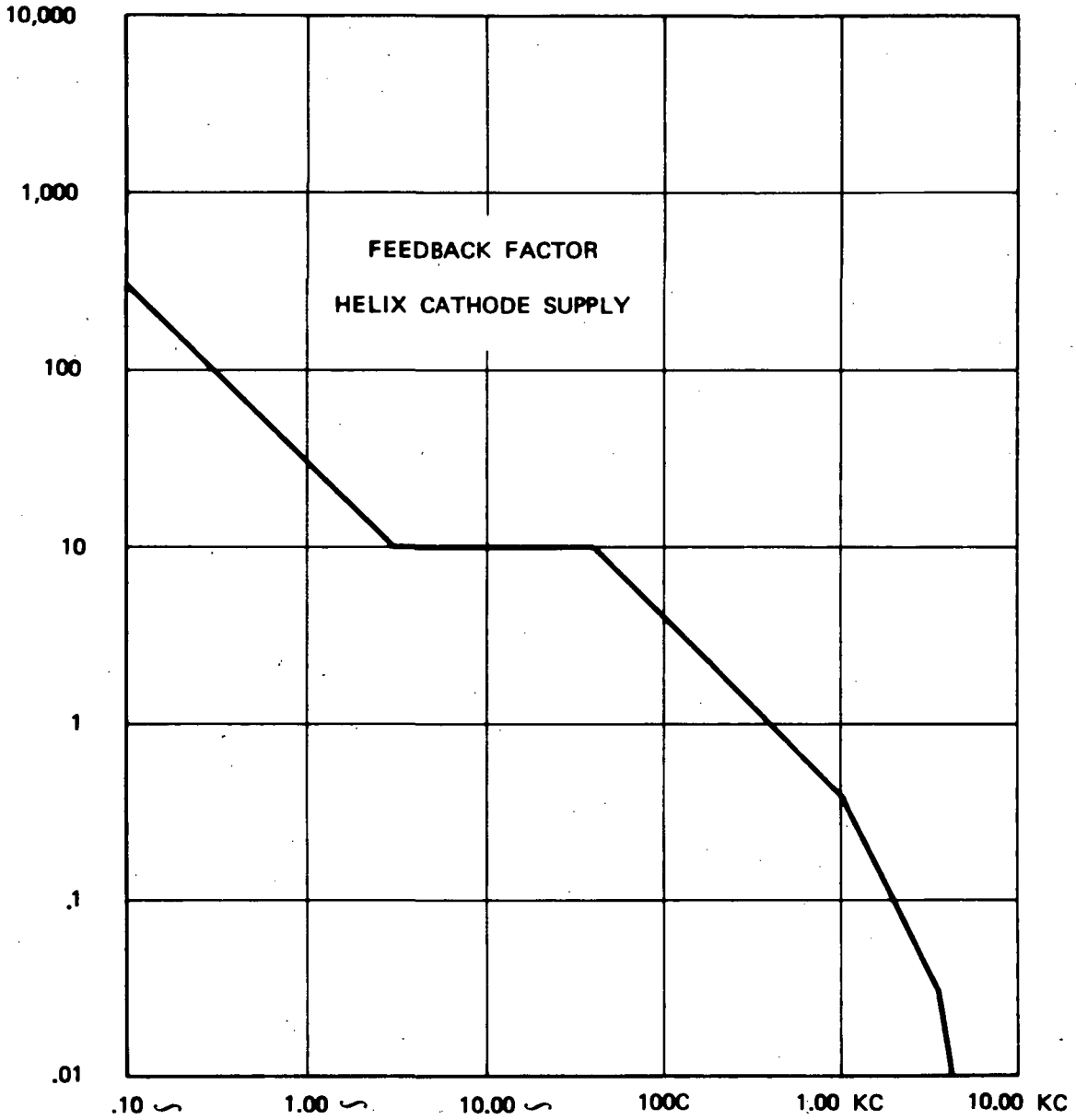

Figure 36 Feedback factor characteristics, cathode supply.

At low frequency the operational amplifier is allowed to approach full open loop gain. The feedback factor, dependent on the gain of the μA 741 IC, therefore becomes very high resulting in excellent line and load regulation. With line variation of ± 1 volt and load variation from zero to full load, the 3600 volt output varies less than 0.5 volts, or less than 0.02%.

The voltage reference supply consists of two dual transistors constituting a temperature compensated current source, in turn feeding a temperature compensated reference diode. The circuit exhibits excellent performance, better than actually needed. The circuit will, therefore, be simplified in later supplies.

Another key function of this supply is to increase the voltage at a linear rate up to +6.4 volts in approximately 250 msec. This will cause the linear voltage regulator to feed the dc/dc converter a likewise linearly increasing voltage starting at zero. The current demand to charge up the high voltage filter capacitors will, therefore, be constant and no excess inrush current will be demanded by the supply.

The output ripple performance is mostly governed by the amount of filtering after the dc/dc converter. The filter installed in this engineering unit is physically small and designed to affect the feedback factors outside the unity cross-over frequency. The filter therefore becomes less efficient, and as for this supply, unable to meet the final specifications. The ripple voltage is approximately 200 mV peak-to-peak at full resistive load, well within the original set of specifications. However, with the floating collector supplies connected to the cathode terminal, a capacitance-coupled noise loop is created to ground through the transformer windings, increasing the ripple to 3.0 volts peak-to-peak. Loading the supply with the TWT, this ripple increases to 3.5 volts peak-to-peak.

Since the ripple specifications have been tightened to 100 mV peak to peak, the following circuit changes are suggested to be implemented:

1. Increase the physical and electrical size of the filter and bring the first filter double pole of the feedback factor well inside unity cross-over frequency.

2. Make the inductors four-terminal devices to facilitate filtering in both feed and return lines.

These changes will insert high impedance in the mentioned noise loops (filter inductors in the collector supplies will also be made four-terminal devices) and eliminate the injected ripple. The first filter section will be composed of L = 10 H and C = 0.3 μf, an improvement of 1500 over the present filter.

The present engineering model operates satisfactorily from -55°C to +80°C. During the next development phase it is expected that overall performance, after implementation of the intended modifications, is going to exceed all revised and tightened specifications. In addition it will add several percentage points to overall efficiency.

The performance is summarized in Table XI.

TABLE XI CATHODE SUPPLY PERFORMANCE

Output Range		Tot. Req. %	Ripple volts ptp	Operating Temperature	Efficiency %
Voltage kV	Current mA				
3.15-4.05	zero-22	0.02	3.5	-55°C to +80°C	91

PULSE WIDTH MODULATOR

The pulse width modulator is schematically shown on Figure 37. The prime objective of this circuit is to convert the input power buss to a preregulated intermediate power buss, and to output two floating high voltage supplies to the collector of the TWT.

All power used by the TWT passes through the PWM. The complete circuit has, therefore, been designed with maximum efficiency in mind. The control element is a magnetic amplifier which modulates the time frame during which power is transmitted to the outputs. To yield the highest possible efficiency the magnetic amplifier has been located in the base drive circuits of the power switching transitors. At this point the lowest possible control power is required. The control device is, therefore, quite small and requires very little control power. A maximum of 8 mA, supplied by the linear IC μA741, is required to fully control up to 280 watts passed by the PWM.

The magnetic amplifier is made of 1/8 mil orthonol material. This insures the best possible squareness ratio, good gain, and best possible pass current rise times. The control winding is common to both base drives, a feature which allows set and reset power to transfer between the cores. The bonus is higher efficiency and lower control power. To adjust for any mismatch between parameters in each side of modulated converter, such as core saturation level, diode voltage mismatch, transistor storage times, etc., an adjustment winding has been implemented in the magnetic amplifier. This winding is thus capable of realigning the current wave symmetry in the transformer such that no core saturation

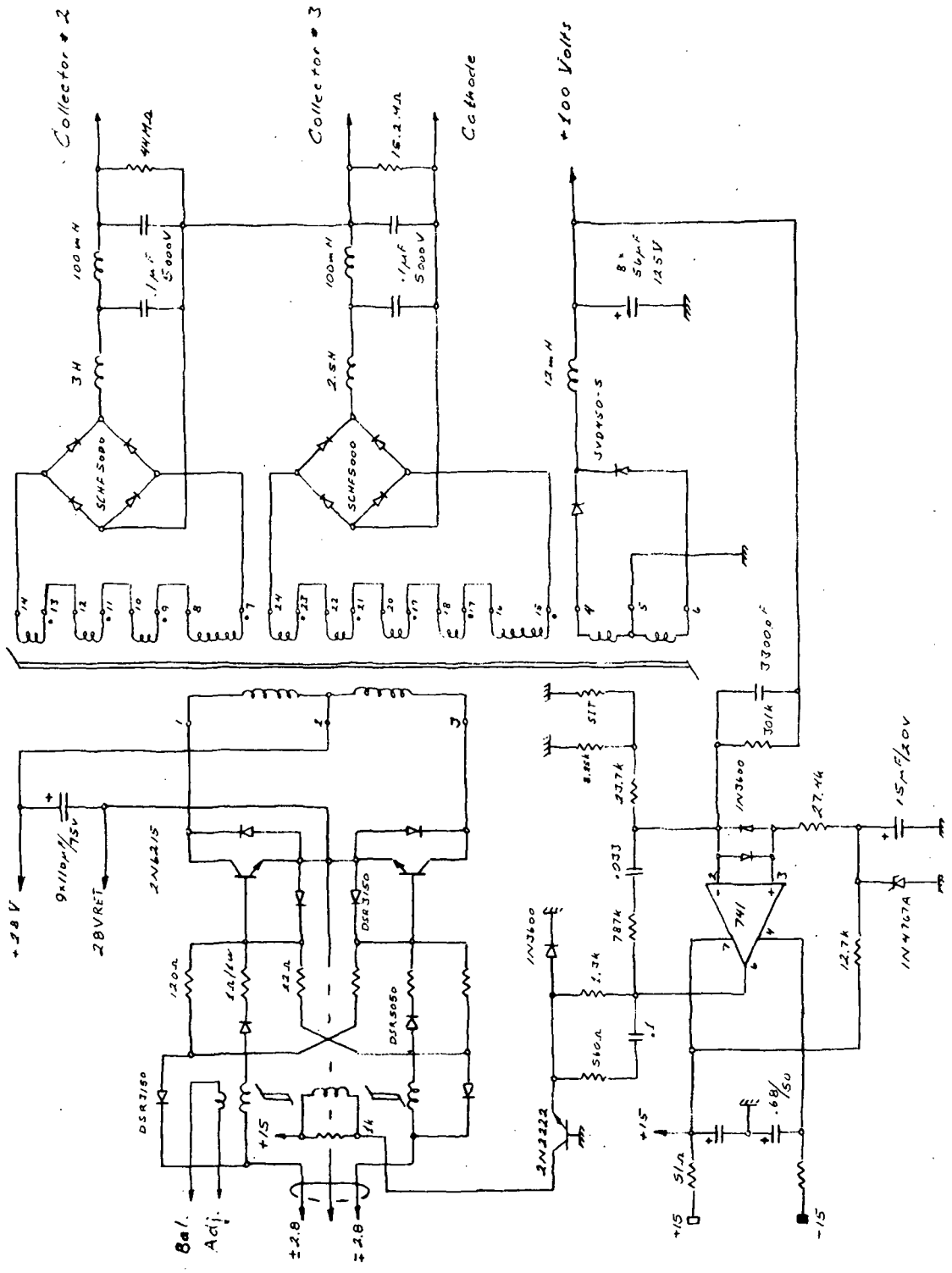

Figure 37 Pulse width modulator.

occurs to reduce efficiency and cause excess ripple on the outputs. To minimize the mentioned problems, several critical components like magnetic amplifier cores, commutating diodes, transistor V_{be}, and transistor current gain, were matched. To protect the power transistors and maintain high efficiency, diodes were placed in parallel with the power transistors. When one transistor seizes to conduct the energy stored in the primary leakage inductance of the transformer will transfer over to its bifilar second half, decrease the voltage on that primary such that the diode becomes forward biased. The stored energy will, therefore, flow back into the power buss, and equally important, the transistor which just ceased conducting will only see a voltage spike twice the power supply voltage.

The preregulated +100 volts output serves as the sensing point for the feedback control. The high voltage collector supplies are, therefore, indirectly controlled by the loading on the preregulated buss. The internal impedance of the collector supplies, however, combined with the steady loading of the TWT at saturation, yields adequate regulation. When the TWT is turning on or operating below saturation, the collector supplies are only lightly loaded, and in such a collector current distribution pattern, that one or both of the supplies are peak charged and delivering higher than normal voltage. This effect of interaction depresses the TWT less to facilitate very safe TWT turn on and also very effectively redistributes the collected beam current during RF drive such that maximum overall efficiency is obtained.

To facilitate wide adjustment ranges in the collector supplies, both high voltage windings are furnished with several binary stepped auxiliary windings. Connected in an aiding or bucking manner an output adjustment range of up to $\pm$450 volts with a resolution 30 volts, equivalent to 2% to 3%, is obtained. This resolution meets the requirements for the TWT. However, if necessary the preregulated output can be adjusted up to $\pm$1 volt which in turn improves the above mentioned resolution by a factor of two.

The feedback factor versus frequency is shown on Figure 38. The mid-frequency value is approximately 50 at full load. At 62 Hz the output LC filter starts rolling off at 12 dB/octave. This slope is kept up to 150 Hz at which point the "zero" in the feedback string brings it back to 6 dB/octave. This slope is kept through unity cross-over at 1.0 kHz and beyond to a safe frequency level. To avoid sub-harmonic oscillations special efforts were made to keep unity cross-over no higher than 20% of the chopping frequency. At low frequency the operational amplifier is allowed to approach full open loop gain. The value of the feedback factor, dependent on the voltage gain of the μA741 IC, becomes very high resulting in excellent line and load regulation of the +100 volts buss. Measured values indicated regulation better than 0.05%.

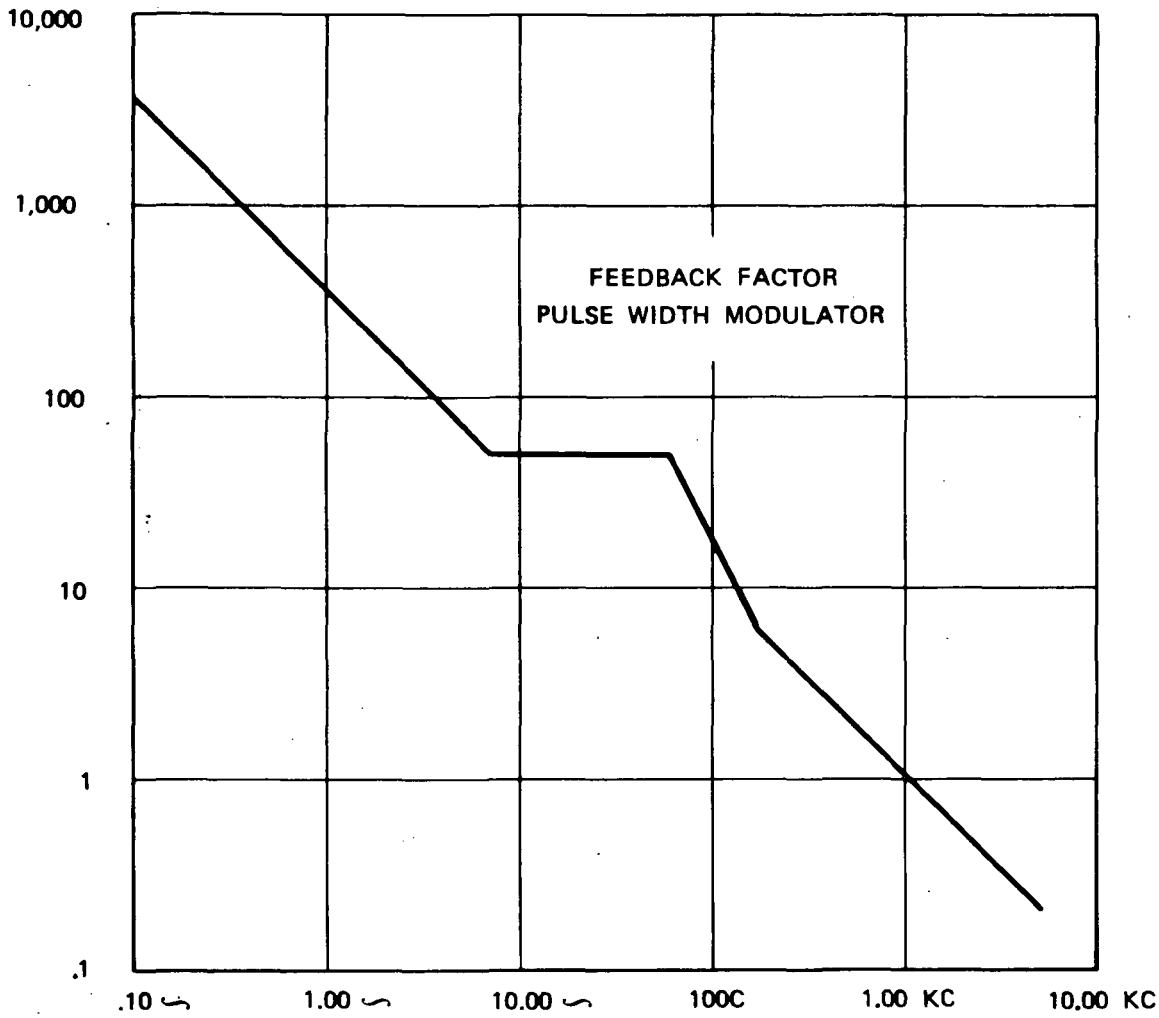

Figure 38 Pulse width modulator.

Due to heavy filtering the ripple on all outputs are very good. The +100 volts has approximately 100 mV peak to peak at full load. Operating in an independent mode (grounded separately) the collector ripples are also excellent. However, when both floating supplies are staggered and referenced to the cathode supply, the ripple increases to beyond specifications. This is caused by capacitive coupling between transformer windings creating a loop of noise currents. Since the filter inductors are all two-terminal devices and only filtering the rectifier feed line in all supplies, the noise current is free to flow in all rectifier return lines. This current will, therefore, flow directly into the filter capacitors and create high ripple voltages. Peak-to-peak value of the spikes were measured up to 8 volts on collector No. 2.

The next supply will have four-terminal inductors in all filters. This way both rectifier feed and return lines will provide high impedance to block the mentioned noise current. As mentioned earlier maximum efficiency was strived for in the module. A theoretical value of 94% was estimated as maximum obtainable at 220 watts thoughput. However, unforeseen problems reduced this goal down to 90%. The loss mechanism is excessive current ringing in the primary half of the transformer. The reflected winding capacitance together with the transformer leakage inductances for a series resonant circuit. Due to low core loss and low winding resistance the equivalent circuit Q becomes high and little damping is present. The resulting current ringing dissipates excessive power resulting in reduced efficiency.

To reduce this problem, the next transformer design will exhibit considerably lower paracitic values together with a core which becomes quite lossy at the anticipated resonance frequency. In this manner, the Q of the circuit will be drastically reduced at the ringing frequency resulting in a minimum amount of current ringing.

During turn-on of this supply the magnetic amplifier is none-biased and all reference voltages are at ground potential. As the oscillator is turned on the housekeeping voltage is brought up rapidly to enable all feedback amplifiers to become quickly operational. However, the reference source, driven by the same supply, will come up at a controlled rate for approximately 250 msec. The magnetic amplifier will, therefore, quickly block any power transfer through the modulator transistors, a possibility which is also prevented due to the use of choke input filters. As the voltage of the reference supply starts increasing, the feedback amplifier is in complete control and the output voltages will, rise at the same rate. Steady voltage rise on the filter capacitors means constant current demand which in turn will control the system inrush current to any desired fixed level.

The present engineering model operates satisfactorily from -55°C to +80°C. It is expected that the performance after the intended modifications during the next phase of the program is going to exceed all specifications, and in addition add a comfortable increase to the overall efficiency.

A performance summary is listed in Table XII.

TABLE XII PULSE WIDTH MODULATOR PERFORMANCE

Preregulated Supply				Collector No. 2			Collector No. 3			Op. Temp.	Efficiency
Voltage volts	Current Amp	Tot. Req. %	Ripple V_{p+p}	Voltage kV	Current mA	Ripple V_{p+p}	Voltage kV	Current mA	Ripple V_{p+p}	°C	%
100	0-1.2	0.05	0.1	1.29-1.71	0-35	8	.65-1.55	0-90	8	-55 to +80	90

OSCILLATOR AND AUXILIARY POWER SUPPLY

This circuit is shown in Figure 32. The primary objective of this circuit is to deliver a constant frequency and voltage drive for all converters in the supply and to furnish house-keeping voltage of ±15 volts for all feedback amplifiers and reference circuits.

The oscillator frequency is governed by a saturable core in its feedback loop. This approach yields high reliability and low power dissipation. The circuit can be switched on and off by controlling the dc current flow to the bases of the oscillator transistor. The frequency of oscillation and output levels are controlled by the supply voltage. To maintain constant levels the oscillator drives a high efficiency wrap-around boost regulator circuit. Driven at twice the oscillator frequency this circuit elevates the supply voltage to the oscillator to +35 volts. Excellent frequency and output level stability is obtained from -55°C to +80°C.

The converter base drive outputs have been separated into four independent drives. This was implemented to avoid ground loops as the different loads are physically separated throughout the TWTA.

EMI FILTER

The Electromagnetic Interference Filter is shown in Figure 39. The 28 volts power buss is connected through a Bendix 21-2000216-26P connector. Three pins, ABC and DEF, are connected in parallel to facilitate minimum connector losses in the respective current feed and return connectors. The TWTA is grounded through two parallel pins, G and H. The ON/OFF input signal, pin J, has a separate ground, Signal Ground, at pin K and should be connected to the amplifier ground external to the amplifier.

The output of the described filter is connected to another filter capacitor bank of 990 μf. As shown in Figure 40, above 400 Hz the two filter sections start rolling off towards 24 dB/octave. The total resistance of all four inductors is approximately .010 m ohms. Steady-state power dissipation is therefore nominally 1 watt or less. It should be emphasized that this filter has not been implemented as a result of specification requirements. Instead, it has been installed as an engineering experiment. Equivalent dc resistance was made quite low and corner frequencies were chosen without definite or specific reasons. The filter may, therefore, not perform to some eventually required specifications. In fact, with the corner frequencies of the two filter sections virtually identical, and since there is no dampening of the high Q-values of the inductors, some combination of input voltage and pulse width modulator load will make this particular filter to resonate. Outside this range, however, which is quite narrow, the filter exhibits good characteristics. Substantial engineering knowledge has, therefore, been acquired as a result of its implementation.

During the next phase of the program it is expected that planned computer simulation of the filter and load will yield good and stable filter-PWM combination.

MECHANICAL DESIGN

The final package of the 1221H power supply is shown in Figure 41. The supply is composed of five separate modules where each one performs a different function. Observing the picture, the module at the top corner is the experimental EMI filter. It is partially covered by the bracket which holds the power connector. Some of the filter capacitors are visible, and the attached circuit board contains the turn ON/OFF and delay circuits. The total package is screw-mounted to the base plate. The weight of the filter is 2.03 lbs.

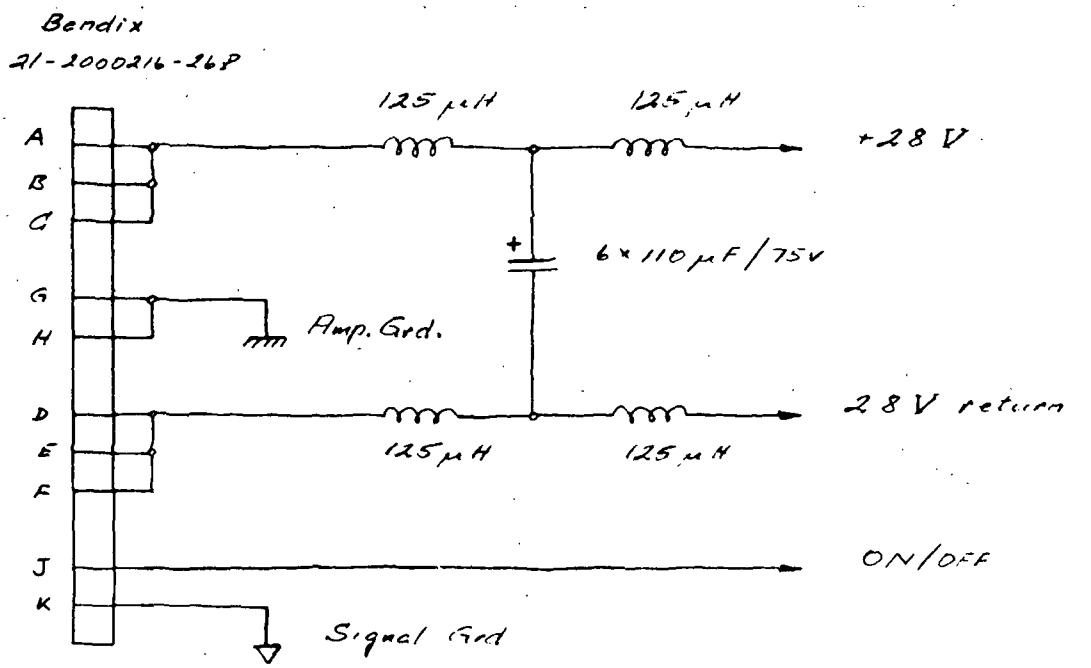

Figure 39 EMI filter.

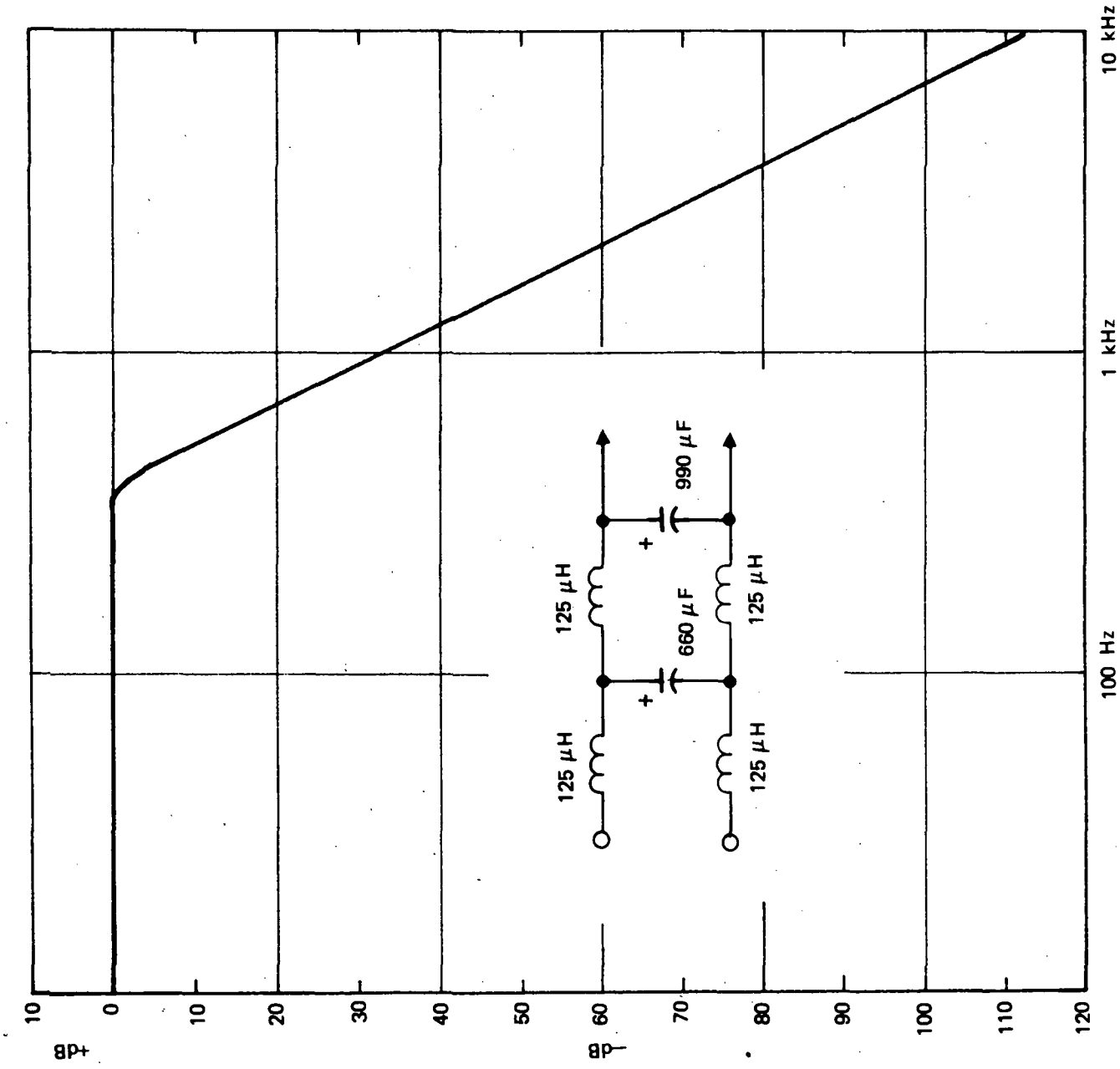

Figure 40 EMI filter characteristic.

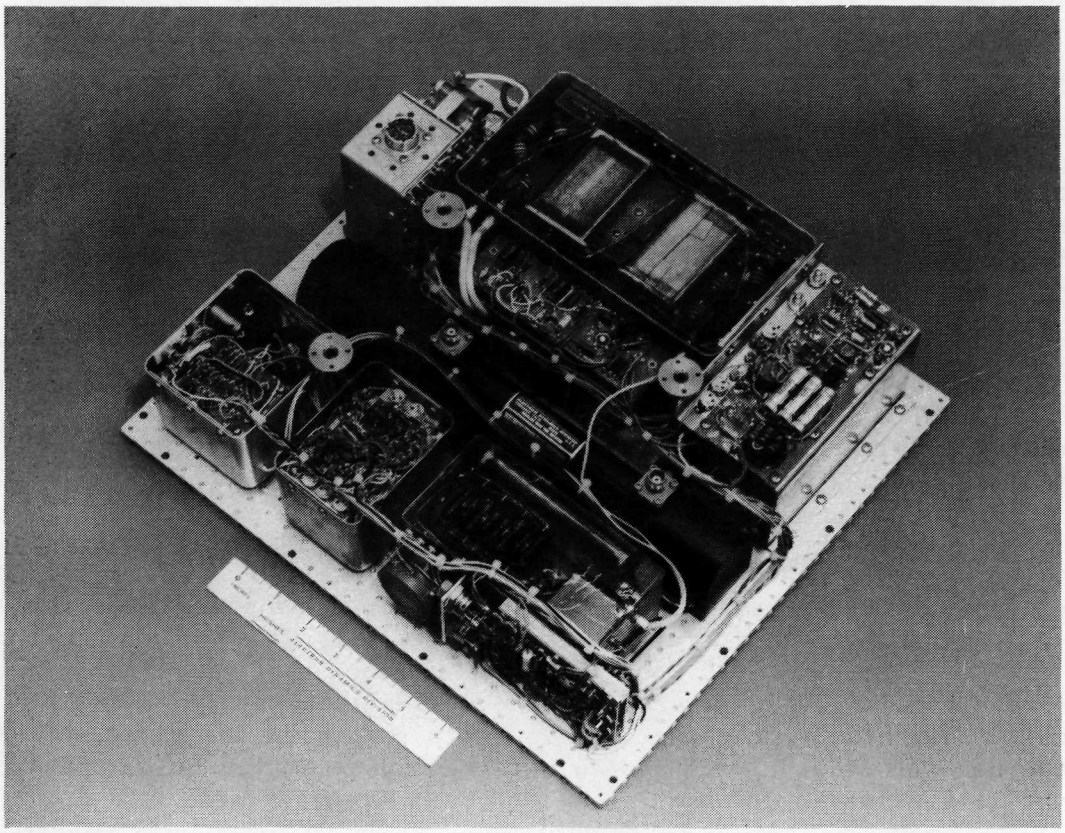

Figure 41 Photograph of 1221H power supply.

The next module in the clockwise direction is the pulse width modulator. The metal box contains the high voltage collector supply transformer, the rectifiers, and the filter circuits. Prior to vacuum-potting this box with Sylgard 184, every and all components were de-greased and cleaned with Freon TA solution. The circuits attached to this box contain all the low voltage drive and control circuitry, and the filter circuits for the preregulated +100 volts. Total weight of PWM is 10.53 lbs.

The module in the bottom corner is the helix-cathode supply. Like the PWM module, the high voltage section of this module is vacuum-potted with Sylgard. The low voltage drive circuits are mounted on the side of the box. Total weight is 3.0 lbs.

The adjacent module contains the anode and heater circuits. The high voltage components are placed in the lower half of the box and covered with potting material. The top half of the box contains the low voltage drive circuitry. The module weighs 1.1 lbs.

The box in the left hand corner contains the modulation anode circuit. The high voltage section is again potted in the lower part of the box with the drive circuits unpotted in the upper half. The weight is 1.6 lbs.

All modules are secured to the base plate by mounting screws inserted from the reverse side of the plate. Heat paste have been used between the boxes and the base plate to optimize thermal characteristics. The base plate weighs 2.95 lbs.

Three mounting posts can also be observed. Their function is to secure the cover of the amplifier. The posts are also tubular such that additional bolts can be used to secure the TWTA to its mounting surface. Total weight of the mounted supply is 19.22 lbs.

PERFORMANCE OF 1221H POWER SUPPLY

The data shown in Table XIII is presented to illustrate the level of accomplishments attained in the development program. For comparison the design goals are also included. It can be seen that while some goals are not exactly met, the majority of the objectives are met and comfortably exceeded.

TABLE XII 1221H POWER CONDITIONER DESIGN ACHIEVEMENTS

Parameter	Design Goal	Present Achievements
Operating Temperature	-55 to +70°C	-55°C to +70°C
Partial Pressure	Through Critical	Not fully implemented
Dynamic Environment		Not fully implemented
Input Voltage	22 to 34 V	24 to 34 V
Inrush Current	None	<150% of dc steady state value
EMI Filtering	None	Experimental circuit installed
OUTPUTS		
Helix Voltage*	3.4 - 4.0 kV	3.2 - 4.2 kV
Regulation	18 volts	<1.0 V
Ripple	.02%	.01%
Current Load	10 - 20 mA	Zero - 22 mA
Collector Voltage No. 2*		.8 - 1.9 kV
Regulation	3%	Self adjusting
Ripple	.5%	.5%
Current Load	30 - 45 mA	25 - 35 mA
Collector Voltage No. 3*	.9 - 1.5 kV	.8 - 1.6 kV
Regulation	3%	Self adjusting
Ripple	.5%	.05%
Current Load	30 - 40 mA	25 - 90 mA
Anode Voltage**	50 - 350 V	-400 to +400 V
Regulation	3%	1.5%
Ripple	.5%	.2%
Current Load	0 - .2 mA	0 - .2 mA

* With respect to cathode potential
** Relative to ground

TABLE XIII (continued)

Parameter	Design Goal	Present Achievements
Heater Voltage*	5 - 6.5 VDC	5.6 - 6.2 VDC
Regulation	3%	4.5%
Ripple	30 mA	20 mA
Current Load	.4 - .6 A	.2 - .5 A
PROTECTION LOGIC		
Input Over Current	None	None
Input Over Voltage	None	Yes
Input Under Voltage	None	Yes
Helix Over Load	None	None
Aut. Sequencing	None	Yes
TELEMETRY		
Input Current	None	None
Helix Current	None	None
Heater Voltage	None	None
EFFICIENCY		
Overall	82%	84.5%
Pulse Width Mod.		90%
Cathode Helix		90.5%

* With respect to cathode potential

V. THE 1222H THERMAL DESIGN

THE HEAT PIPE SYSTEM

The requirement to reduce the heat flux through the cooling surface of the TWTA to a figure less than 1.5 watts per square inch, and the constraint that 150 watts of waste heat would have to be rejected through this surface, defined the base plate surface area. Further constraints on weight prevented the use of a massive block of copper or aluminum to achieve a level temperature and even heat flow through each square inch of surface.

The solution was a system of heat pipes to move waste heat from a localized source, the collector area of the tube, out over the entire base plate, selected to be approximately 14-1/2 x 13 inches for the engineering model. To be effective this system must weigh less than a homogeneous slab of material which could achieve the same thermal results and must function efficiently over all gravity orientations, at zero gravity, and for the required unit lifetime. The total development problem, therefore, included construction and thermal tests of the individual heat pipes and the total assemblies, but also an analysis of effects which might limit life. These effects from our past experience would be associated with incompatibility of materials or with contaminants introduced during fabrication. Finally, life tests of a variety of heat pipes were conducted to back up our choice of materials and to evaluate possible alternatives.

THE THERMAL PROBLEM

Figure 42 shows the loading of the base plate due to the losses in the tube and in the power supply. Note that the major load is at one end of the tube package which is located near the center of the baseplate. The losses in the power supply modules are better distributed but are not sufficient to balance the tube load. An additional problem lies in the fact that the 100 watt heat generator is electrically isolated from ground and is operated at 2600 volts off ground. A three-part system is used to level the thermal load. The three parts were built and evaluated separately and then also evaluated as an assembly.

THE COLLECTOR TO MOUNTING BASE HEAT PIPE

A radial heat pipe serves to move the 100 watts of energy across the electrical isolation required between collector and ground. No conduction path is provided except through the vacuum seal ceramic isolator, a poor thermal conductor in this application. Vaporized fluid is condensed on an outer cylinder and, through a wick system, is returned to the hot collector for reuse. This collector cross section is shown schematically in Figure 43. The fluid used is perchlorethylene. To improve the high voltage standoff the system is purged and backfilled with Freon 116 before final sealing.

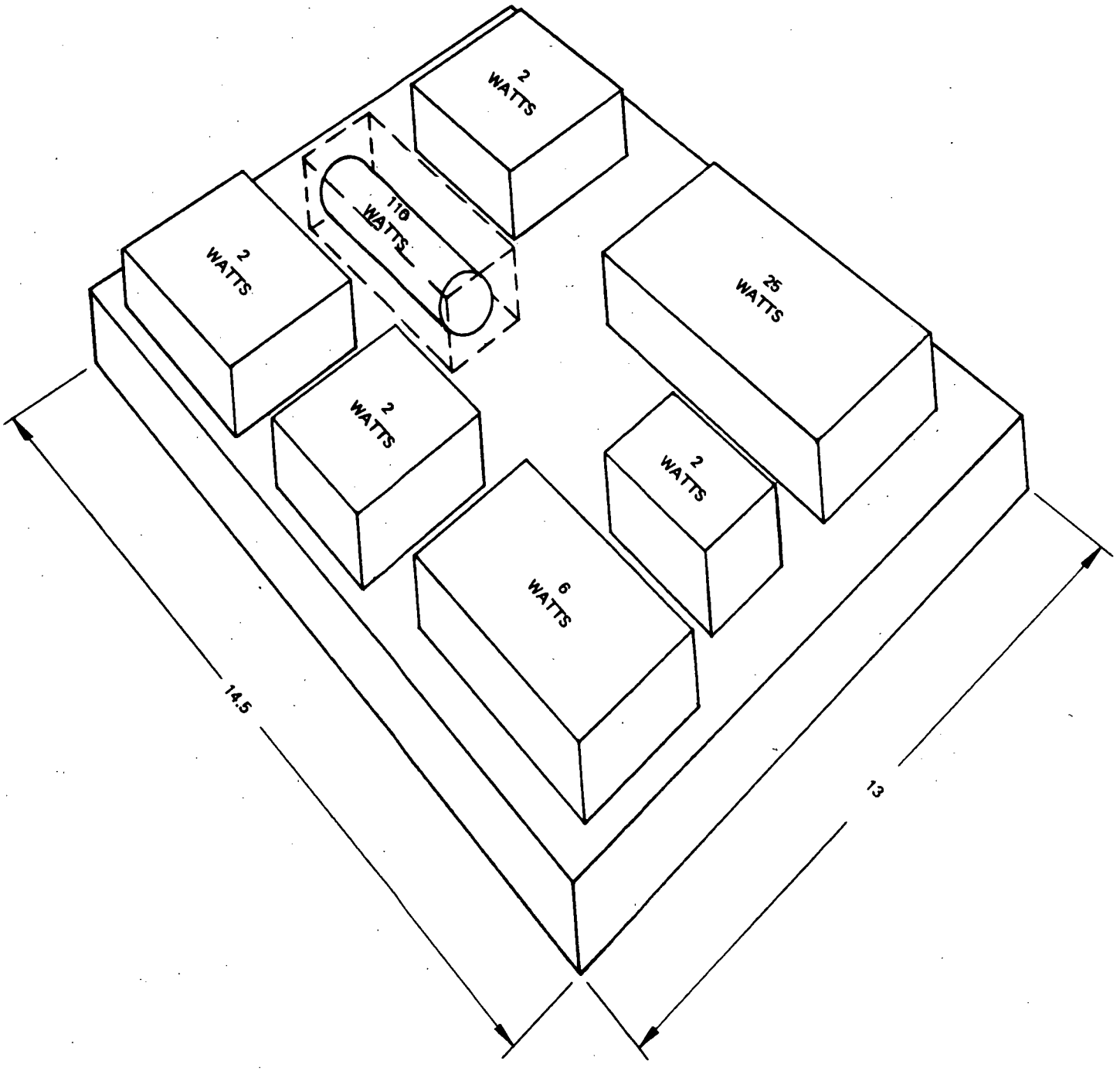

Figure 42 Schematic of thermal load.

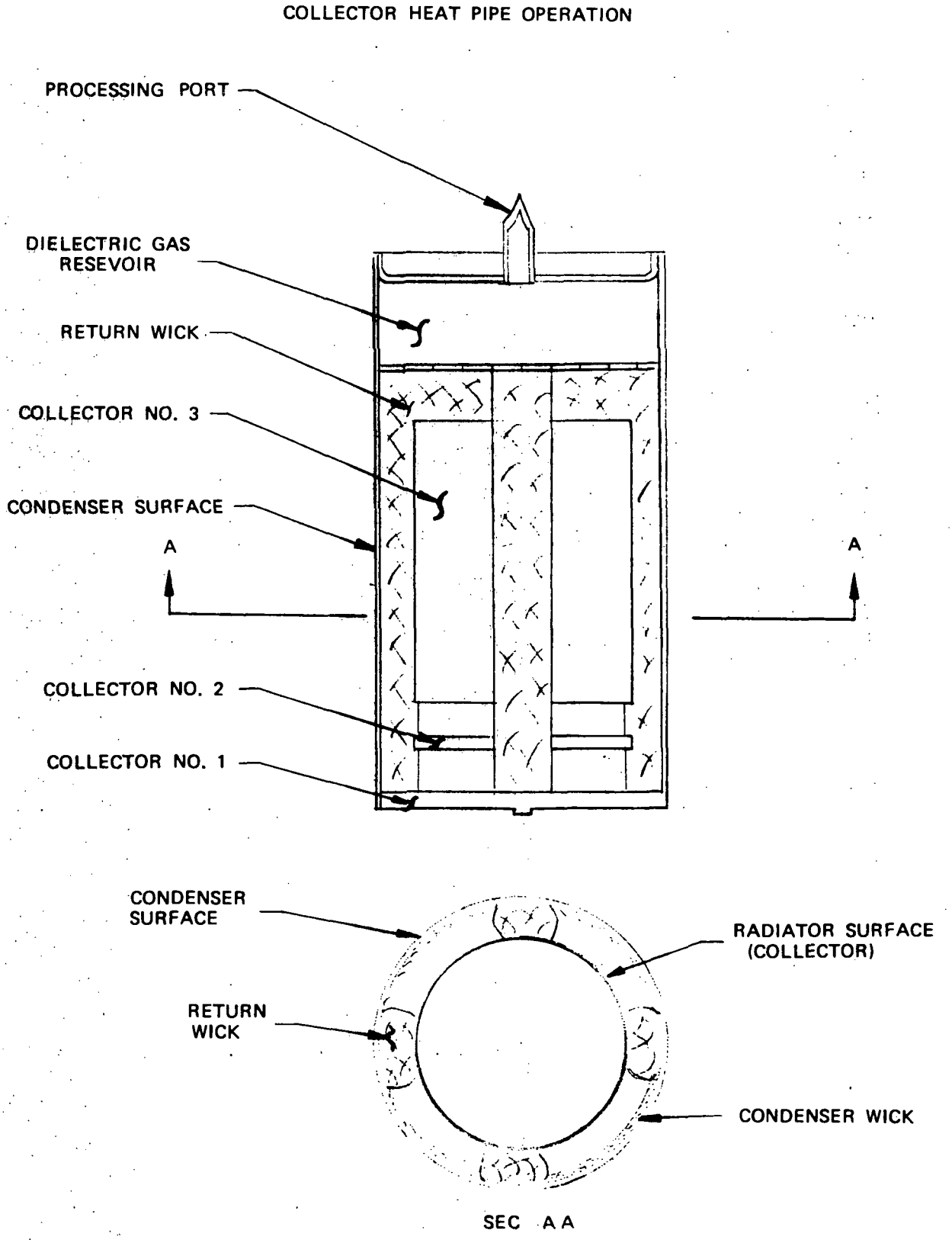

Figure 43 Collector heat pipe operation.

THE MOUNTING BASE HEAT PIPES

With the heat transferred to the mounting base at the collector end of the tube the problem is only partly resolved. The heat must now be spread along the major axis of the tube, a length of 12 inches. The mechanism used is a set of axial heat pipes clamped to the tube mounting base. Two sets of pipes, each 1/4 inch in diameter, are used. There are 3 pipes in each set. In addition, conduction through the aluminum base also contributes to the heat transfer. The heat pipes are stainless steel in this case, using methanol as the working fluid. Since the footprint of the tube mounting base is 27 square inches, the thermal density at the tube mouting base-baseplate interface is 3.7 watts per square inch.

THE BASE PLATE HEAT PIPES

Having leveled the thermal density along the tube axis by use of cylindrical heat pipes in the mounting base, it now remains to transfer heat transverse to the tube axis, out into the base plate. This is accomplished by embedding in the baseplate 50 heat pipes. These are arranged such that all 50 pipes originate under the tube base and extend transverse to the tube axis, to the edge of the base plate. Half of the group extends in each of the two directions away from the tube. Since the power supply modules are also bolted to the base plate, the dissipation from each of the modules is added to the heat transferred from the tube. Since those losses are added near the edge of the base plate their effect is to reduce the heat transfer required to level the thermal density. The heat pipes used in the base plate are also stainless steel using a methanol fluid.

HEAT PIPE DESIGN EVALUATION

In the design of the required heat pipes the operating temperature and power handling capability were firm requirements that had to be met. A variety of optional material had previously been used by Hughes Electron Dynamics Division in other applications, and additional materials were researched and added to the list of possibilities. Some of the materials originally considered are listed to show the number of combinations considered.

Housing Materials

Stainless steel

Aluminum

Monel

Copper

Wick Materials

Copper

Aluminum

Stainless Steel

Nickel

Refrasil (glass fiber)

Fluids

Water

Acetone

Ammonia

Methanol

Perchlorethylene

Dow A

Dow E

DC-200

Hexaflouro Benzene

Incompatibility of some fluid-metal combinations results in an immediate reduction of this group of variables. Considering further the objectives for power handling and operating temperature, initial choices for both the radial collector heat pipe and the axial base plate pipes were made.

The radiator section of the radial collector heat pipe was selected to be copper, the vacuum wall of the tube. Stainless steel was selected for the condenser side which is also the container forming the fluid and dialectic gas reservoir. Refrasil (glass fiber) was selected for the transfer wick material and nickel felt for the wick lining the condenser walls. The fluid choice was not as straightforward with some virtue in each of five different fluids. Hexafluoride benzene had the advantage of a lower operating temperature, but had limited heat transfer capacity in the size collector to be used. Acetone also had a very low radiator operating temperature, but was subject to degradation through inclusion of impurities in the fluid. DC-200 and perchlorethylene in initial tests appeared more stable although operating temperatures were slightly higher. The collector operation with these fluids is shown in Figure 44. This data was taken by operating radial heat pipes designed and built for this program. They closely simulate the heat pipes used on the actual tubes.

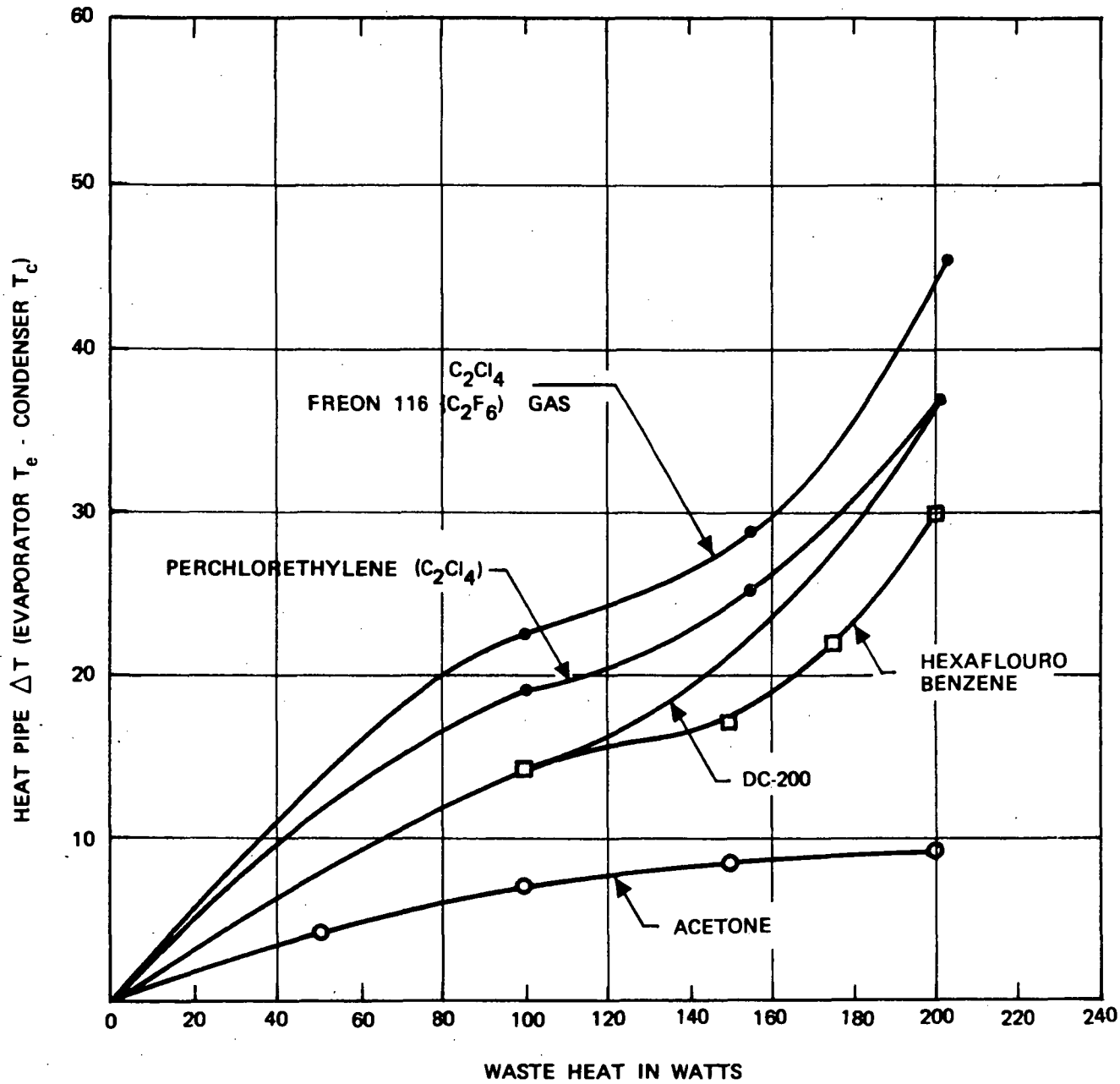

Figure 44 Collector heat pipe operation with various fluids.

Based on the test results and the additional data obtained by analyzing the fluid after the tests, a choice of three fluids for life test was made and ultimately implemented. DC-200, perchlorethylene, and Dow A fluids were used in three separate life test vehicles which were placed on test with 150 watt loads and 1500 volt high voltage standoff (to allow for evaluation of isolation capability as well). It should be pointed out also that, as specified in the design description, an atmosphere of Freon 116 is used to improve high voltage insulation. Leaks which would cause a change in the partial pressures of the vapor phase of the heat pipe fluid and of the Freon would be detected as leakage currents. The life tests were conducted from the fourth to the fifteenth program months. During this time there was no detectable change in the high voltage stand-off capability. The temperature drop between radiator and collector decreased for DC-200 and for Dow A. The temperature drop increased for C_2Cl_4. The data is shown in Table XIV.

TABLE XIV 8000 HOUR LIFE TEST RESULTS, COLLECTOR HEAT PIPES

Fluid	Start Life Test	End Life Test
DC-200	64°C	50°C
C_2Cl_4	46°C	86°C
Dow A	108°C	82°C

Note that the initial reluctance to use Dow A (high Δt) has been washed out by changes in performance of the C_2Cl_4 test vehicle. The best performance has, however, been DC-200 in terms of stability. Results of the life test will be considered in the specification of future units. The change in Δt of C_2Cl_4 would have raised the collector temperature about 30°C, an acceptable deviation.

Several varieties of the axial heat pipes were built and evaluated. The ability to transfer heat with gravity both aiding and opposing fluid flow was tested. Figure 45 shows typical performance waves in which the power handling was tested for various heat pipe lengths. If 8 watts is taken as the heat load, then this particular pipe should not be longer than about 6 inches. Actual heat pipes used were less than 6 inches long and were increased to 1/4 inch diameter to increase the power transfer capability.

Based on initial tests fluid choices of methanol and acetone were made. Also the choices of tubing, which is a condenser at one end and a radiator at the other end, were reduced to aluminum and stainless steel. Dynaloy X-7, a stainless steel felt, was used as

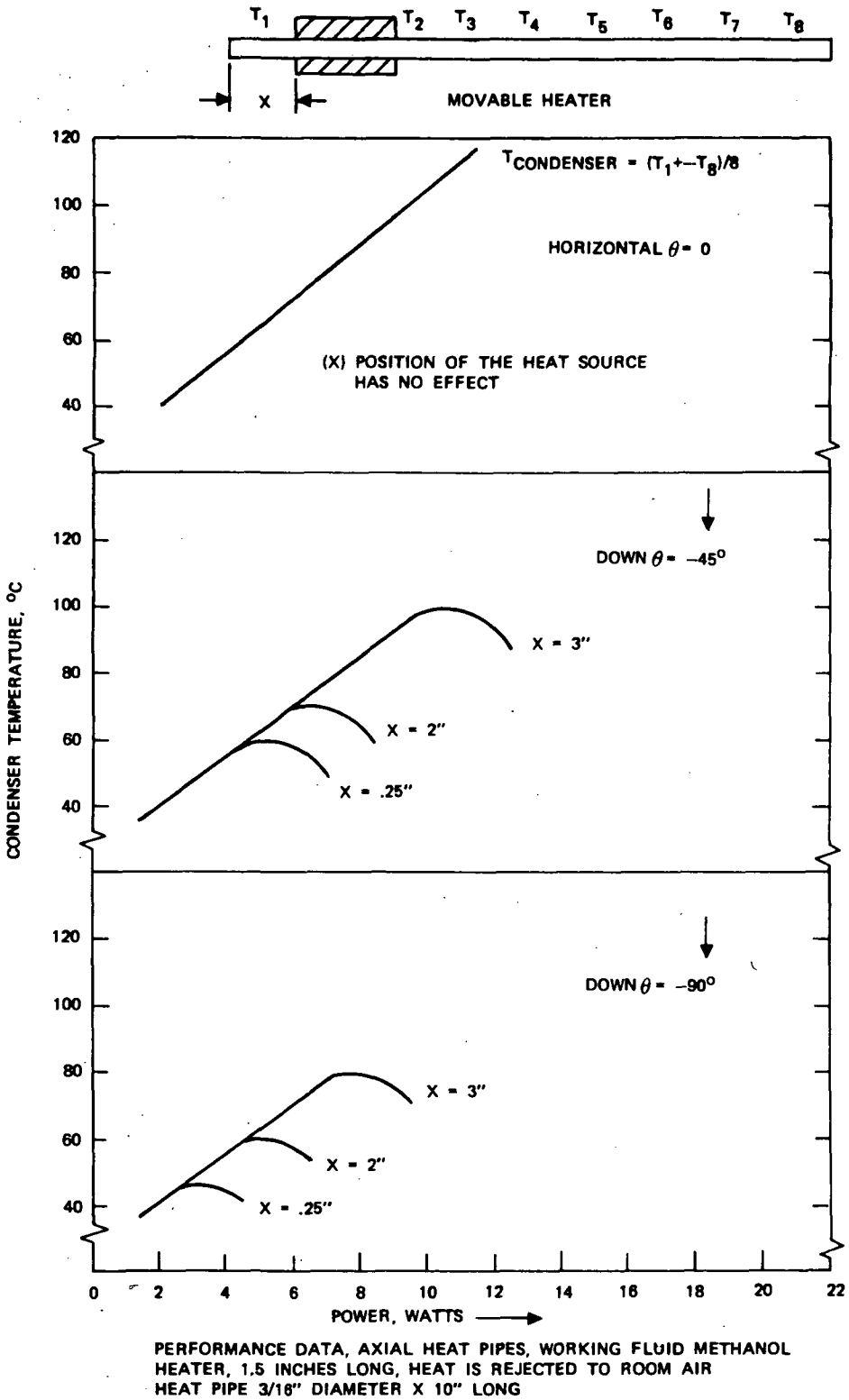

Figure 45 Performance data, axial heat pipes.

the wick. Four each of three combinations were built for life test. The three combinations are shown in Table XV. A fourth possible combination, aluminum-methanol, was not attempted because of known incompatibility problems.

TABLE XV AXIAL HEAT PIPE, LIFE TEST CONFIGURATIONS

Tubing	Wick	Fluid	Quantity
Stainless Steel	Dynaloy	Methanol	4
Stainless Steel	Dynaloy	Acetone	4
Aluminum	Dynaloy	Acetone	4

The life test was run for 14 months. Within three months, degradation of the stainless steel-acetone combinations were noted and after four months the heat pipes no longer functioned. The remaining two combinations were continued successfully to the end of the test period.

Because of the problem with acetone the decision was made to use the stainless steel-methanol combination in both the base plate and the tube mounting base.

HEAT PIPE SYSTEM PERFORMANCE

In addition to providing a low, even heat dissipation density the tube and power supply must maintain itself at temperatures which allow for safe, reliable operation as heat sink temperatures vary and reach a maximum of 80°C. Heat pipes feature a property which can be utilized to predict what temperatures will be reached for given heat sink temperatures. When operated within its rated power handling capability, the heat pipe radiator temperature will be governed by the fluid use. For example, the collector using perchlorethylene fluid will stabilize at approximately 150°C regardless of the cool side temperature.

Table XVI illustrates what the temperature profile becomes for the two extremes of heat sink temperature.

TABLE XVI TEMPERATURE PROFILES FOR TWTA OPERATION

	LOW TEMPERATURE OPERATION	HIGH TEMPERATURE OPERATION
Base Plate	-20°C	+70°C
Tube Mounting Plate	0°C	+80°C
Collector Condenser Cylinder	+10°C	+90°C
Collector Temperature	+150°C	+150°C
Heat Transferred	100 watts	100 watts

Note that because the thermal impedance of the heat pipes is variable, dependent on the vapor pressure of the fluid, the temperature drop from radiator to condenser changes with heat sink temperature to maintain the desired collector temperature. This will remain true as power transferred is changed with a ±50% range. For further increases in heat transferred in this particular sized collector the high side temperature would rise in proportion to the added power.

The base plate heat pipe system is shown in Figure 10. The base plate is constructed in two identical halves using a tape controlled milling operation. Half-circular grooves are cut for each required pipe, in each half plate. The two half plates are then clamped together and the grooves are finished reamed to the heat pipe diameter. The halves are then separated, the pipes are installed with a thermal compound added, and the halves are reclamped together. All modules are then bolted to the base plate as required.

One evaluation of the heat pipe system is shown in Figure 46. In this test the TWTA is operating at saturation and 150 watts are being dissipated as heat. The base plate is positioned horizontally with the base plate above the heat generators. The heat transfer is, therefore, to natural convection upward. (No fans were used.) The temperature was allowed to stabilize and the numbers in Figure 46 were obtained. Note that the variation across the base plate is 22°C. The highest temperature, 59°C, is offset from the centerline as is the tube mounting position in this design.

TEMPERATURE PROFILE
HEAT SINK BASEPLATE

1222H TWTA
SERIAL EM NO. 2

BASEPLATE IN HORIZONTAL PLANE, BASEPLATE
ON TOP (UNIT INVERTED)
NATURAL CONVECTION COOLING ONLY

37	39	40	40	40	40	39	38.5	38	37.5
40	42	43	44	44	43.5	42.5	42	41	39.5
43	45	46.5	47.5	47.5	47	45	44.5	43.5	42.5
45	47.5	49	52	52.5	51	49	47.5	46.5	45
48	50	53.5	54.5	54.5	52	50.5	49	48.5	47
50	53	55	57.5	57.5	55	52	50.5	50	47.5
50.5	53	55	57.5	59	57	52	51.5	50	48
50.5	53	55	57	57	57	53	51.5	50	48
50.5	52	53.5	55	55	53.5	52	51	49.5	49

ALL NUMBERS IN
DEGREES CENTIGRADE

SATURATION OPERATION
150 WATTS THERMAL LOAD

Figure 46 Temperature profile, heat sink base plate.

VI. THE 1222H TWTA PERFORMANCE SUMMARY

One TWTA was produced as part of the development program. This unit was electrically evaluated and delivered to NASA. Figure 47 is a photograph of the complete amplifier. Figure 48 shows the inside of the package with the tube and all power supply components in place.

Weight and power budgets, as they were established with fabrication of this unit, are shown in Tables XVII and XVIII.

The package size is 13.06 inches x 14.45 inches x 3.9 inches high excluding the power/control connector. RF connectors are recessed and do not impact on the outline dimensions.

Although the power budget is made for the condition of a 28-volt line the variation in output power or efficiency is minimal with changes in line voltage. This is shown in Figure 49.

Additional 1222H data taken is shown in this report. Drive level effects are shown in Figures 50, 51, 52, and 53.

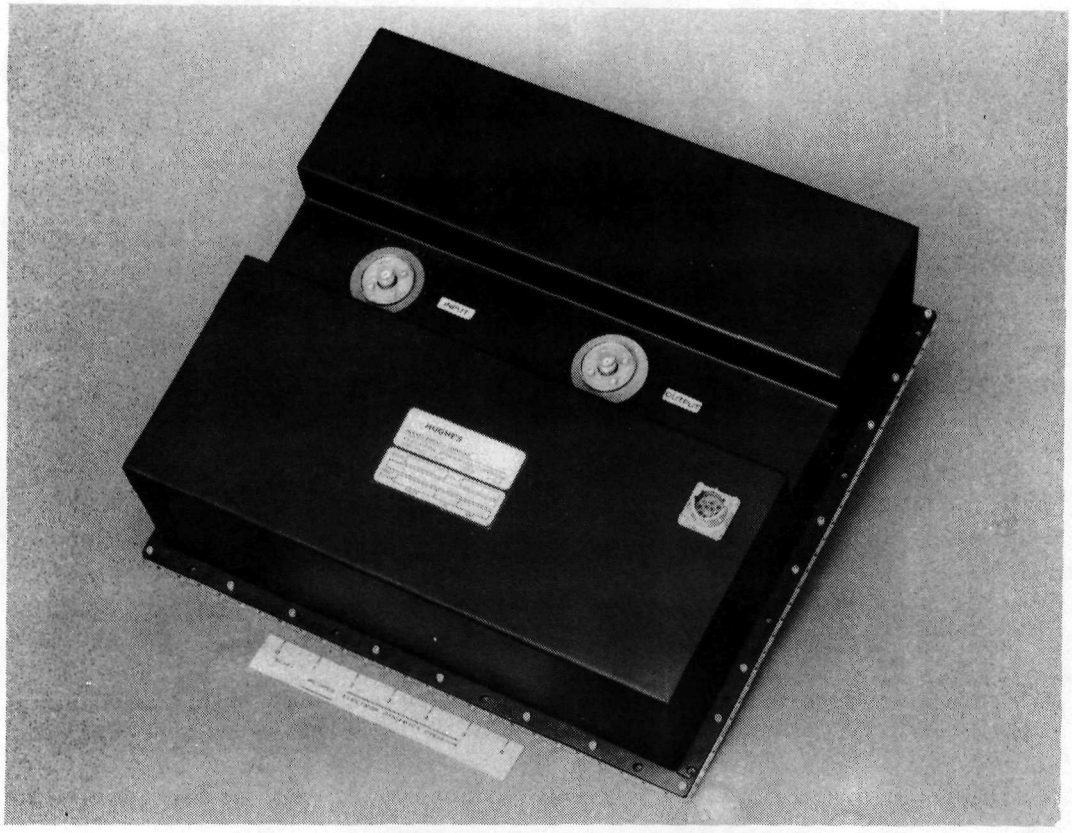

Figure 47 The 1222H TWTA.

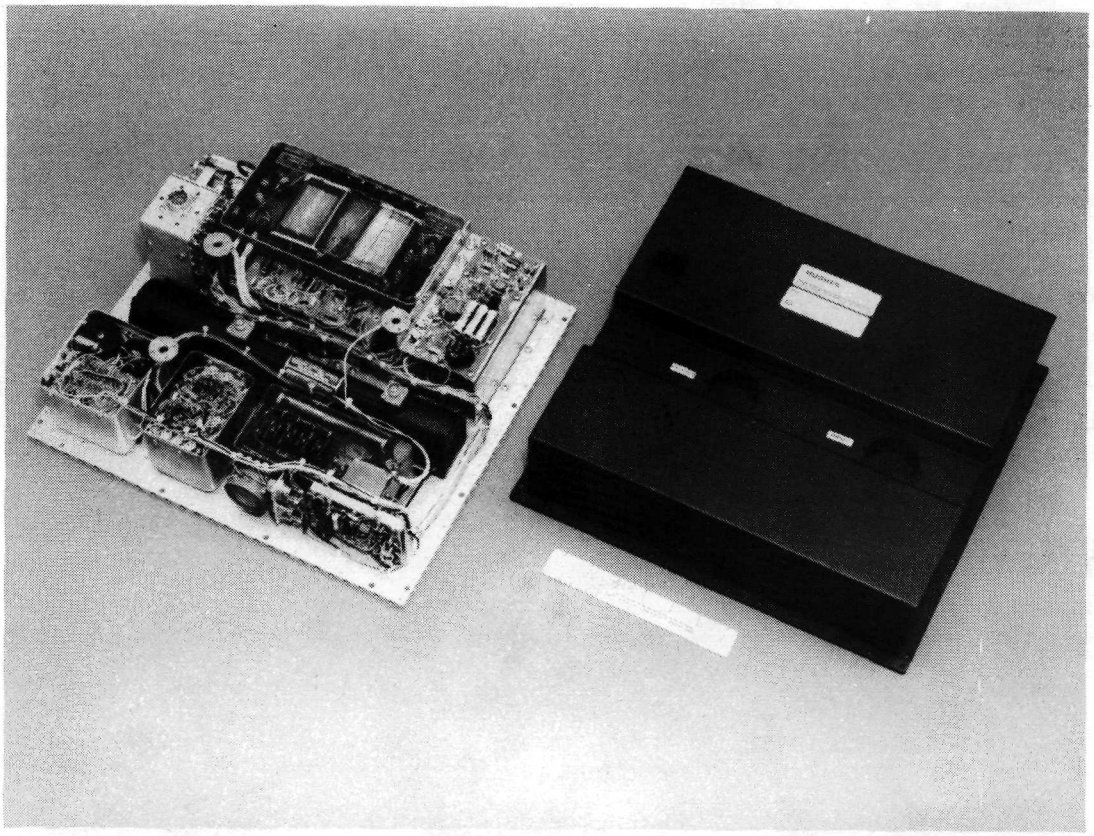

Figure 48 The 1222H TWTA with cover removed.

TABLE XVII 1222H WEIGHT BUDGET

Tube	3.87 lbs
Base Plate	4.63 lbs
Power Supply	18.3 lbs
Cover	2.0 lbs
Misc. Hardware	0.5 lb
Total	29.3 lbs

TABLE XVIII 1222H POWER BUDGET, 28-VOLT LINE

RF Output Power	92 watts
TWT Power	110 watts
Power Supply Losses	36 watts
Total	238 watts

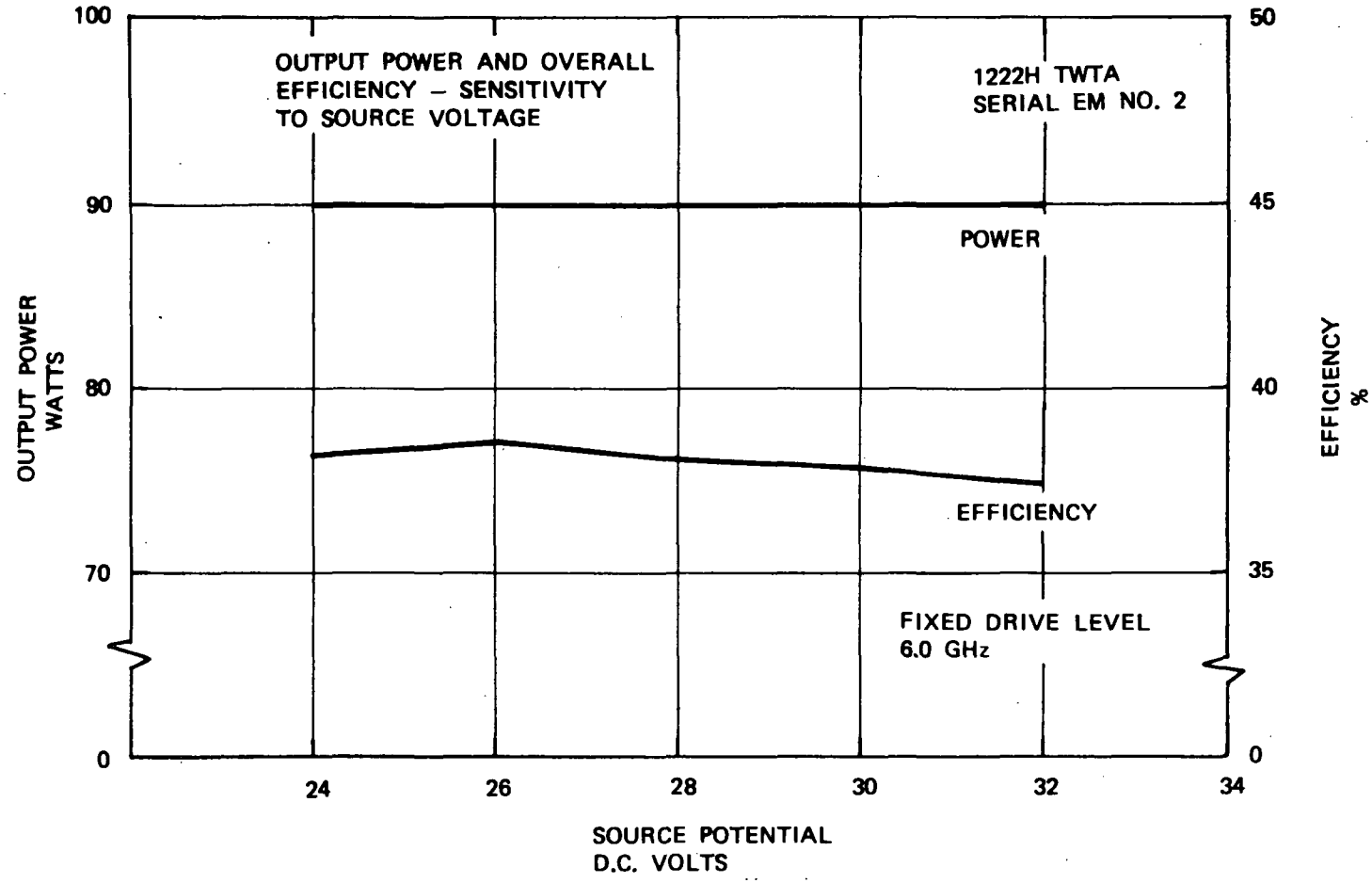

Figure 49 1222H output power and efficiency variation with line voltage.

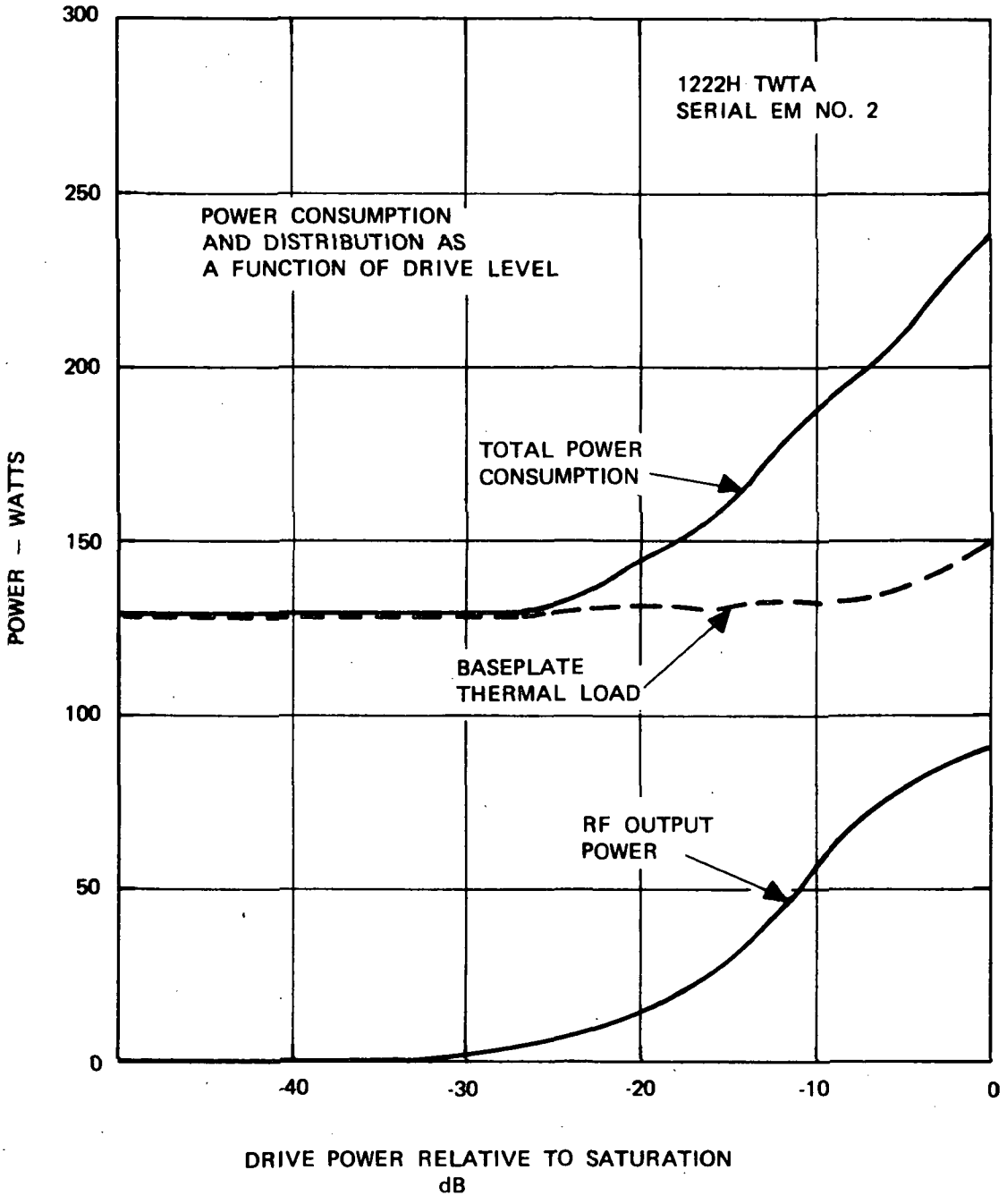

Figure 50 1222H power consumption and distribution, variation with drive level.

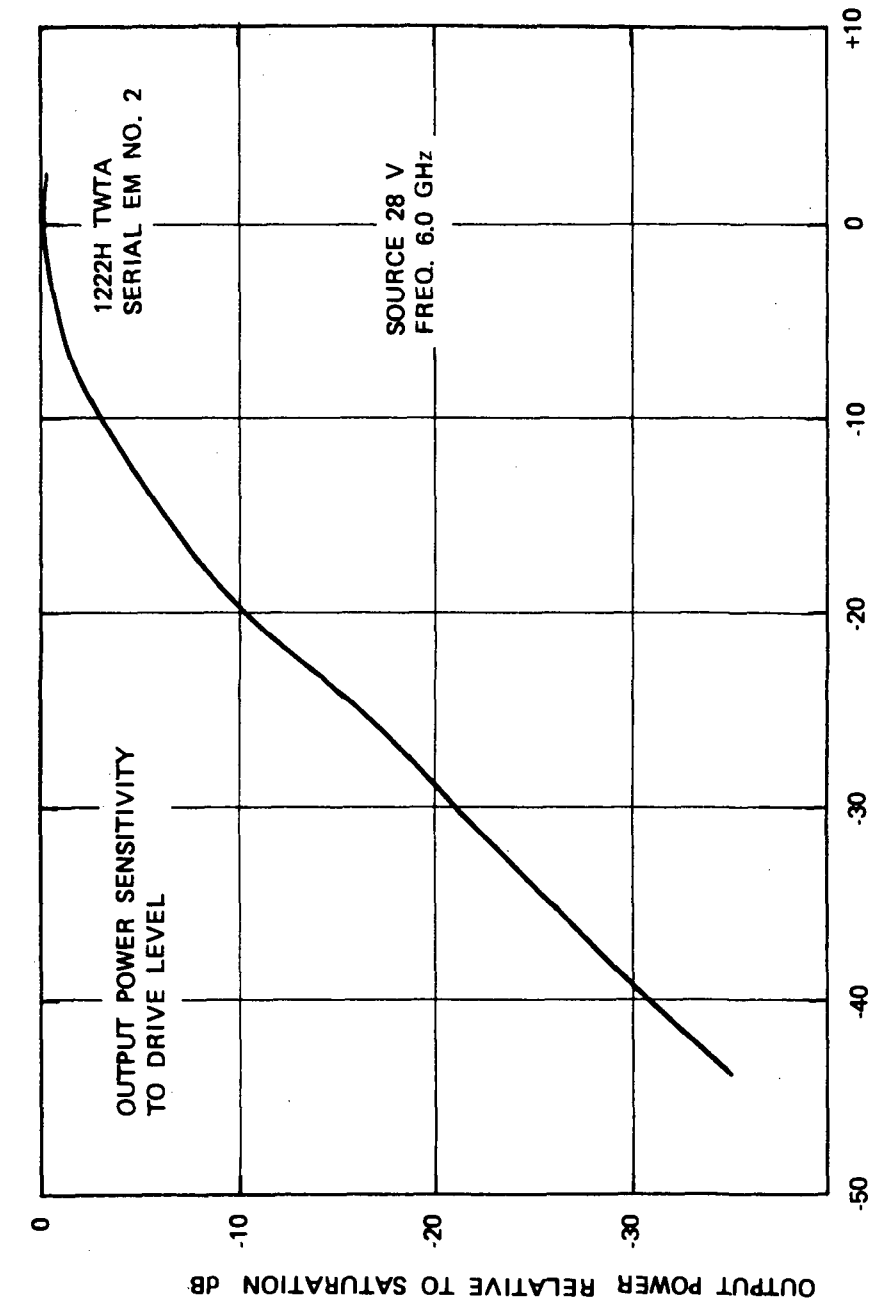

Figure 51 1222H output power, variation with drive level.

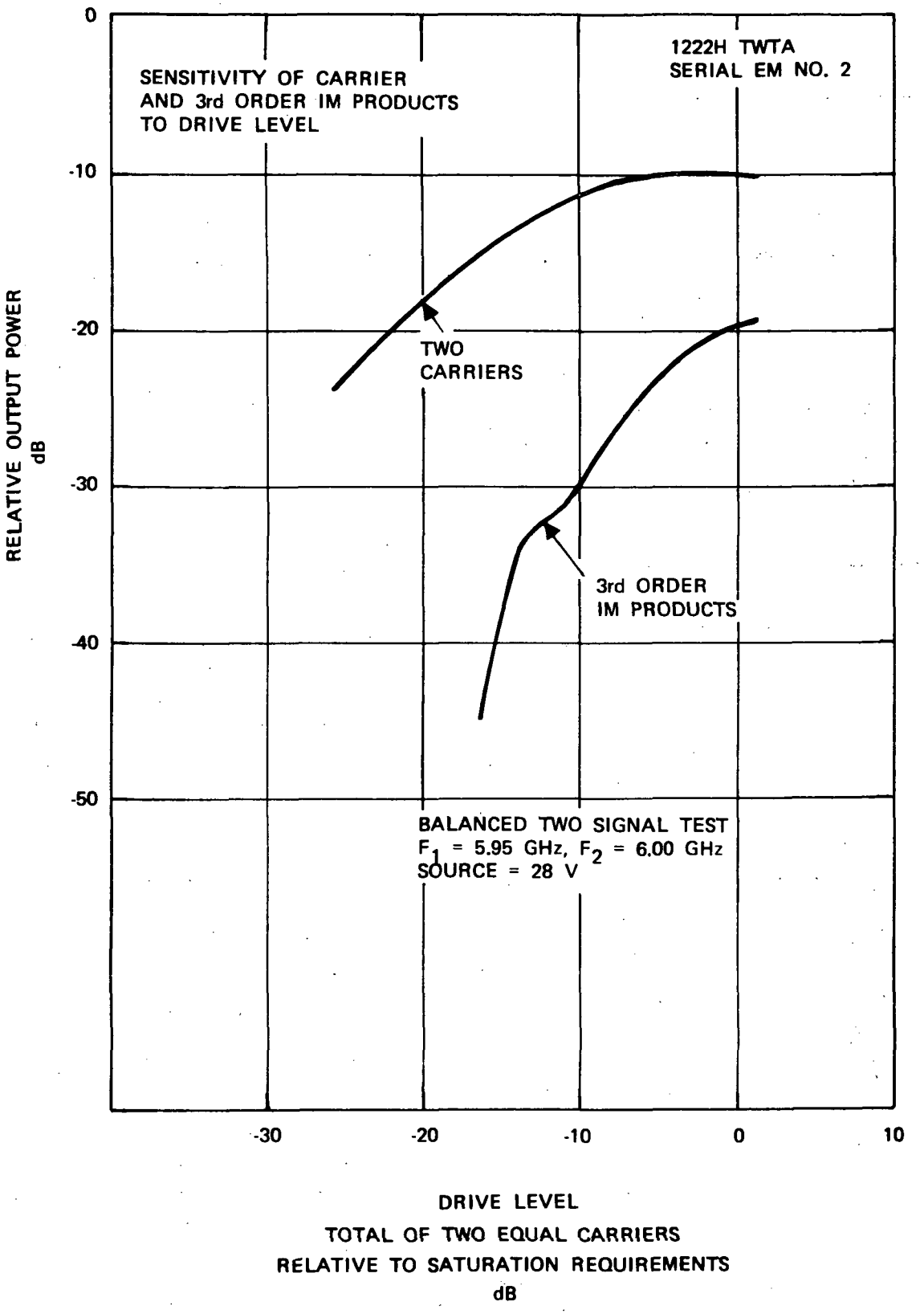

Figure 52 122H third order intermodulation, variation with drive level.

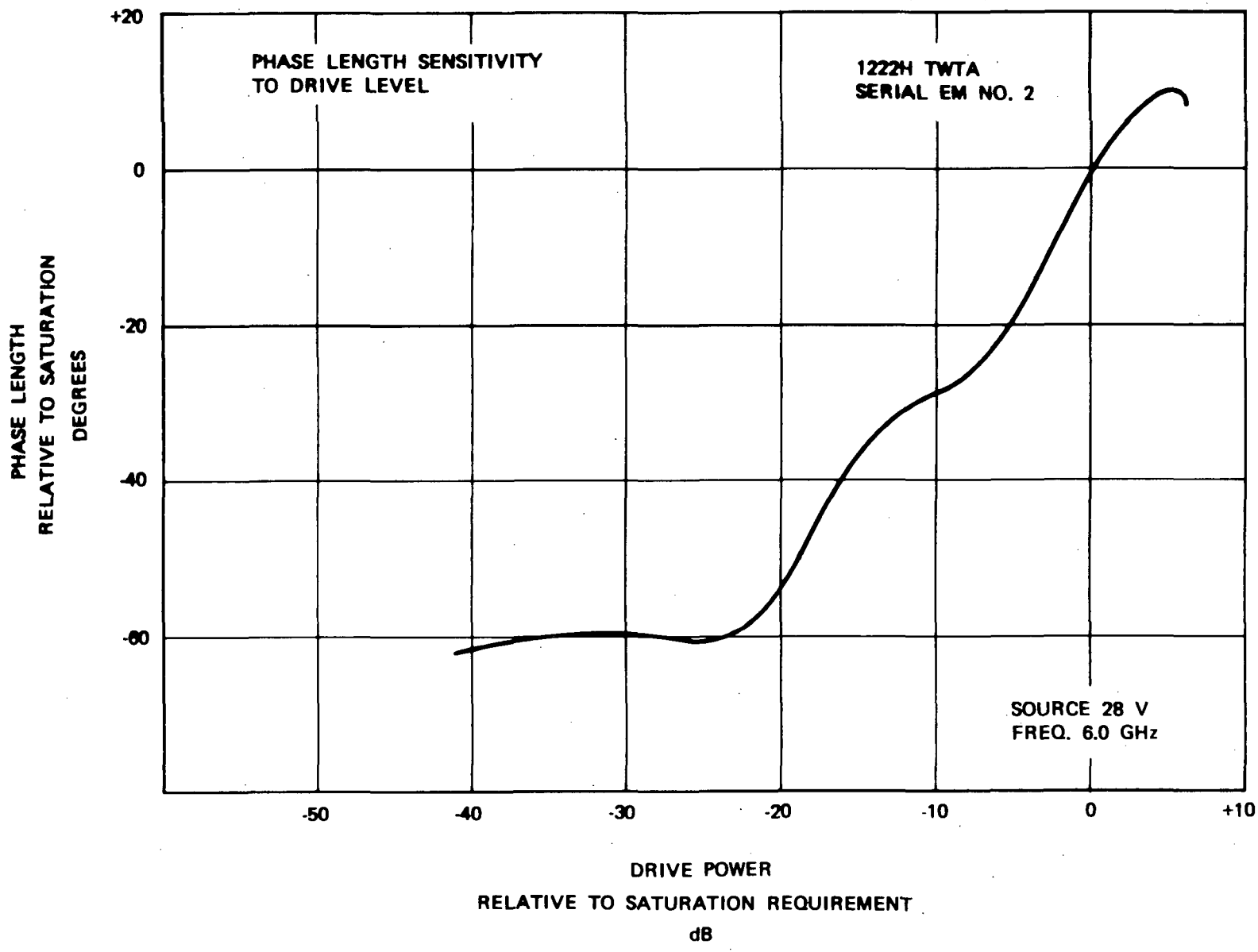

Figure 53 1222H phase length, variation with drive level.

Figure 50 is especially interesting in that it illustrates the impact of an efficient two stage collector. Because of redistribution of interception current as drive level changes, the power drawn by the tube varies with drive level. The increase in input power required as drive level is changed from no drive to full drive is only slightly more than the amount of RF power delivered. As a result the thermal load varies only slightly, from 130 to 150 watts as a function of drive level.

A well shaped transfer curve is shown in Figure 51 indicating that good small signal performance could be expected and the third order IM product level, shown in Figure 52, is also normal. The phase length versus drive, from which AM/PM conversion is obtained, is shown in Figure 53. At saturation the slope of the curve (AM/PM conversion) is only 4^{o}/dB.

Frequency variant effects are shown in Figures 54, 55, and 56. With one exception these are all direct functions of tube capability since they are unaffected by the power supply. These curves indicate, as was seen in the 279H tube data, that the tube is centered low with respect to the 5.925 to 6.425 GHz band. Gain level and slope, and gain ripple are all well within requirements. Over a 500 MHz band, selecting the best 500 MHz, the power variation is 0.3 dB. This may be reduced slightly by better frequency centering, but all tubes evaluated have varied approximately this much. The significance of this data is that the design power level must account for this much variation since minimum power level will be rated at band edge.

The one exception mentioned, the data which does include the effects of the power supply, is the efficiency plotted in Figure 55. This is overall efficiency including power supply losses. Over the same best 500 MHz band the efficiency ranges from 38.5% to 37%. The variation in efficiency of 0.16 dB is less than that of power output because of the benefits of the two stage collector mentioned earlier in this report. The efficiency attained here meets minimum goals. Planned improvements will raise overall efficiency at least 3 percentage points.

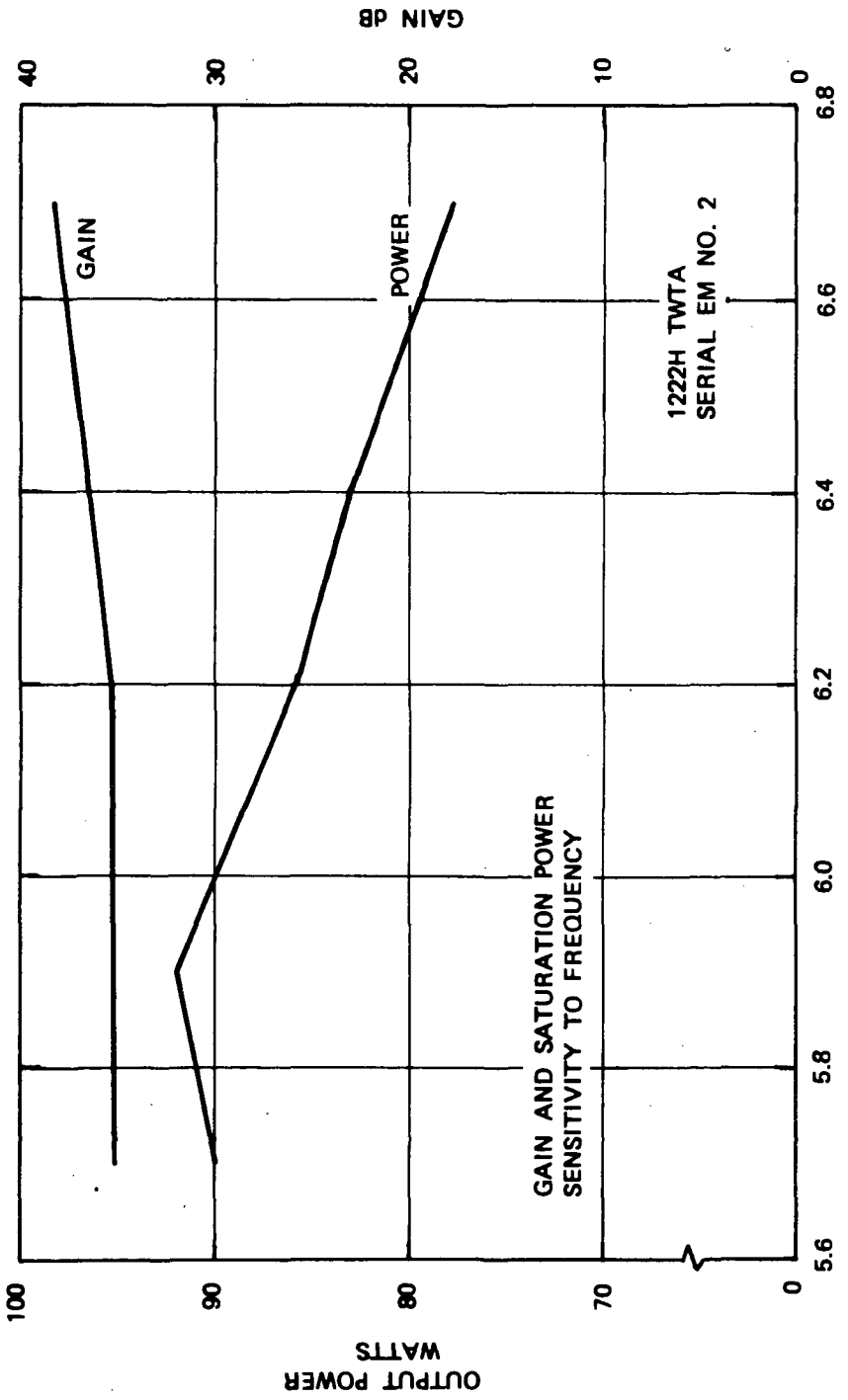

Figure 54 1222H gain and saturation power variation with frequency.

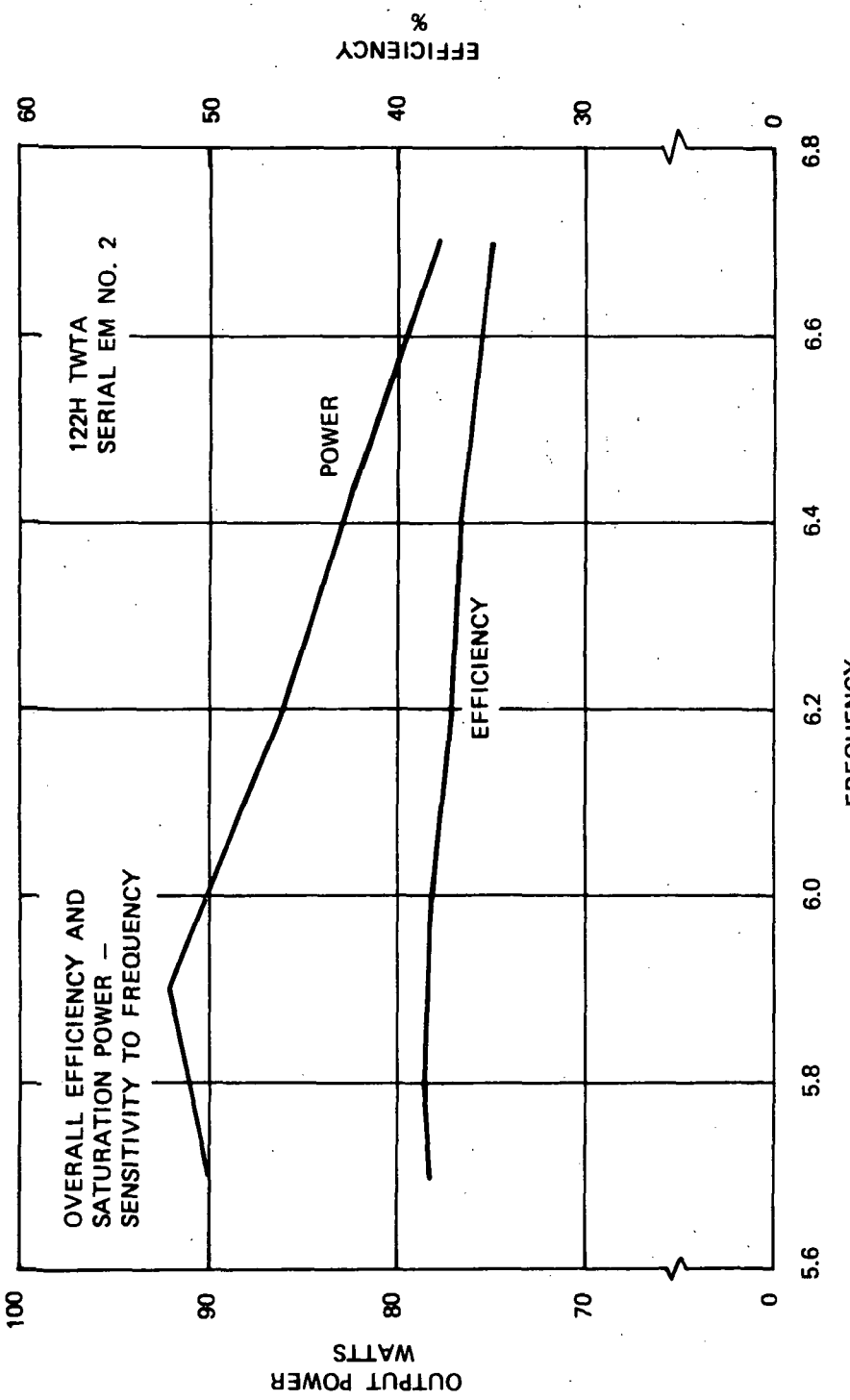

Figure 55 1222H efficiency and saturation power variation with frequency.

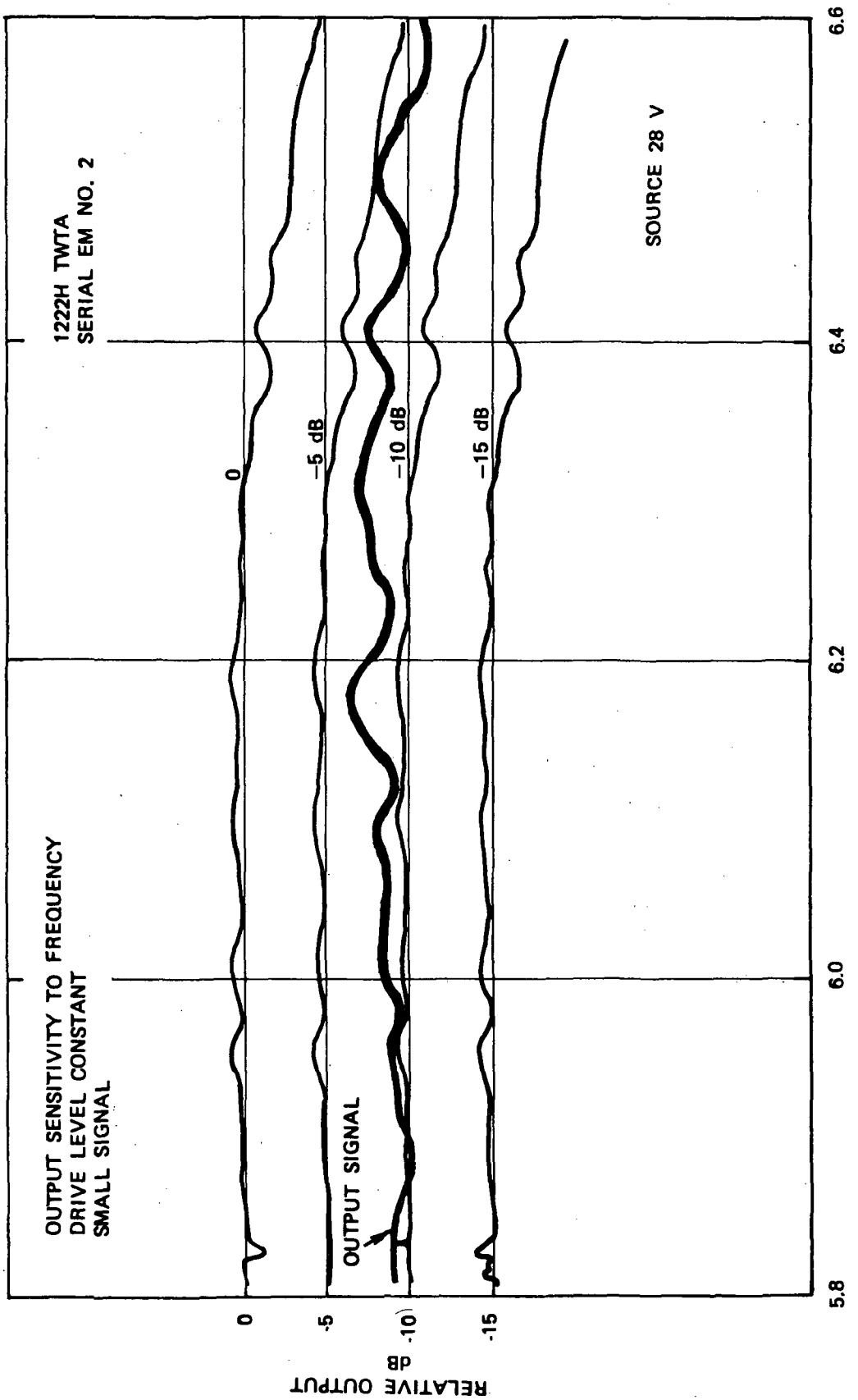

Figure 56 1222H small signal gain ripple variation with frequency.

VII. DISCUSSION OF RESULTS

The most significant result of this program is the documentation, by test results, that high efficiency can be combined with good communication performance in high power traveling-wave tube amplifiers. A second very important accomplishment, the reduction of density of waste heat rejected from the unit, points up the fact that heat pipes can be used in straightforward fashion to relieve what would otherwise be a severe limit on the use of high power devices in spacecraft in which high density thermal loads cannot normally be handled.

It is also felt that limitations on experimental effort by virtue of available time and funds prevented attaining the predicted efficiency of the tube. It is expected that with modifications of a minor nature to the helix taper and to the collector electrode geometry, several percentage points in efficiency can be attained. This estimate is based partially on data taken in this program and partially on extrapolation from similar Hughes Electron Dynamics Division designs in which the same design techniques were used and better performance was obtained.

The power supply efficiency of 85% is good considering the need for two collector supplies. A new look at requirements based on actual tube performance could benefit the power supply efficiency since early estimates of required regulation were much more severe than experience has indicated we actually need. Relaxation here would result in reduced complexity as well as reduced losses.

The package size is partly based on the operating power level and partly based on the requirement for a low density for rejected (waste) heat. We are presently within both size and weight requirements for the total amplifier.

Our average base plate thermal power density is less than 1.0 watt per square inch. This average, however, will not be attained in certain gravity situations in which thermal power flow to one half of the base plate or the other will be favored and the peak loading will increase. Consequently the area of the base plate should not be significantly reduced below the present size even though the average loading appears low.

One of the more interesting side effects noted may also become an important feature with regard to the thermal capacity and thermal control capability of spacecraft. Redistribution of intercept current as basic efficiency changes across the band, or as drive level is altered, changes the power drain from the source in an amount very nearly equal to the change in RF output power. This is as opposed to low power, lower efficiency units in which the drain from the source is essentially constant regardless of operating condition. As a result of the redistribution of current essentially all power drawn, above a fixed loss of 150 watts,

is delivered as RF power. The thermal load is, therefore, nearly constant at 150 watts. This can be of major significance if output power level must be altered since the constant thermal load eliminates the need for fast response in the spacecraft waste heat removal system.

VIII. RECOMMENDATIONS FOR FUTURE WORK

THE TRAVELING-WAVE TUBE

During the course of this development program a number of tube iterations were evaluated. These were modifications of the initial computer design. All were evaluated with a single type of collector, also computer designed.

Data generated by this program and by other similar programs lead to the conclusion that additional modifications to the circuit taper in conjunction with collector modifications will result in increases in overall efficiency to well over 50%. A goal of 55% would be well in line with other available data.

This work could take the form of a tube design with a demountable collector such that a family of circuit designs can be evaluated with a single collector or, conversely, modified collectors could be easily evaluated with a circuit of known characteristics.

THE POWER SUPPLY

The final design consists of several modules, each of which has been through an analysis of operating characteristics. Each does its job well and the resultant power supply meets or exceeds all original goals set for it.

Now that tube sensitivities to voltage level changes are well known it would be worthwhile to reconsider the power supply design. Constraints which were originally imposed are no longer necessary. For instance, regulation in the helix circuit is less critical than that demanded of low power tubes. Significant reduction in complexity, and some reduction in size and improvement in reliability must result from such an assessment.

EVALUATION OF ENVIRONMENTAL CAPABILITY AND RELIABILITY

In order to be able to make a quantitative statement of the ability of the unit to withstand the rigors of a launch operation and subsequent operation in space, a formal qualification program should be undertaken. Units for this program should be constructed with flight quality parts and appropriate burn-in of the power supply; the tube and the integrated amplifier should be conducted.

Following exposure to the required environmental extremes the units should be placed on operating life test to assess both failure rate and eventually the design life by extending the life test to cathode depletion.

It is suggested that an environmental test of two units and a life test of six units would be appropriate considering the ultimate mission.

IX. CONCLUSIONS

This program required the development of a high efficiency C-Band TWT and associated power supply. The total design was also concerned with the ultimate mission use as a highly reliable communication system power amplifier for space applications.

A velocity tapered tube approach was taken with special consideration given to avoidance of "overvoltage" techniques or other efficiency enhancement devices which might degrade the usefulness of the design in communication systems.

A well regulated solid state power supply capable of conditioning over 200 watts of dc power for the TWT was also designed, again with a high reliability mission in mind.

The successful delivery of the engineering model TWTA incorporating one each of tube and power supply points up the fact that a unit such as is described by the contract specification is a reality. The approach of tube operation at low perveance and at synchronism can result in high overall efficiency and good communication type performance if proper circuit and collector design techniques are employed.

NASA CR-112125

DISTRIBUTION LIST

NAS1-10417

	No. Copies
NASA Langley Research Center Hampton, VA 23365	
Attn: 122/Acquilla D. Saunders	1
115/Raymond L. Zavasky	1
139A/Technology Utilization Office	1
490/Bruce M. Kendall	35
NASA Ames Research Center Moffett Field, CA 94035	
Attn: 202-3/Library	1
233-15/John Dimeff	1
NASA Flight Research Center P. O. Box 273 Edwards, CA 93523	
Attn: Library	1
NASA Goddard Space Flight Center Greenbelt, MD 20771	
Attn: Library	1
520.0/Dr. Robert J. Coates	1
NASA Manned Spacecraft Center 2101 Webster Seabrook Road Houston, TX 77058	
Attn: JM6/Library	1
EE3/Meridth W. Hamilton	1
EJ/William C. Bradford	1
NASA John F. Kennedy Space Center Kennedy Space Center, FL 32899	
Attn: IS-DOC-12L/Library	1
DD-EDD-21/William R. McMurran	1
Jet Propulsion Laboratory 4800 Oak Grove Drive Pasadena, CA 91103	
Attn: 111-113/Library	1
161-213/Robert S. Hughes	1
NASA Lewis Research Center 21000 Brookpark Road Cleveland, OH 44135	
Attn: 54-1/Henry W. Plohr	1
54-5/Rubert E. Alexovich	1
54-5/Francis E. Kavanagh	1
54-5/Dr. Henry G. Kosmahl	1
54-5/Gerald J. Chomos	1
54-5/Norbert Stankiewicz	1
54-5/Peter Ramins	1

NASA CR-112125

DISTRIBUTION LIST
NAS1-10417

	No. Copies
National Aeronautics & Space Administration Washington, DC 20546	
Attn: EC/Dr. Richard B. Marsten	1
ECC/A. M. Greg Andrus	1
REM/Edward C. Buckley	1
MHE/Richard C. Livingston	1
ECF-2/Eugene Ehrlich	1
NASA Marshall Space Flight Center Huntsville, AL 35812	
Attn: Library	1
PD-DO-EC/Edward C. Hamilton	1
S&E-ASTR-IR/Dane O. Lowrey	1
Defense Documentation Center Cameron Station (Building 5) Alexandria, VA 22314	
Attn: DDC-IRS	1
Office of Assistant Secretary of Defense (Research and Engineering) Washington, DC 20301	
Attn: Technical Library, RM 3E1065	1
Director Advanced Research Projects Agency The Pentagon Room 2b 285 Washington, DC 20301	1
Commanding General U. S. Army Electronics Command Fort Monmouth, NJ 07703	
Attn: AMSEL-RD-MAT	1
AMSEL-RD-LNA	1
AMSEL-XL-D	1
Director Naval Research Laboratory Washington, DC 20390	
Attn: Howard O. Lorenzen, Code 4530	1
Rome Air Development Center (EMTLD) Griffiss Air Force Base, NY 13440	
Attn: Documents Library	1
Haralambe Chiosa, EMATE	1
Systems Engineering Group Wright-Patterson Air Force Base, OH 45433	1
Electronic Systems Division (ESTI) L. G. Hanscom Field Bedford, MA 01731	1

NASA CR-112125

DISTRIBUTION LIST

NAS1-10417

	No. Copies
Commander Air Force Cambridge Research Laboratories L. G. Hanscom Field Bedford, MA 01731	
Attn: CRZC	1
CRIM. Walter Rotman	1
Advisory Group on Electron Devices 201 Varick Street 9th Floor New York, NY 10014	1
COMSAT Corporation 2100 L. Street, N.W. Washington, DC 20037	
Attn: Roberts Strauss	1
Varian Associates 611 Hansen Way Palo Alto, CA 94304	
Attn: Dr. Wayne Abraham	1
Litton Industries Electron Tube Division 960 Industrial Road San Carlos, CA 94070	
Attn: W. R. Day	1
General Electric Company Tube Department Microwave Tube Operation Schenectady, NY 12305	
Attn: R. Dehn	1
DCASR, San Francisco 866 Malcolm Road Burlingame, CA 94010	
Attn: James M. Graham	1
Watkins-Johnson Company 333 Hillview Avenue Stanford Industrial Park Palo Alto, CA 94304	
Attn: Dr. David Bates	1
Dr. Lester Roberts	1
NASA Scientific & Technical Information Facility P. O. Box 33 College Park, MD 20740	14 plus reproducibl